

CORRELATION OF THEORETICAL TURBULENT SKIN
FRICTION WITH PRESTON-TUBE MEASURE-
MENTS ON A SUBSONIC CONE

By

AMIR NASSIRHARAND

Bachelor of Science in Mechanical Engineering

Oklahoma State University

Stillwater, Oklahoma

1980

Submitted to the Faculty of the Graduate College
of the Oklahoma State University
in partial fulfillment of the requirements
for the Degree of
MASTER OF SCIENCE
December, 1981

Thesis
1981
N268c
cop. 2



CORRELATION OF THEORETICAL TURBULENT SKIN
FRICTION WITH PRESTON-TUBE MEASURE-
MENTS ON A SUBSONIC CONE

Thesis Approved:

Joy D. Reed

Thesis Adviser

A. W. Moub

W. G. Lilley

Norman D. Durham

Dean of Graduate College

ACKNOWLEDGMENTS

I wish to express my gratitude to every single member of my family for their understanding, encouragement, and many sacrifices.

I am most grateful to my major adviser, Dr. Troy D. Reed, for his invaluable assistance and guidance throughout this study and in the preparation of the final manuscript.

This study was sponsored by NASA-Ames Research Grant No. NAG 2-76.

TABLE OF CONTENTS

Chapter	Page
I. INTRODUCTION	1
II. BASIC TOOLS USED TO CARRY OUT THE TURBULENT BOUNDARY LAYER CALCULATIONS	7
Allen's Correlation	7
Musker's Equation	9
Wu and Lock Computer Code	12
STAN-5 Computer Code	14
III. THE METHOD DEVELOPED TO COMPLETE THE TURBULENT BOUNDARY LAYER CALCULATIONS	18
IV. DEVELOPMENT OF THE GOVERNING EQUATIONS	27
V. ANALYSIS OF DATA AND THE CORRELATION EQUATION	35
VI. SUMMARY AND CONCLUSIONS	55
A SELECTED BIBLIOGRAPHY	57
APPENDIXES	58
APPENDIX A - THE MINI-BASIC COMPUTER CODE	59
APPENDIX B - TABULATED VALUES OF TOTAL PRESTON-TUBE PRES- SURE, EFFECTIVE CENTER OF THE PROBE AND SKIN FRICTION COEFFICIENT ALONG THE SURFACE OF THE CONE FOR 19 CASES	101

LIST OF TABLES

Table	Page
I. Wind Tunnel Cases Studied to Develop the Correlation Equation (NASA Ames 11-ft TWT)	6
II. Comparison of Skin Friction Coefficient Values by Modeling the Cone with Three Different Methods	24
III. Preston-Tube Pressure, Effective Center of the Probe, and Skin Friction Coefficient Along the Surface of the Cone For Run Number 29.440	102
IV. Preston-Tube Pressure, Effective Center of the Probe, and Skin Friction Coefficient Along the Surface of the Cone For Run Number 61.636	103
V. Preston-Tube Pressure, Effective Center of the Probe, and Skin Friction Coefficient Along the Surface of the Cone For Run Number 60.635	104
VI. Preston-Tube Pressure, Effective Center of the Probe, and Skin Friction Coefficient Along the Surface of the Cone For Run Number 25.376	105
VII. Preston-Tube Pressure, Effective Center of the Probe, and Skin Friction Coefficient Along the Surface of the Cone For Run Number 59.634	106
VIII. Preston-Tube Pressure, Effective Center of the Probe, and Skin Friction Coefficient Along the Surface of the Cone For Run Number 23.346	107
IX. Preston-Tube Pressure, Effective Center of the Probe, and Skin Friction Coefficient Along the Surface of the Cone For Run Number 40.547	108
X. Preston-Tube Pressure, Effective Center of the Probe, and Skin Friction Coefficient Along the Surface of the Cone For Run Number 58.633	110
XI. Preston-Tube Pressure, Effective Center of the Probe, and Skin Friction Coefficient Along the Surface of the Cone For Run Number 70.726	111

Table	Page
XII. Preston-Tube Pressure, Effective Center of the Probe, and Skin Friction Coefficient Along the Surface of the Cone For Run Number 21.318	112
XIII. Preston-Tube Pressure, Effective Center of the Probe, and Skin Friction Coefficient Along the Surface of the Cone For Run Number 41.548	114
XIV. Preston-Tube Pressure, Effective Center of the Probe, and Skin Friction Coefficient Along the Surface of the Cone For Run Number 57.632	116
XV. Preston-Tube Pressure, Effective Center of the Probe, and Skin Friction Coefficient Along the Surface of the Cone For Run Number 72.748	117
XVI. Preston-Tube Pressure, Effective Center of the Probe, and Skin Friction Coefficient Along the Surface of the Cone For Run Number 19.289	118
XVII. Preston-Tube Pressure, Effective Center of the Probe, and Skin Friction Coefficient Along the Surface of the Cone For Run Number 42.549	120
XVIII. Preston-Tube Pressure, Effective Center of the Probe, and Skin Friction Coefficient Along the Surface of the Cone For Run Number 56.631	121
XIX. Preston-Tube Pressure, Effective Center of the Probe, and Skin Friction Coefficient Along the Surface of the Cone For Run Number 43.550	122
XX. Preston-Tube Pressure, Effective Center of the Probe, and Skin Friction Coefficient Along the Surface of the Cone For Run Number 15.231	123
XXI. Preston-Tube Pressure, Effective Center of the Probe, and Skin Friction Coefficient Along the Surface of the Cone For Run Number 44.551	124

LIST OF FIGURES

Figure	Page
1. Flat Plate Boundary Layer	3
2. AEDC Boundary Layer Transition Cone	5
3. Inviscid Pressure Distribution About a 10° Cone (Wu & Lock)	13
4. Terminology for Setting Up STAN-5	19
5. Determination of the Location of the Match Point and the Corresponding Preston-Tube Pressure	21
6. Variation of Effective Height of Probe in Laminar Boundary Layers	37
7. The Corrected Variation of Effective Height of Probe in Laminar Boundary Layers	38
8. Criterion for Discarding Unsuitable Cases	40
9. Criterion for Selection of Suitable Data Points	41
10. Variation of the Effective Height of Probe in Turbulent Boun- dary Layers	42
11. Preston-Tube/Turbulent-Skin-Friction Correlation Based on a Variable Effective Probe Height	44
12. Deviation of Skin Friction Coefficient Predicted by Equation (5.5) from Theoretical Values	45
13. Skin Friction Distribution Along the Surface of the Cone for Run Number 15.231	47
14. Skin Friction Distribution Along the Surface of the Cone for Run Number 40.549	48
15. Comparison of k_{eff} Distribution Along the Surface of the Cone Using the New Correlation and Allen's Correlation for Run Number 15.231	49

Figure	Page
16. Comparison of k_{eff} Distribution Along the Surface of the Cone Using the New Correlation and Allen's Correlation for Run Number 40.549	50
17. Comparison of k_{eff} Distribution as a Function of $U_T h / \nu_w$ Using Allen's Correlation and New Correlation for Run Number 15.231	51
18. Comparison of k_{eff} Distribution as a Function of $U_T h / \nu_w$ Using Allen's Correlation and New Correlation for Run Number 40.549	52
19. Simplified Flow Chart for the Mini-Basic Computer Code . . .	61

NOMENCLATURE

a	speed of sound (FT/S) ($\sqrt{\gamma R g_c T}$)
B	constant in logarithmic region of mean velocity distribution 5.0 (dimensionless)
c_f	skin friction coefficient ($2\tau_w/\rho_e U_e^2$) (dimensionless)
\bar{c}_f	nondimensional difference between skin friction coefficient ($(c_{f,t} - c_{f,c})/c_{f,t}$)
c_p	pressure coefficient based on the difference between a Pitot and static pressure reading ($(P_p - P_w)/q_\infty$) (dimensionless)
d	geometric parameter - ft (see Figure 4)
D	external diameter of a round Pitot tube - inches
D_{eq}	equivalent external diameter of the oval shaped Pitot probe used in NASA Ames experiments (inches) (see Equation 4.26)
F_1	Allen's first calibration parameter (see Equation (2.1)) (dimensionless)
F_2	Allen's second calibration parameter (see Equation (2.2)) (dimensionless)
F_3	Fenter-Stalmach's first calibration parameter (see Equation (2.5)) (dimensionless)
F_4	Fenter-Stalmach's second calibration parameter (see Equation (2.6)) (dimensionless)
g_c	conversion factor (32.174 LBM-FT/S)
h	external height of face of the oval probe (0.0097 inches)

k_{eff}	nondimensional effective center of the Pitot probe (see Equation (3.2))
L	axial length of cone (44.5 inches)
M	Mach number (dimensionless)
P	pressure (LBF/FT ²)
q	dynamic pressure (LBF/FT ²)
r	recovery factor (0.884) (dimensionless)
R	gas constant (53.35 LBF-FT/LBM- ⁰ R for air)
R_D	Reynolds number for compressible flow based on diameter D (see Equation 4.22) (dimensionless)
Re_{ft}	freestream unit Reynolds number - 1/ft (see Equation (4.3))
Re_{θ}	Reynolds number based on the product of U_e/ν_e and boundary-layer momentum thickness.
T	temperature - ⁰ R
T^*	nondimensionalized temperature (see Equation (5.4))
u	mean velocity inside boundary layer - FT/S (see Equation (2.8))
U_e	velocity at outer edge of boundary layer - FT/S
U_{pt}	velocity calculated from Preston-tube data-FT/S
U_{τ}	classical wall-shear-stress velocity-FT/S($\sqrt{\tau_w/\rho_w}$)
U_{∞}	freestream velocity - Ft/S
x	axial distance from physical nose of cone - inches
X_4	the location within the laminar boundary layer which has the same Preston-tube pressure as that of the match point (inches) (see Figure 5)
X_c	surface distance along the surface of the cone measured with reference to virtual origin - FT

X_{eq}	surface distance between match point and virtual origin - FT (see Figure 4)
X_{MP}	surface distance between match point and tip of the physical cone - FT (see Figure 4)
X_0	surface distance measured with reference to tip of the physical cone - FT
X_t	distance along surface of cone from apex to onset of boundary-layer transition - FT (see Figure 5)
X_T	distance along surface of cone from apex to end of boundary-layer transition (see Figure 5)
X^*	logarithm of the square of a Reynolds number based on the product $U_{pt} y_{eff}/\nu_w$ (dimensionless) (see Equation 5.3)
y	distance normal to the cone surface - FT
y_{eff}	effective height of face of Preston-tube which is defined to be the height above the wall of an undisturbed streamline which has a total pressure equal to the measured Pitot pressure - FT
Y^*	dimensionless shear stress for compressible, nonadiabatic flow (see Equation (5.2))

Greek Letters

δ	boundary layer thickness
ϵ_m	eddy diffusivity for momentum conservation (dimensionless)
γ	specific heat ratio (1.4 for air)
κ	von Karman constant 0.41
μ	absolute viscosity (LBF-S/FT)

ν	kinematic viscosity (FT^2/S)
Π	wake-strength parameter 0.5
ρ	density of fluid (LBM/FT)
τ	shear stress (LBF/FT^2)
θ	cone half-angle (5°) (see Figure 3)

Subscripts

aw	at adiabatic wall conditions
e	at outer edge of boundary layer
FP	flat plate
i	at initial station of turbulent boundary layer calculations
pt	calculated based on Preston-tube data
t	total
w	at the wall of physical cone
∞	at freestream conditions

Superscripts

$\hat{}$	evaluated at the reference temperature of Sommer and Short (see Equation (2.9))
---------------------	--

CHAPTER I

INTRODUCTION

In the area of fluid mechanics, the concept of boundary layer transition is still one of the major areas of research. It is an indisputable fact that a better understanding of boundary layer transition will further improve the progress of a wide variety of industries. For example, the auto industry is one of the major areas of industry that uses the concept of a boundary layer to design the shape of an automobile. The drag coefficient of an actual automobile may vary from a value of one to an ideal value of two tenths depending on the shape of the automobile. Achieving low values of drag coefficient reduces the rate of gas consumption of automobiles. Another major industry that heavily depends on the understanding and control of fluid movement is the aerospace industry. The aerospace industry uses the concept of the boundary layer to design aircraft which meet different missions. The design of wings and the prediction of important parameters such as lift, drag, and skin friction require a good understanding of the boundary layer. The concept of a boundary layer is also used in the turbomachinery industry and fluid power control systems.

The concept of a boundary layer was first introduced by Prandtl in 1904 (1). The term boundary layer is due to the fact that a thin layer of fluid near the boundary of a moving body is retarded by fluid viscosity. Boundary layer theory can be illustrated by considering the flat

plate shown in Figure 1. First of all, one should recognize two distinct regions of the boundary layer: (1) a laminar boundary-layer region and (2) a turbulent boundary-layer region. The region that corresponds to transition from the laminar boundary layer to the turbulent boundary layer is referred to as the transition region.

The overall objective of this research project is to investigate the possibility of using pressure measurements, obtained with Pitot tubes resting on the surface of a ten-degree cone, to develop a method which could be used to characterize the flow quality of a given transonic wind tunnel. For a given transonic wind tunnel, the freestream turbulence and noise inside the wind tunnel cause appreciable errors and inaccuracies in the results of wind tunnel experiments. For example, if a given model is tested in different wind tunnels at ostensibly identical Mach number, unit Reynolds number, and dynamic pressure, different values of lift and drag, for example, are measured. Ideally, the measurement of different variables (e.g., lift and drag) for a given model should be independent of the wind tunnel used. However, in practice this is not the case. If there were a method that could be used to characterize the flow quality of existing wind tunnels, then the measurements of different parameters and variables for a given model would be consistent and independent of the wind tunnel that is used to carry out the experiments. It is interesting to note that a satisfactory method has not yet been developed that can be used to characterize flow quality of a transonic wind tunnel.

The specific objective of the work presented herein is to correlate Preston-tube pressure measurements within turbulent boundary layers on a

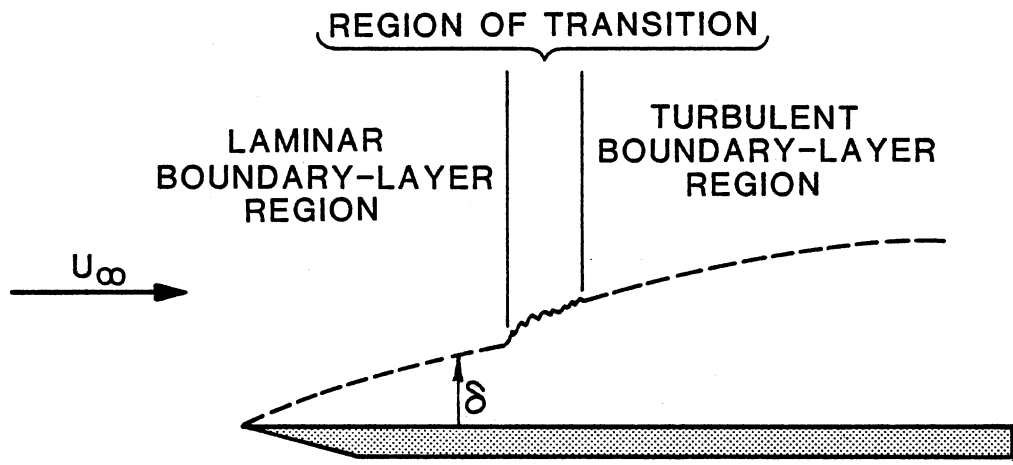


Figure 1. Flat Plate Boundary Layer

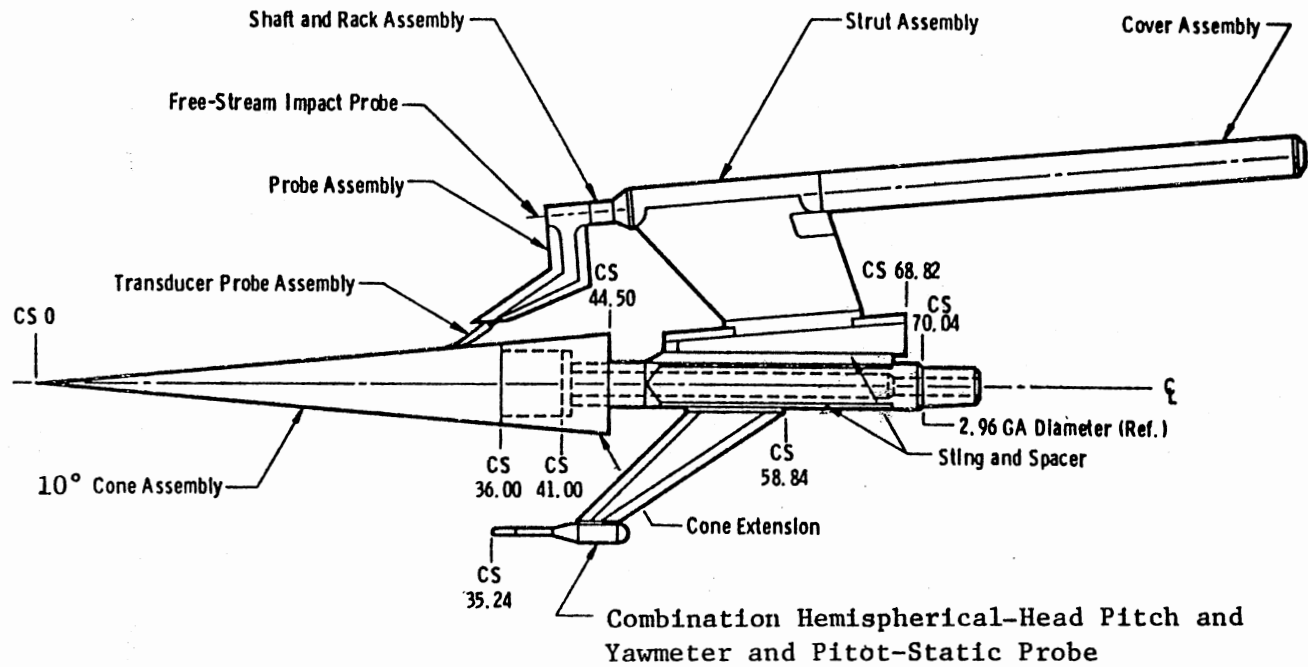
sharp ten-degree cone to the corresponding theoretical values of the skin friction coefficient.

In 1975, tests were conducted at Ames Research Center of the National Aeronautics and Space Administration (NASA) to obtain the distribution of Preston-tube pressures along the surface of a sharp ten-degree cone for different freestream conditions. The Preston-tubes, which were used in these tests, were oval-shaped Pitot tubes. The cone and apparatus were primarily designed to detect boundary layer transition. The subject cone was designed by engineers at Arnold Engineering Development Center (AEDC). For this reason, this cone is referred to as the AEDC Boundary-Layer-Transition Cone. The instrumentation of the AEDC Cone is shown in Figure 2 (2). The NASA Ames 11-ft Transonic Wind Tunnel (TWT), located at Moffett Field, California, was used to carry out these experiments.

A total of 19 cases are used to develop the correlation between Preston-tube measurements and the corresponding values of skin friction coefficient. The run numbers and the corresponding freestream conditions are presented in Table I.

The STAN-5 computer code, which was developed at Stanford University, is used to solve the boundary layer conservation of mass, momentum, and energy equations (3). The Wu and Lock (4) computer code, which calculates the inviscid pressure distribution, is used to specify the boundary conditions along the outer edge of the boundary layer. The Mini-Basic computer code has been developed by the author to obtain all the necessary input information for the STAN-5 computer code. Finally, the Preston-tube pressure measurements are correlated to the corresponding theoretical skin friction coefficient values by means of a least-squares technique.

NOTE: CS = Cone Station = Distance in inches aft of the nose



Source: Dougherty and Fisher (2, p. 7).

Figure 2. AEDC Boundary Layer Transition Cone

TABLE I
 WIND TUNNEL CASES STUDIED TO DEVELOP
 THE CORRELATION EQUATION
 (NASA AMES 11-FT TWT)

Run No.	Case No.	M_∞	$Re_{ft} \times 10^{-6}$	q_∞ psf
29.440	1	0.30	4	230
61.636	2	0.40	3	246
60.635	3	0.50	3	302
25.376	4	0.50	4	404
59.634	5	0.60	3	357
23.346	6	0.60	4	477
40.547	7	0.60	5	586
58.633	8	0.70	3	408
70.726	9	0.70	4	538
21.318	10	0.70	4	548
41.548	11	0.70	5	680
57.632	12	0.80	3	453
72.748	13	0.80	4	605
19.289	14	0.80	4	617
42.549	15	0.80	5	761
56.631	16	0.90	3	492
43.550	17	0.90	5	842
15.231	18	0.95	4	693
44.551	19	0.95	5	873

CHAPTER II

BASIC TOOLS USED TO CARRY OUT THE TURBULENT BOUNDARY LAYER CALCULATIONS

Allen's Correlation

Allen's (5) correlation is the primary tool that is used to start the turbulent-boundary-layer calculations. Allen developed a set of Preston-tube calibration equations which relate measurements of Preston-tube pressure to measured values of turbulent skin friction. These equations were developed for compressible turbulent boundary layers on flat plates in supersonic flows. The test data were obtained for adiabatic wall conditions. The resulting empirical Preston-tube calibration equations were developed by Allen in 1977. The two calibration parameters F_1 and F_2 are defined by the following equations.

$$F_1 = \frac{\rho_w}{\rho_e} \cdot \frac{\mu_e}{\mu_w} \cdot R_D \cdot \frac{U_p}{U_e} \quad (2.1)$$

$$F_2 = \sqrt{\frac{\rho_w}{\rho_e}} \cdot \frac{\mu_e}{\mu_w} \cdot R_D \cdot \sqrt{c_f} \quad (2.2)$$

Allen used a linear least-squares curve fit of the data, and the resulting linear equation was

$$F_1 = 5.85 (F_2)^{1.132} \quad (2.3)$$

The experimental data were compared with the correlated values obtained

from Equation (2.3). The results were unsatisfactory at higher Reynolds numbers. For this reason, Allen tried a second-order least-squares curve fit. The equation for this fit was found to be

$$\log_{10} F_2 = 0.01239 (\log_{10} F_1)^2 + 0.71814 \log_{10} F_1 - 0.4723 \quad (2.4)$$

Again, the experimental data was compared with the values obtained from Equation (2.4). It was concluded that Equation (2.4) fits the data very well at both low Reynolds numbers and high Reynolds numbers. The root mean square (rms) error in scatter of skin friction was five and one half of one percent. A third-order least-squares curve fit was also obtained by Allen; however, no appreciable improvement in accuracy of the fit was observed.

As mentioned before, Equation (2.4) was found to be a better representation of the data when compared to Equation (2.3). For this reason, Equation (2.4) is used for the work presented herein.

There exists other Preston-tube calibration equations. For example, the Fenter-Stalmach (5) calibration equation is

$$F_3 = F_4 (4.06 \log_{10} F_4 + 1.77) \quad (2.5)$$

where

$$F_3 = \frac{\rho_w}{\rho_e} \frac{\mu_e}{\mu_w} \sqrt{\frac{5+M_e^2}{M_e}} \cdot R_D \cdot \sin^{-1} \left[\frac{M_e}{\sqrt{5+M_e^2}} \cdot \frac{U_{pt}}{U_e} \right] \quad (2.6)$$

$$F_4 = \sqrt{\frac{\rho_w}{\rho_e}} \cdot \frac{\mu_e}{\mu_w} \cdot R_D \cdot \sqrt{c_f} \quad (2.7)$$

The problem with the above calibration equation and other similar Preston-tube calibration equations is the fact that the data collapse is not good at higher Reynolds numbers.

Allen's correlation has some advantages compare to the other correlations. For example, Allen's correlation is simple, can be solved for c_f explicitly, and it fits the data over a large range of Reynolds numbers ($3 \times 10^3 < Re_\theta < 8 \times 10^4$).

As mentioned before, Allen's correlation was developed for circular Preston-tubes in supersonic flows with zero pressure gradient. However, this research focuses on subsonic flows about cones with favorable pressure gradients. Therefore, one might expect some errors when Allen's correlation is applied to the AEDC Cone data. Allen's correlation is primarily used to evaluate the skin friction coefficient at the starting point of the turbulent boundary layers. Furthermore, it is assumed that any errors at the start of the turbulent boundary calculations are lost as the boundary layer develops downstream.

Musker's Equation

Musker's (6) mean-velocity-profile equation is another primary tool that is used to start the turbulent-boundary-layer calculations. Musker's equation is used to estimate the velocity profile and the boundary layer thickness at the initial station which are required input to the STAN-5 computer code in order to start a calculation of the turbulent boundary layer.

Musker developed the mean-velocity-profile equation in 1979. This equation has the following form.

$$\frac{u}{U_\tau} = \frac{1}{\kappa} \log_e \frac{yU_\tau}{\nu} + B + \frac{\Pi}{\kappa} \left\{ 6 \left(\frac{y}{\delta}\right)^2 - 4 \left(\frac{y}{\delta}\right)^3 \right\} + \frac{1}{\kappa} \left(\frac{y}{\delta}\right)^2 \left(1 - \frac{y}{\delta}\right) \quad (2.8)$$

The recommended values for κ , B , and Π in the above equation are 0.41, 5.0, and 0.5, respectively. Musker's mean-velocity profile gives the

boundary layer profile formed on a smooth wall and is valid from the wall to the outer edge of the boundary layer. Furthermore, Musker's equation was derived for incompressible flows. The derivation and the detailed analysis of Equation (2.8) is given by Musker (6).

The primary advantage of using Equation (2.8) to estimate the initial velocity profile and the initial turbulent boundary layer thickness is the fact that the boundary conditions are satisfied both at the wall and at the outer edge. Another advantage of Equation (2.8) is its simplicity. Musker's equation expresses mean-velocity, u , as an explicit function y ; therefore, it is easy to apply. However, one has to be careful when using Equation (2.8). Equation (2.8) is derived based on the assumption that the flow is incompressible while the flows considered herein are compressible. Therefore, one should not apply Musker's mean-velocity-profile equation, as it appears in Equation (2.8), to a compressible flow field. However, with proper definition of fluid properties, one is able to apply Equation (2.8) to compressible flow fields. In order to do this, a reference temperature must be introduced. Obviously, the value of this reference temperature is higher than the edge temperature but less than the wall temperature. In other words, the selected reference temperature serves as an "average" value for temperature across the boundary layer. Then, all the fluid properties that appear in Equation (2.8) must be evaluated at this reference temperature. Consequently, fluid properties (e.g., density and viscosity) evaluated at the selected reference temperature serve as the "average" values for the fluid properties across the boundary layer. Thus, when the reference kinematic viscosity is used in Equation (2.8), Musker's mean-velocity-profile equation can be applied to compressible, turbulent boundary layers.

The reference temperature derived by Sommer and Short (1) for compressible turbulent boundary layers has been selected for use herein. This reference temperature is calculated via the following equation.

$$T' = T_e (0.55 + 0.035 M_e^2) + 0.45 T_w \quad (2.9)$$

For the wind-tunnel tests, it is known that wall temperatures are very close to the adiabatic values given by

$$T_{aw} = T_e \left(1 + r \frac{\gamma-1}{2} M_e^2\right) \quad (2.10)$$

As discussed above, Musker's mean-velocity profile is used to estimate the initial turbulent-boundary-layer thickness and the corresponding velocity profile at the initial station. The initial turbulent-boundary-layer thickness is easily estimated by imposing the boundary-layer-edge conditions on Equation (2.8). At the outer edge of the boundary layer, the following boundary conditions apply

$$u = U_e \quad (2.11)$$

and

$$y = \delta \quad (2.12)$$

The following equation is obtained by imposing the outer-edge conditions to Equation (2.8).

$$\delta_i = \left\{ \exp\left(\frac{U_e}{U_\tau} - B - \frac{2\pi}{\kappa}\right) \kappa \right\} \cdot \left\{ \frac{v_e}{U_\tau} \right\} \quad (2.13)$$

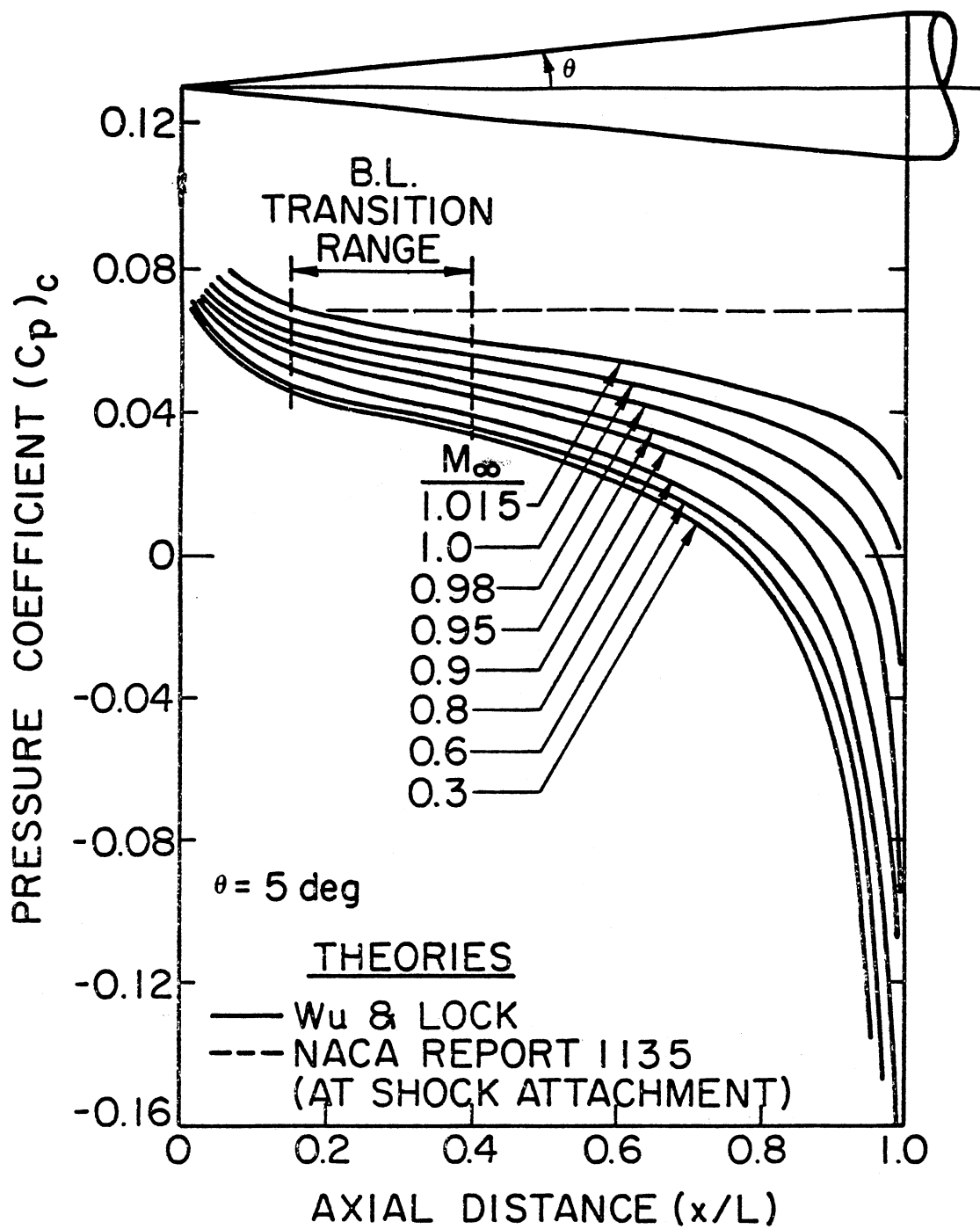
With the known edge velocity and the turbulent-boundary-layer thickness, one can easily use Equation (2.8) to estimate the initial velocity profile of the turbulent boundary layer. This velocity profile is input to the STAN-5 computer code.

Wu and Lock Computer Code

The Wu and Lock (4) computer code is another basic tool that is needed to calculate the turbulent boundary layer. This computer program was developed by Wu and Lock at the University of Tennessee Space Institute.

For a given Mach number, cone semivertex angle, azimuth angle, and angle of attack one can use the Wu and Lock computer code to obtain the inviscid pressure distribution along a ray of a sharp-nose cone. Figure 3 presents the Wu and Lock inviscid pressure distribution for a 10-degree cone at zero angle-of-attack and transonic Mach numbers. Along with the pressure distribution, the Wu and Lock computer printout includes the inviscid velocity distribution along the surface of the cone. For a detailed analysis of the development of the Wu and Lock computer code one should refer to Wu and Lock (4).

The rest of this section includes a brief discussion of how the Wu and Lock computer program is used to obtain the inviscid boundary conditions along the surface of the cone. The match point is defined to be the estimated location of the initial station at which a fully-developed turbulent boundary layer begins. For reasons that will become apparent in the next chapter, the inviscid boundary conditions ahead of the tip of the physical cone must be obtained. For this reason, the velocity distribution upstream of the match point is obtained by a simple linear extrapolation of the Wu and Lock velocity distribution upstream of the match point. Unfortunately, the Wu and Lock computer output does not provide the inviscid velocity distribution at evenly spaced locations along the axis of the cone. Whereas, the STAN-5 computer code works better when the inviscid boundary conditions are evenly spaced. From previous Oklahoma



Source: Wu and Lock (4, p. 39).

Figure 3. Inviscid Pressure Distribution About a 10° Cone (Wu & Lock)

University (OSU) work, the inviscid boundary conditions are evenly spaced by means of a simple computer program. This program has been modified by the present author so that it accepts the data directly from the Wu and Lock computer printout. This modified program is used as one of the subroutines in the Mini-Basic computer code. This is done for two reasons. Firstly, it is desirable to obtain the edge velocity directly from the Wu and Lock data. This saves time and eliminates possible errors that may be introduced by obtaining the edge velocity for each single STAN-5 computer run by means of hand calculations. The second reason is that this subroutine uses other information within the Mini-Basic computer code, and the printout is in the desired format that can directly be input to the STAN-5 computer code.

STAN-5 Computer Code

The STAN-5 computer code is the primary boundary-layer calculation tool that is used in this project (3). This computer code is used to solve the boundary layer conservation equations, and it is specifically used to estimate the theoretical, skin friction coefficient. The STAN-5 computer program was developed by Crawford and Kays (3) at Stanford University. This computer code is an extension of work originally done by Patankar and Spalding (7) in 1967. In this section, it is intended to give a brief description of the operation of STAN-5. A detailed analysis of the theory behind the STAN-5 computer code is beyond the scope of this report. For a complete understanding of the STAN-5 computer code, one should consult Patankar and Spalding (7). However, if one is interested only in the basics of how to use the program, he should consult the STAN-5 Manual (3). This manual discusses the theory in

reasonable detail. Furthermore, it gives adequate instructions to properly use this sophisticated computer code. The following discussion, which is a brief description on the operation of the STAN-5 computer code is based on the information given in the STAN-5 Manual.

The conservation equations of a given boundary layer are impossible to solve analytically. For this reason, with the progress of the technology of digital computers, it has become routine to use finite-difference techniques to solve the boundary layer equations. The STAN-5 computer program is such a program and employs difference methods to solve the conservation of mass, momentum, and energy equations. Some of the basic features of STAN-5 computer code are discussed in this part of the report.

The STAN-5 computer code uses the concept of eddy diffusivity for momentum conservation, ϵ_m , in order to solve for the Reynolds shear stress. There are three options for modeling the eddy diffusivity which appears in the conservation of momentum equation. The first option is to use the Prandtl mixing-length model. The second option is to use the constant eddy diffusivity model. The turbulent-kinetic-energy model was selected for use in this project. The STAN-5 Manual suggests that the turbulent-kinetic-energy model for ϵ_m should be used if there are significant amounts of freestream turbulence which is one of the primary sources of inaccuracy in wind-tunnel experiments.

Computation of the flow field near the wall is the last feature of STAN-5 that is discussed here. The STAN-5 computer code uses the Couette flow equations to compute the flow field near the wall region. In order to achieve this, STAN-5 has two options. The first option numerically integrates the Couette flow equations over the region of high velocity

gradient. This option, which is referred to the "Wall Function," saves computation time. The second option, which bypasses the "Wall Function," continues the finite difference equations down to the wall with a progressively finer spacing. Although the STAN-5 Manual suggests bypassing the "Wall Function" only for flows with large pressure gradients, the wall function is bypassed for the present work because this results in a smoother distribution of skin friction.

There are a number of flag parameters that must be input to the STAN-5 computer code. These flag parameters are fully explained in the STAN-5 Manual. Besides these flag parameters, the initial static pressure, the initial velocity profile, and the inviscid boundary conditions along the outer edge of the boundary layer must be input.

The initial static pressure is obtained from the following equation.

$$P_{e,i} = P_{\infty} \left(\frac{1 + 0.2M_{\infty}^2}{1 + 0.2M_{e,i}^2} \right)^{\gamma/\gamma-1} \quad (2.14)$$

However, in order to solve for $P_{e,i}$, one has to know $M_{e,i}$. This Mach number is related to velocity and temperatures by the following equations.

$$U_{e,i} = M_{e,i} \sqrt{\gamma g_c R T_e} \quad (2.15)$$

$$T_e = T_{t,\infty} (1 + 0.2 M_{e,i}^2)^{-1} \quad (2.16)$$

$U_{e,i}$ is obtained from the Wu and Lock computer code. With the known value of $T_{t,\infty}$ one can combine Equations (2.15) and (2.16) to solve for $M_{e,i}$. With the known value of $M_{e,i}$, Equation (2.14) is used to solve for $P_{e,i}$. Equation (2.8) is used to specify the mean-velocity-profile

at about 40 points across the boundary layer. Finally, the proper inviscid boundary conditions, which are obtained from the Wu and Lock computer code, are input to the STAN-5 computer code.

CHAPTER III
THE METHOD DEVELOPED TO COMPLETE
THE TURBULENT BOUNDARY
LAYER CALCULATIONS

A unique method has been developed to complete the turbulent-boundary-layer calculations. In this chapter an overall perspective of this method is presented. This chapter discusses the theory behind the method used to execute the turbulent-boundary-layer calculations. The detailed analysis of the governing equations of this method is presented in the next chapter. Furthermore, Appendix A presents the step-by-step procedure used in the turbulent-boundary-layer calculations.

At this point, two sets of information are available. The first set of information is the primary variables of the wind tunnel for a given run. The primary variables for a given run include freestream Mach number, unit Reynolds number, and the freestream dynamic pressure. The second set of information is the Preston-tube pressure distribution along the surface of the cone. Determination of the location of the imaginary point at which the turbulent boundary layer has zero thickness and the location of match point are necessary information that must be obtained first. The imaginary location at which zero thickness occurs is defined to be the virtual origin of the turbulent boundary layer. The variable X_{eq} is defined to be the distance between the match point and virtual origin. This terminology is defined in Figure 4. Note that the location

$$d = (0.5) / \cos 5^\circ \text{ ft}$$

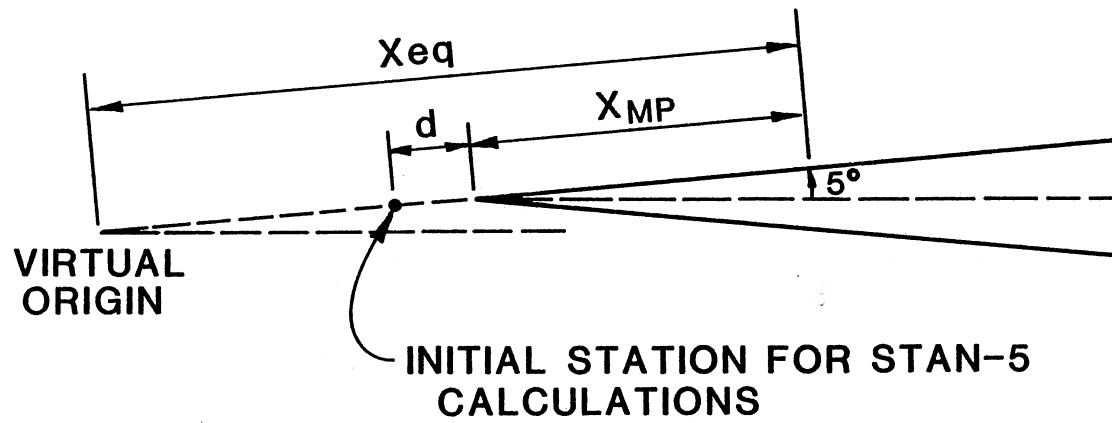


Figure 4. Terminology for Setting Up STAN-5

of the virtual origin may be downstream as well as upstream of the tip of the physical cone. The location at which the maximum Preston-tube pressure occurs could be used as the match point. However, this is not a valid choice because at this location the boundary layer may still be affected by transition. For this reason, the following method is used to assure that the match point is in the fully-developed turbulent-boundary-layer region. Figure 5 shows the Preston-tube pressure distribution along the surface of the cone for a typical case. The point at which the Preston-tube pressure distribution curve corresponding to the turbulent boundary layer diverges from that of the rest of the boundary layer is defined to be the match point. A French curve may be used to do this task. This is indicated by dashed lines in Figure 5. In order to locate the virtual origin, Allen's correlation is used to obtain an estimation of skin friction coefficient at the match point. Note that this is just an estimation. Then, the flat plate equations are used to estimate the location of the virtual origin on a flat plate. This result is then transformed by using Tetervin's (8) transformation to obtain the corresponding location of the virtual origin on the ten-degree cone.

The next step is to set up STAN-5 and start the boundary layer calculations. As was mentioned before, the Wu and Lock computer code and Musker's mean-velocity profile are used to define the inviscid boundary conditions and the initial velocity profile, respectively. In order to save computer time, STAN-5 is run with the initial station located no more than six inches ahead of the physical cone. This is an axial distance. If the location of the virtual origin is such that

$$(X_{eq} - X_{MP} - 0.5/\cos 5^{\circ}) < 0 \text{ ft} \quad ,$$

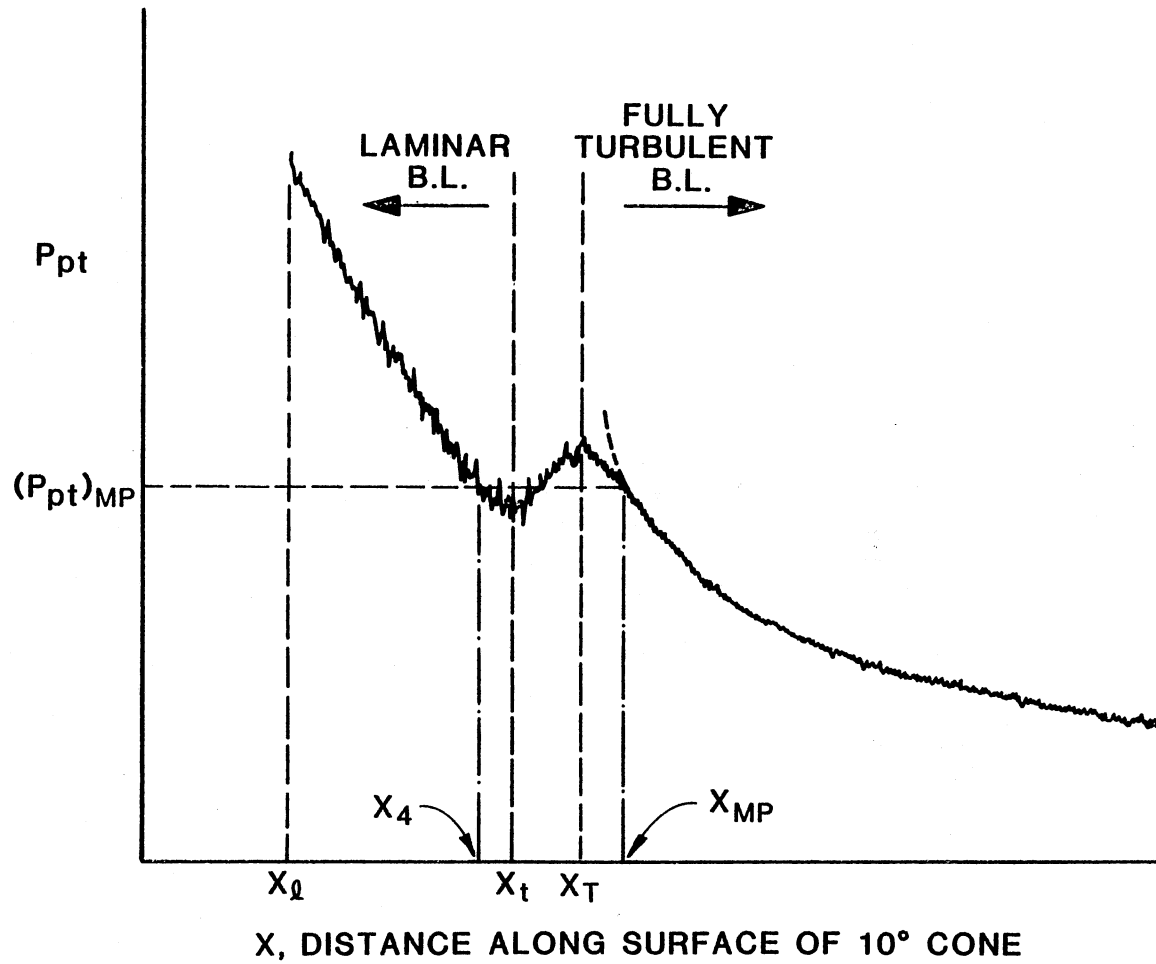


Figure 5. Determination of the Location of the Match Point and the Corresponding Preston-Tube Pressure

then the initial station for beginning computations of the boundary layer is located at one inch downstream of the virtual origin. In this case surface distance is used. It should be mentioned that there are no well-defined criteria for choosing the initial station at which the turbulent-boundary-layer calculations begin. The distances of six inches upstream of tip of the cone or one inch downstream of the virtual origin are based on past experience with STAN-5. Starting STAN-5 very close to the virtual origin uses too much computer time if the location of the virtual origin is located a distance far ahead of the tip of the cone. As the boundary layer develops, any errors at the beginning of the calculations are normally lost as the conservation equations are solved downstream.

The cone is assumed to be an axisymmetric body. The inviscid boundary conditions along the surface of the cone are obtained from the Wu and Lock computer code and are input to STAN-5 by specifying the velocity at a series of points along the surface of the cone and the corresponding radius of the body at those locations. Due to the structure of STAN-5, the virtual origin is the reference point from which distance and radius are measured. From Figure 4, it is apparent that the radial distance is equal to the surface distance times the sine of the cone half-angle. This is the method used to model the cone. However, one could argue this method is not valid due to the fact that the specified radius of a point on the cone corresponds to the radius of the imaginary cone and not to that of the physical cone. Consequently, one could conclude that transverse curvature effects are not modeled correctly. The fact is that transverse curvature effects become important when the radius of the body is of the same order of magnitude as that of the boundary layer thickness.

transverse curvature effects become even more important when the radius of the body is much less than the turbulent-boundary-layer thickness. None of the above cases apply here. In fact, the ratio of the boundary layer thickness to the radius of the body is rather small. Thus, transverse curvature effects are not expected to be a significant source of error in the present work. In order to check this, the cone was modeled using two other methods for a sample run. The sample run was selected as being a worst case. As was mentioned above, the higher the ratio of the turbulent-boundary-layer thickness to the radius of the body the higher is the error in the skin-friction calculations. For this reason, the case that has a high Mach number and low unit Reynolds number was chosen. This corresponds to Run Number 56.631 which was selected to check the significance of any errors introduced by improper modeling of body radius. The first method simply lets the radial distance correspond to the physical cone rather than the imaginary cone. This is possible since the virtual origin is downstream of the tip of the cone for this particular case (see Appendix B, Table XVIII). The second method is to model the cone as a cylinder upstream of the match point, and for the points downstream of the match point let the radial distance correspond to the physical cone. STAN-5 was run twice in order to calculate the skin friction coefficient along the surface of the cone with these two different modeling procedures. The results are tabulated in Table II. The maximum error due to modeling the radius of the cone is about three percent. It should be noted that this is the worst case. In all the other other cases under study, the ratio of the turbulent-boundary-layer thickness to the radius of the body is smaller than that of this sample run. In summary, the method used to model the cone in

TABLE II
 COMPARISON OF SKIN FRICTION COEFFICIENT
 VALUES BY MODELING THE CONE WITH
 THREE DIFFERENT METHODS

Case No. 16: $M_\infty = 0.90$, $Re_{ft} = 3 \times 10^6$

No.	(1)	(2)	(3)	(4)
1 ($\approx X_{MP}$)	1.3183	0.003589	0.003535	0.003534
2	1.4193	0.003450	0.003380	0.003391
3	1.5190	0.003368	0.003284	0.003295
4	1.6169	0.003298	0.003208	0.003216
5	1.7191	0.003238	0.003140	0.003145
6	1.8207	0.003188	0.003090	0.003088
7	1.9628	0.003112	0.003021	0.003020
8	2.0667	0.003080	0.002992	0.002987
9	2.2092	0.003026	0.002943	0.002942
10	2.4225	0.002946	0.002876	0.002875

- (1) - Distance along the surface of the cone measured from tip of the cone, ft.
- (2) - Skin friction coefficient obtained by the method used to model the cone to carry out the skin friction calculations for all the cases (radial distance corresponds to the imaginary cone).
- (3) - Skin friction coefficient obtained by letting the radial distance correspond to the physical cone rather than imaginary cone.
- (4) - Skin friction coefficient obtained by modeling the cone as a cylinder upstream of match point, and for the points downstream at match point letting the radial distance correspond to the physical cone.

well within the accuracy of the wind-tunnel data and the numerical techniques being used.

After completing tasks of modeling and obtaining other necessary information that must be input to STAN-5, the turbulent-boundary-layer calculations are initiated. The skin friction coefficient at the match point is calculated by STAN-5 and is compared to the value obtained from Allen's correlation for the same local flow conditions. If the calculated skin-friction coefficient by means of STAN-5 is larger (smaller) than that calculated by means of Allen's correlation, then it is concluded that the turbulent boundary layer at the match point is too thin (thick). So, the virtual origin must be shifted forward (backward) in order to obtain a thicker (thinner) boundary layer. A one-seventh power law is used to relocate the virtual origin.

$$\frac{x_{eq,1}}{x_{eq,2}} = \left(\frac{c_{f,2}}{c_{f,1}} \right)^{1/7} \quad (3.1)$$

This process is continued until the skin friction coefficient calculated by STAN-5 computer code is within plus or minus a half of one percent of that calculated by Allen's correlation. At that point, it is concluded that an acceptable initial velocity profile is obtained. Next the STAN-5 computer code is run to solve the boundary layer equations along the surface of the cone all the way up to the point where the wind-tunnel data ends.

This procedure is repeated for all the cases. Then, for each case, a modified version of STAN-5 is run to obtain the effective height of the probe. The effective height of the probe is the distance from the wall at which the total pressure within the theoretical boundary layer equals the measured Preston-tube pressure. The effective height of the probe,

y_{eff} is nondimensionalized by the following relation.

$$k_{\text{eff}} = \frac{y_{\text{eff}}}{h/2} \quad (3.2)$$

In other words, k_{eff} is a measure of the location of the effective center of the probe.

Obtaining the values of k_{eff} concludes the turbulent-boundary-layer calculations. The values of total Preston-tube pressure, effective center of the probe, skin friction coefficient, location of match point, and the location of the virtual origin is tabulated in Appendix B for 19 different wind-tunnel flow conditions.

CHAPTER IV
DEVELOPMENT OF THE GOVERNING
EQUATIONS

So far, the basic procedures, which were followed during this research project, have been described. In this chapter, additional details of the method described in Chapter III are presented.

For a given case, the first step is to calculate the freestream thermodynamic and kinematic properties of the fluid (air). This is a fairly simple task since the primary wind-tunnel flow parameters are given. These parameters are defined as follows.

$$q_{\infty} = \frac{1}{2} \rho_{\infty} U_{\infty}^2 \quad (4.1)$$

$$M_{\infty} = \frac{U_{\infty}}{a} = U_{\infty} (\gamma R g_c T_{\infty})^{-1/2} \quad (4.2)$$

$$Re_{ft} = \frac{\rho_{\infty} U_{\infty}}{\mu_{\infty}} \quad (4.3)$$

From Equation (4.2) one can solve for U_{∞} and substitute the result into Equation (4.1). The resulting equation is

$$q_{\infty} = (1/2 \gamma M_{\infty}^2) \frac{(RT_{\infty})}{\rho_{\infty}} \quad (4.4)$$

The equation of state for a thermally perfect gas is

$$P = \rho RT \quad (4.5)$$

Substituting Equation (4.5) into Equation (4.4) and solving for freestream static pressure, P_∞ , results in the following relation.

$$P_\infty = \frac{2q_\infty}{\gamma M_\infty^2} \quad (4.6)$$

The freestream total pressure, $P_{t,\infty}$, is obtained from the following isentropic relation.

$$\frac{P_{t,\infty}}{P_\infty} = \left(1 + \frac{\gamma-1}{2} M_\infty^2\right)^{\gamma/\gamma-1} \quad (4.7)$$

Now substitute Equation (4.6) in to Equation (4.7) and solve for the freestream total pressure, $P_{t,\infty}$.

$$P_{t,\infty} = \left(1 + \frac{\gamma-1}{2} M_\infty^2\right)^{\gamma/\gamma-1} \cdot \left(\frac{2q_\infty}{\gamma M_\infty^2}\right) \quad (4.8)$$

In order to obtain the freestream total temperature, multiply Equation (4.2) by Equation (4.3), and divide the resulting equation by Equation (4.1). This results in the following equation.

$$\frac{M_\infty Re_{ft}}{q_\infty} = \frac{U_\infty}{\sqrt{\gamma RT_\infty}} \frac{P_\infty U_\infty}{\mu_\infty} \frac{2}{P_\infty U_\infty^2} = \frac{2}{\mu_\infty (g_c \gamma RT_\infty)^{1/2}} \quad (4.9)$$

The Sutherland's (1) relation for absolute viscosity, μ , is

$$\mu = \frac{(2.27) (T_\infty)^{1.5}}{T_\infty + 198.6} \times 10^{-8} \quad (4.10)$$

When Equation (4.10) is substituted into Equation (4.9) and rearranged, the following equation is obtained.

$$\left(\frac{M_\infty^2}{q_\infty} \cdot Re_{ft} \cdot \frac{2.27 \times 10^{-8}}{2} \cdot \sqrt{\gamma g_c R} \right) T_\infty^2 - T_\infty - 198.6 = 0 \quad (4.11)$$

Equation (4.11) is an explicit equation in T_∞ , and it can easily be solved for the freestream static temperature. The freestream total temperature is obtained finally from the following isentropic equation.

$$T_{t,\infty} = T_\infty \left(1 + \frac{\gamma-1}{2} M_\infty^2 \right) \quad (4.12)$$

The equation of state (Equation 4.5) is used to calculate density of the air. The Sutherland's relation for absolute viscosity, Equation (4.10), is used to calculate absolute viscosity, μ . The kinematic viscosity, ν , is defined as the ratio of absolute viscosity to density.

The second step is to use Allen's correlation to estimate the skin friction coefficient at the match point. In order to solve Allen's Preston-tube calibration equations (2.1 and 2.2), the following parameters must be calculated: (1) edge temperature, (2) edge pressure, (3) edge velocity, (4) reference temperature, (5) velocity based on Preston-tube data, and (6) Reynolds number based on the diameter of a circular Pitot probe.

Before solving for the edge temperature, one has to solve for the edge Mach number. In order to solve for this Mach number, the following procedure should be followed. The pressure coefficient is defined as follows.

$$c_p = \frac{P_e - P_\infty}{\frac{1}{2} \rho_\infty U_\infty^2} = \frac{P_e - P_\infty}{q_\infty} \quad (4.13)$$

By rearranging terms in Equation 4.13, one obtains:

$$\frac{q_{\infty} c_p}{P_{\infty}} + 1 = \frac{P_e}{P_{\infty}} = \frac{P_e}{P_t} \cdot \frac{P_t}{P_{\infty}} \quad (4.14)$$

The following equation is obtained by substituting appropriate isentropic relations for the pressure ratios occurring in Equation (4.14).

$$\frac{q_{\infty} c_p}{P_{\infty}} + 1 = \left(\frac{1 + 0.2 M_{\infty}^2}{1 + 0.2 M_e^2} \right)^{\gamma/\gamma-1} \quad (4.15)$$

By rearranging terms in Equation (4.15), one obtains:

$$M_e = \left[-5 + 5 (1 + 0.2 M_{\infty}^2) \left(1 + \frac{q_{\infty} c_p}{P_{\infty}} \right)^{1-\gamma/\gamma} \right]^{\frac{1}{2}} \quad (4.16)$$

Note that c_p is obtained from the Wu and Lock computer code. With the known edge Mach number, M_e , one can use the following isentropic relation to solve for the edge temperature, T_e .

$$T_e = T_{t,\infty} (1 + 0.2 M_e^2)^{-1} \quad (4.17)$$

With the known values of c_p , P_{∞} , and q_{∞} , Equation (4.13) can be used to calculate the edge pressure. The edge velocity can either be obtained from the Wu and Lock computer code, or it can be calculated by employing an equation similar to Equation (4.2), i.e.,

$$U_e = M_e (\gamma R g_c T_e)^{\frac{1}{2}} \quad (4.18)$$

As discussed before, the Sommer and Short relation for reference temperature, Equation (2.9), is used to calculate the reference temperature, T' .

The velocity based on the Preston-tube data is calculated via the isentropic relations. Starting with Equation (4.2), the following equation can be obtained for U_{pt}/U_e ,

$$\frac{U_{pt}}{U_e} = \frac{M_{pt}}{M_e} \sqrt{\frac{T_{pt}}{T_e}} = \frac{M_{pt}}{M_e} \sqrt{\frac{T_{pt}}{T_{t,pt}}} \sqrt{\frac{T_{t,e}}{T_e}} \sqrt{\frac{T_{t,pt}}{T_{t,e}}} \quad (4.19)$$

$$= \frac{M_{pt}}{M_e} \left(\frac{1 + \frac{\gamma-1}{2} M_e^2}{1 + \frac{\gamma-1}{2} M_{pt}^2} \right)^{\frac{1}{2}},$$

and

$$\frac{P_{pt}}{P_e} = \left(1 + \frac{\gamma-1}{2} M_{pt}^2 \right)^{\gamma/\gamma-1} \quad (4.20)$$

Next, one can use Equation (4.20) to solve for M_{pt} ,

$$M_{pt} = \left\{ \frac{2}{\gamma-1} \left[\left(\frac{P_{pt}}{P_e} \right)^{\gamma-1/\gamma} - 1 \right] \right\}^{\frac{1}{2}} \quad (4.21)$$

In summary, Equation (4.21) is used to calculate M_{pt} and with the known value of M_{pt} , Equation (4.19) is used to obtain U_{pt} .

The Reynolds number based on probe diameter, R_D , is the final piece of information that is needed to solve Allen's calibration equations.

The Reynolds number based on probe diameter, R_D , is defined as

$$R_D = \frac{\rho_e U_e D}{\mu_e} \quad (4.22)$$

The only unknown in the above equation is the diameter of the probe's face. Allen's Preston-tube pressure measurements were carried out by means of circular Preston tubes. In contrast, the measured Preston-tube pressures for this project were obtained by means of oval-shaped Preston tubes. For

this reason, it is necessary to define an "equivalent" probe diameter, D_{eq} , which can be used in place of the diameter which appears in Allen's correlation. Following the suggestion of Patel (9), the diameter of a circular probe is related to the effective height of the probe by

$$D = \frac{2y_{eff}}{k_{eff}} \quad (4.23)$$

Patel suggests a value of 1.3 for k_{eff} for a circular Preston-tube. If one sets $k_{eff} = 1.3$ in Equation (4.23), the following equation is obtained.

$$D = 1.54 y_{eff} \quad (4.24)$$

In the case of non-circular probes y_{eff} is defined as follows.

$$y_{eff} = \left(\frac{h}{2}\right) (k_{eff}) \quad (4.25)$$

In this equation h is the maximum external height of the probe's face. The probe used during the NASA Ames wind-tunnel tests had a height of 0.0097 inches. Substituting Equation (4.25) into Equation (4.24) leads to the definition of an equivalent diameter for the oval-shaped probe used during the NASA Ames tests.

$$D_{eq} = (0.0075) k_{eff} \quad (4.26)$$

In order to obtain a reasonable value for k_{eff} at the start of the turbulent-boundary-layer calculations, the following estimation procedure was used. From the previous work done by Reed and Abu-Mostafa (10), the values of k_{eff} along the surface of the cone for the laminar boundary layer are available. For each case, a straight-line least-squares curve fit was obtained that correlates k_{eff} to distance along the surface of the

cone. Since this fit is only valid in the laminar boundary-layer region, it is not correct to use this fit and blindly apply it to turbulent-boundary-layer calculations. However, the laminar values of k_{eff} can be employed by assuming the locations in the laminar and turbulent boundary layer, which have the same Preston-tube pressure, have approximately the same value of k_{eff} . Thus, the laminar value of k_{eff} , at the location which has the same Preston-tube pressure as measured within the turbulent boundary layer at the match point, is used to estimate an equivalent diameter for use in Allen's correlation. With the known value of D_{eq} , Equation (4.22) is used to calculate R_D .

All the necessary information to solve for skin friction coefficient is then available. Equation (2.1) is used to solve for the calibration parameter F_1 . Next, Allen's correlation Equation (2.4), is used to solve for the calibration parameter F_2 . Finally, the skin friction coefficient is calculated from Equation (2.2).

The third step is to estimate the location of the virtual origin. Unfortunately, the exact location of the virtual origin along the surface of a cone cannot be obtained. However, the flat plate equations may be used to estimate an approximate value of X_{eq} on a flat plate. Then, the flat plate X_{eq} may be converted to the cone X_{eq} . The following equation is used to estimate the flat plate X_{eq} .

$$X_{eqFP} = \left(\frac{g_c \mu'}{0.06 \rho' U_e} \right) \left(\exp \left(\frac{0.455 \rho'}{\rho_e c_f} \right)^{\frac{1}{2}} \right) \quad (4.27)$$

Equation (4.27) is based on an empirical skin friction formula for flat-plate turbulent boundary layers in incompressible flow, viz.,

$$c_f \approx \frac{0.455}{\ln^2 0.06Re_x} \quad (4.28)$$

The following relation between wetted length on a flat-plate and a cone has been suggested by Tetervin (8) in the case of equal skin friction at the two X locations.

$$X_{eq} = (2.268) (X_{eqFP}) \quad (4.29)$$

Once the location of the virtual origin is fixed, the inviscid velocity from the Wu and Lock computer program is extrapolated forward from the match point to obtain the edge velocity at the initial station at which the turbulent-boundary-layer calculations are started with STAN-5. As previously discussed, the remainder of the inviscid boundary conditions are obtained from the Wu and Lock computer code.

The final step is to use Musker's mean-velocity-profile, Equation (2.8), and calculate the initial velocity profile of the turbulent boundary layer. At this point, all the necessary information that must be input to STAN-5 is available.

The procedure discussed above is automated by means of the Mini-Basic computer code. This code is fully documented in Appendix A.

CHAPTER V

ANALYSIS OF DATA AND THE CORRELATION EQUATION

Once the turbulent-boundary-layer calculations are completed, all the necessary information to correlate the Preston-tube pressure to the corresponding theoretical values of skin friction coefficient are available. Based on the work done by Reed and Abu-Mostafa (10), on laminar boundary layers, the following equation is assumed for this correlation:

$$Y^* = A_1(X^*)^2 + B_1(X^*) + C_1(T^*) + D_1 \quad , \quad (5.1)$$

where

$$Y^* = \log_{10} (\tau_w y_{\text{eff}}^2 / \rho_w \nu_w^2) = \log_{10} (U_{\tau} y_{\text{eff}} / \nu_w) \quad , \quad (5.2)$$

$$X^* = \log_{10} (U_{\text{pt}} y_{\text{eff}} / \nu_w)^2 \quad , \quad (5.3)$$

and

$$T^* = \log_{10} (T / T_e) \quad . \quad (5.4)$$

The correlation parameters X^* and Y^* are basically of the same nature as the correlation parameters defined by Allen. From the work done by Reed and Abu-Mostafa, it was found that the effective center of a Pitot probe was a function of U_{τ} , h , M_{∞} , and ν_w . Furthermore, it was learned that accounting for the variation of the effective center of the probe resulted

in less scatter of skin friction coefficient in the laminar boundary layer region. For this reason, unlike Allen, the variation of the effective height of the probe is included in the calibration parameters.

The following method is used to discard the data points that should not be included in the development of a correlation. The values of k_{eff} along the surface of the cone are tabulated in Appendix B for the various wind-tunnel flow conditions. It should be noted that Reed and Abu-Mostafa correlated skin friction coefficient to the corresponding Preston-tube pressure measurements in laminar boundary layers. Their plot of k_{eff} vs. $U_\tau h/\nu_w$ for several cases is shown in Figure 6. This figure corresponds to the laminar boundary layer studies. From this data, it is concluded that the values of k_{eff} should increase as $U_\tau h/\nu_w$ decrease. This means the values of k_{eff} should increase as the surface distance increases. Furthermore, for a given Reynolds number per foot, the values of k_{eff} decrease with increasing Mach number. The distributions of k_{eff} for Run Numbers 57.632 and 29.440 do not exhibit this behavior. Apparently, the k_{eff} 's for these two runs were in error. At the completion of this work, it was found that the Preston-tube pressures for these two runs were read incorrectly. Figure 7 is the corrected laminar k_{eff} distribution. It might be expected that the k_{eff} distribution along the surface of the cone should have the same trend as that of laminar boundary layer studies. However, this is not exactly true. From tabulated results of k_{eff} , it is observed for most of the cases that the values of k_{eff} decrease until they reach a minimum at a location downstream of the match point. Then a continuous increase in k_{eff} is observed. Consequently, it is concluded that the data points preceding the minimum value of k_{eff} should not be included

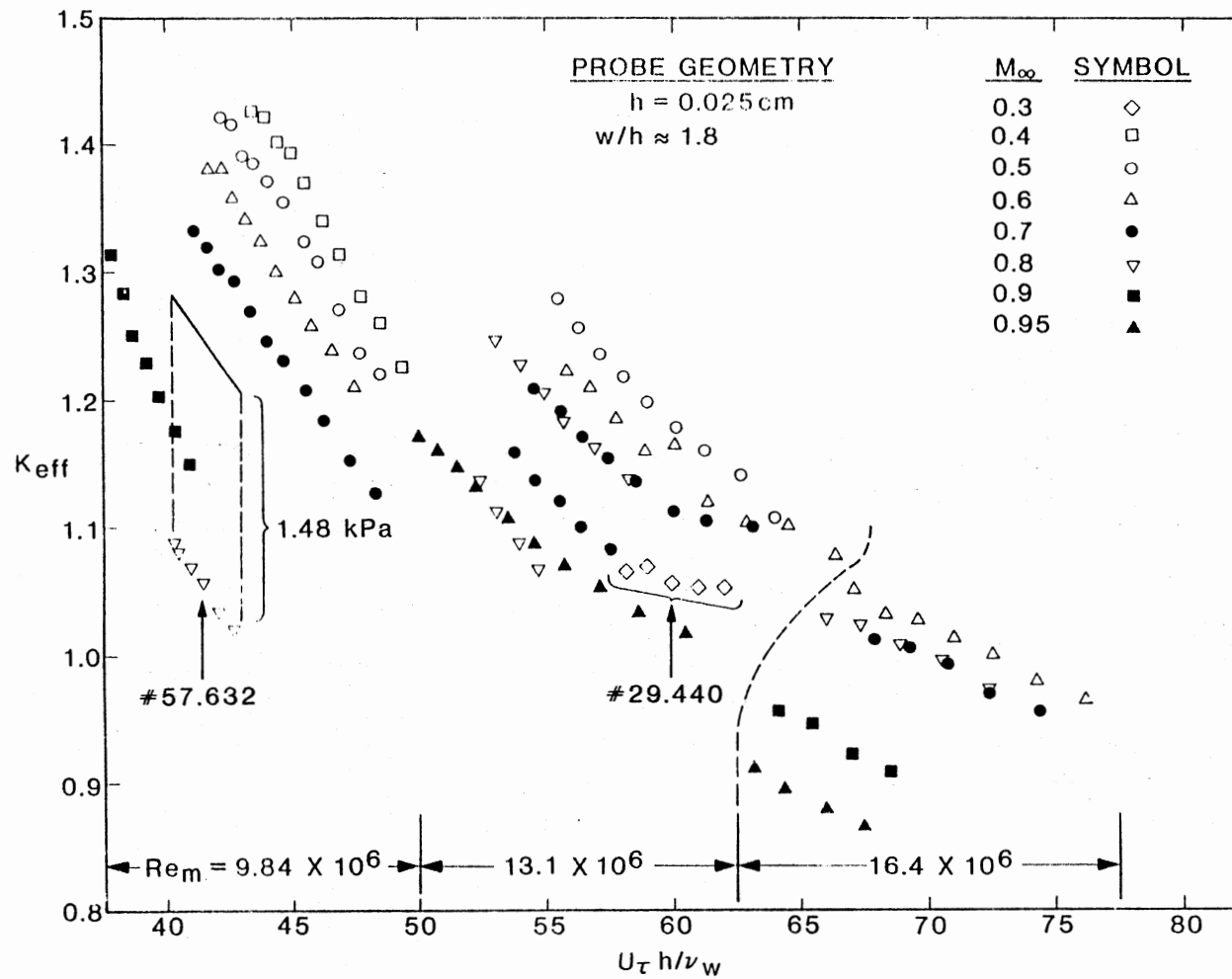


Figure 6. Variation of Effective Height of Probe in Laminar Boundary Layers

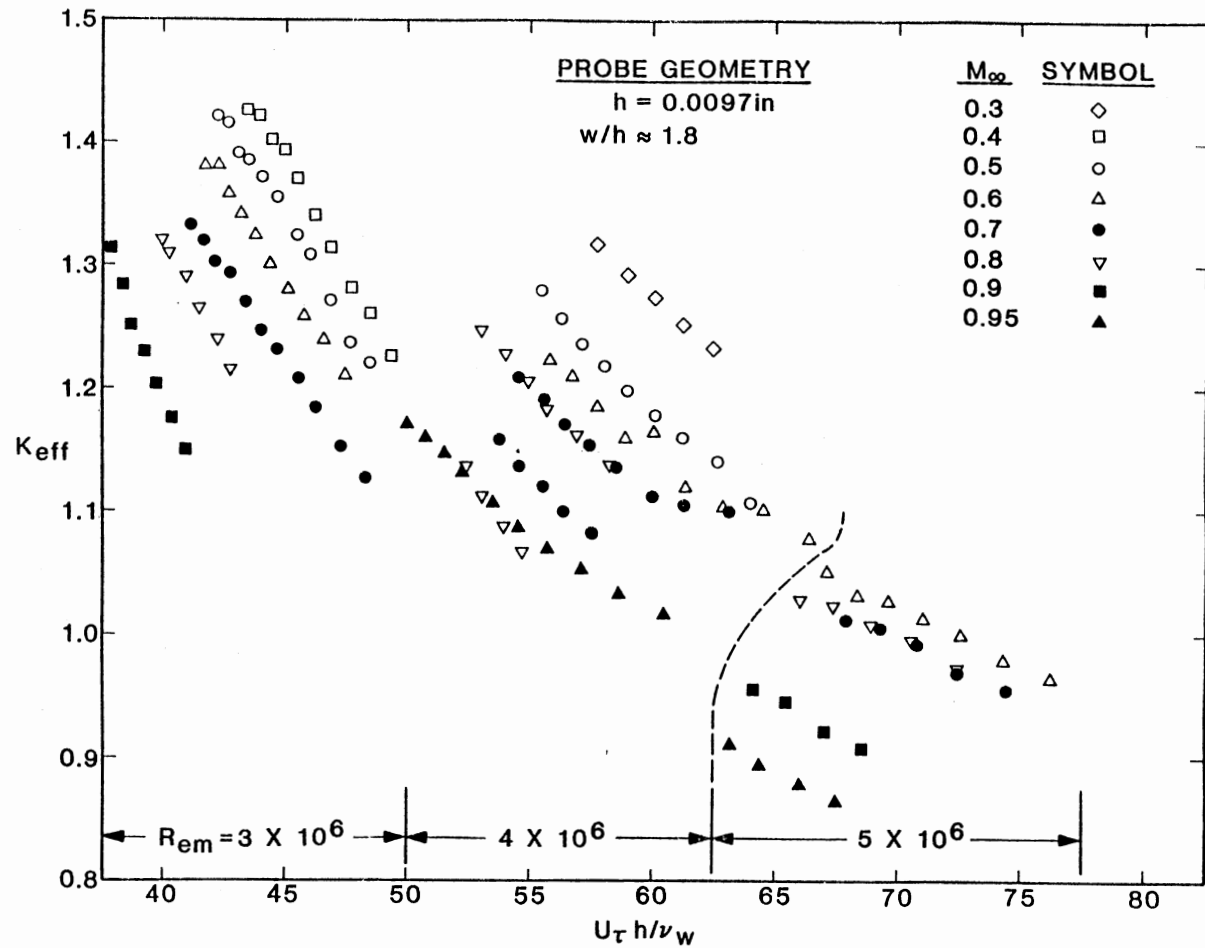


Figure 7. The Corrected Variation of Effective Height of Probe in Laminar Boundary Layers

in the correlation equation. The fact of the matter is that the decrease in k_{eff} downstream of the match point is probably caused by errors in the estimated skin friction coefficient at the match point, i.e., Allen's correlation and the equivalent diameter does not provide the correct skin friction at the match point. However, it is known that the errors in this estimation are lost somewhere downstream of the match point. This is assumed to occur at the location where k_{eff} exhibits a minimum. So, for a given case, all the data points ahead of the minimum value of k_{eff} are discarded. In other words only the data points that show a continuous increase in the values of k_{eff} , following the minimum value of k_{eff} , are set aside for correlation purposes. Figure 8 and Figure 9 illustrate examples of this procedure. Cases that exhibit a behavior similar to Figure 8 are not included in the correlation equation. The cases that exhibit a behavior similar to Figure 9 are used to develop the correlation equation, and only the points that show a continuous increase in the k_{eff} values following the minimum value of k_{eff} are used to obtain the correlation. By employing this method, it is found that Run Numbers 70.726 and 15.231 should also not be used in developing the correlation equation. The distribution of the effective center of the probe vs. $U_t h/v_w$ for 17 cases is shown in Figure 10. As is shown in Figure 10, the distribution of effective center of the probe for Run Number 72.748 is much closer to Run Number 21.318 than it is to Run Number 19.289. Since Run Numbers 72.748 and 19.289 have the same freestream flow conditions (i.e., $M_\infty = 0.8$ and $Re_{ft} = 4 \times 10^6$) except for slight difference in freestream dynamic press, $\Delta q_\infty = 12 \text{ lb}_f/\text{ft}^2$, the distribution of the effective center of the probe for these two cases is expected

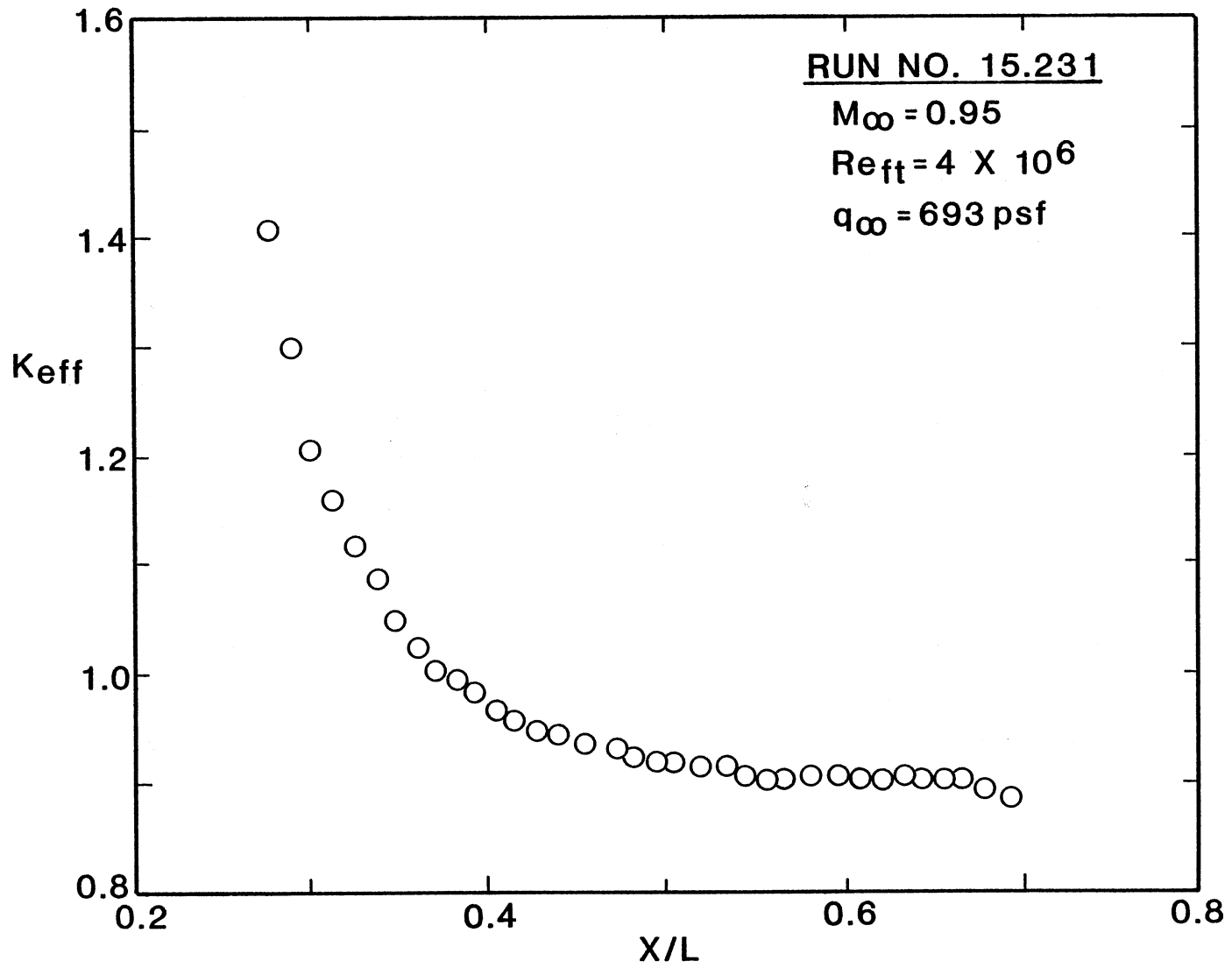


Figure 8. Criterion for Discarding Unsuitable Cases

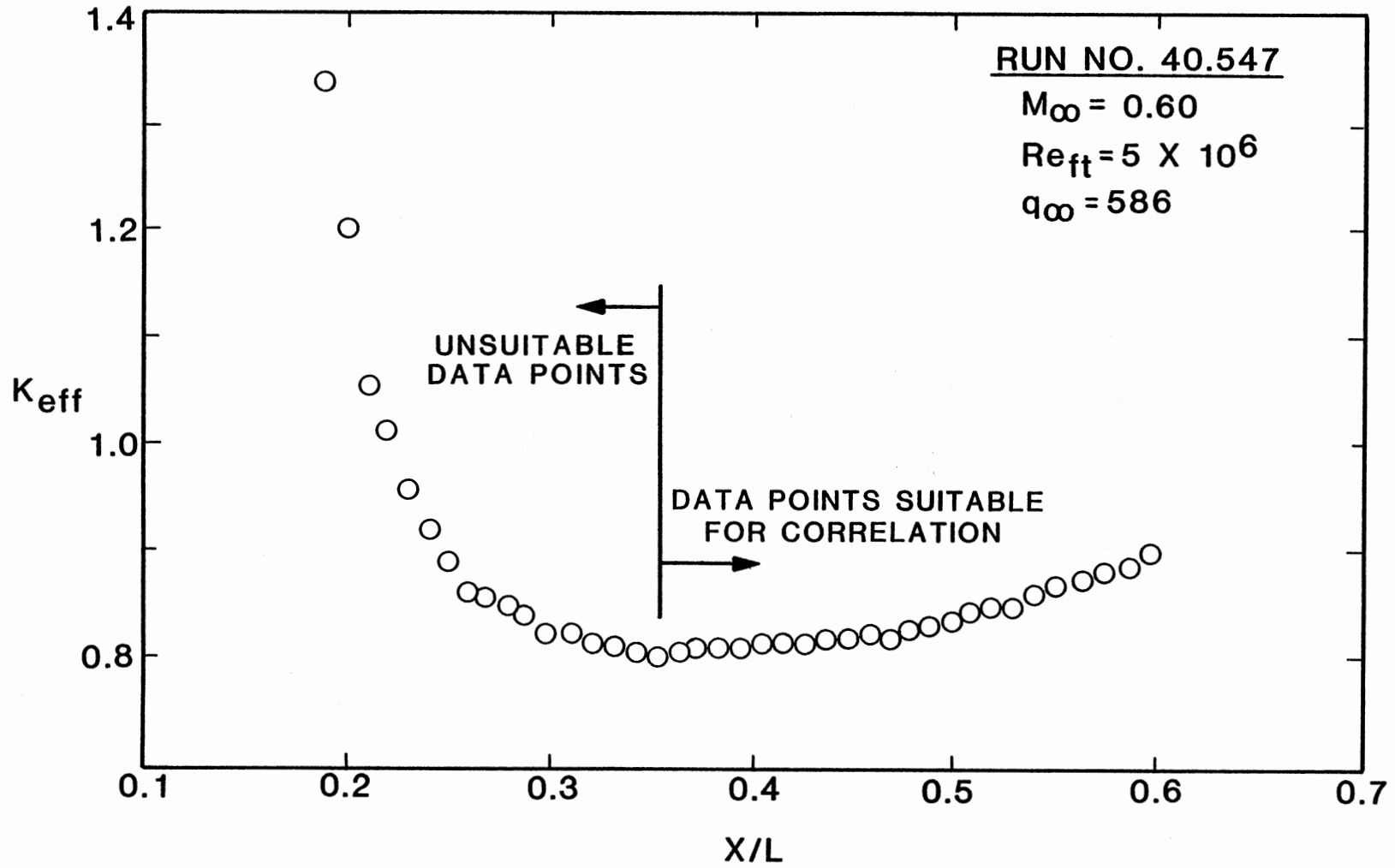


Figure 9. Criterion for Gathering Suitable Data Points

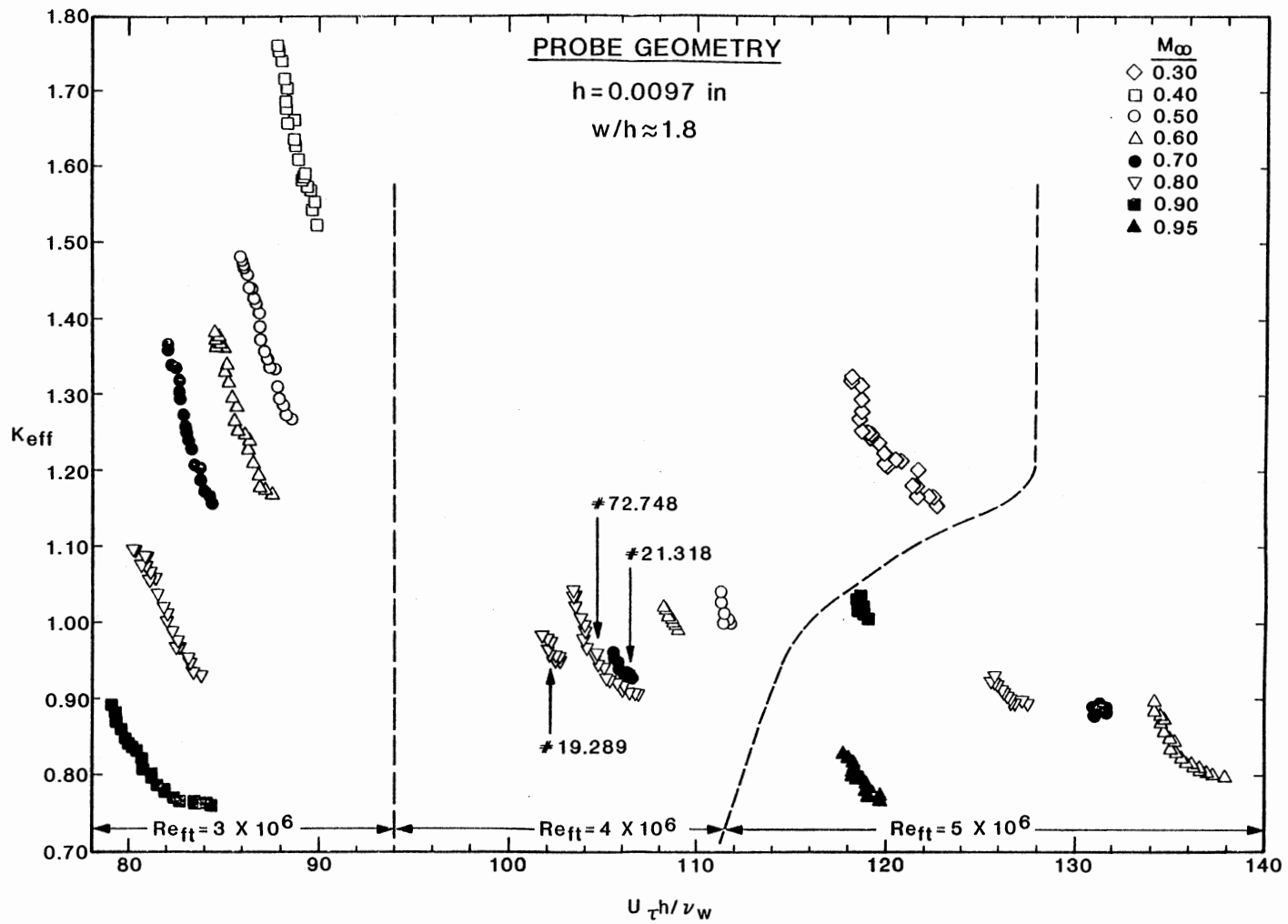


Figure 10. Variation of the Effective Height of Probe in Turbulent Boundary Layers

to be much closer together. Furthermore, by studying Figure 10, it is apparent that the spacing of the distributions of the effective center of the probe among Run Numbers 72.748, 21.318, and 19.289 does not match with the rest of the k_{eff} distributions. However, the spacing of the k_{eff} distributions for Run Numbers 21.318 and 19.289 is similar to the rest of the run numbers. For this reason Run Number 72.748 is not included in the development of the correlation equation. In summary, a total of sixteen cases have been used to develop the correlation equation, and 259 data points have been set aside to obtain the correlation equation. A second-order least-squares curve fit to this data results in the following correlation equation.

$$Y^* = (0.0272) (X^*)^2 + (0.5337) (X^*) + (0.1140) (T^*) - 0.5419 \quad (5.5)$$

Figure 11 is the plot of Y^* vs. Z^* for the individual wind-tunnel data points where Z^* is defined as follows.

$$Z^* = (0.0272)(X^*)^2 + (0.5337)(X^*) + (0.1140)(T^*) \quad (5.6)$$

The corresponding rms value of \bar{c}_f is 1.125 percent. Figure 12 shows the narrow range of scatter in skin friction coefficient. The scatter in skin friction coefficient is very satisfactory, and it is comparable to the Preston-tube calibrations obtained by Patel (9) for incompressible pipe flows. The coefficient of T^* in the correlation Equation (5.5) is very small, and a second correlation equation was obtained by neglecting the effects of variable properties across the probe's face. This equation has the following form.

$$Y^* = (0.0195) (X^*)^2 + (0.6124) (X^*) - 0.7339 \quad (5.7)$$

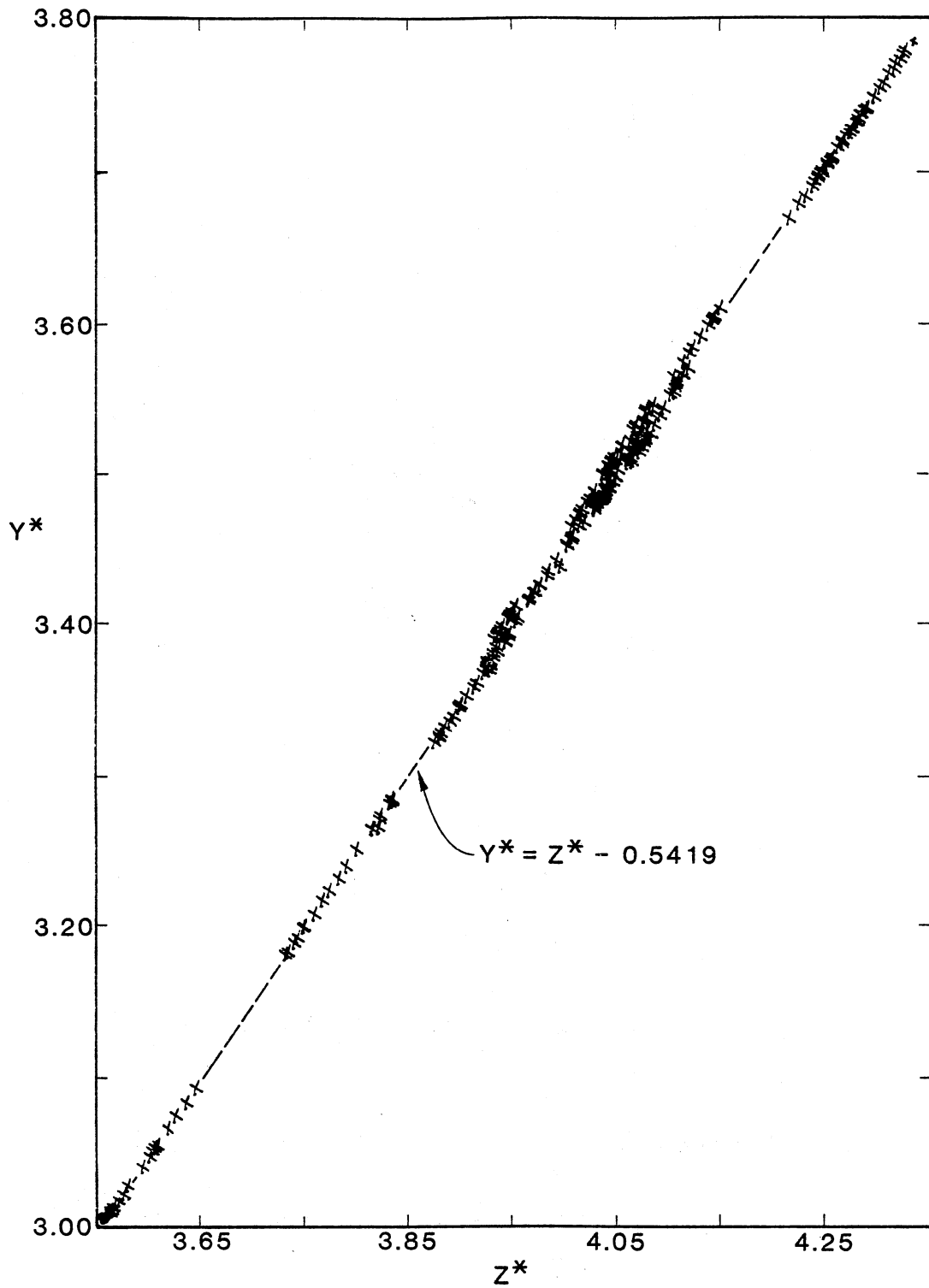


Figure 11. Preston-Tube/Turbulent-Skin-Friction Correlation Based on a Variable Effective Probe Height

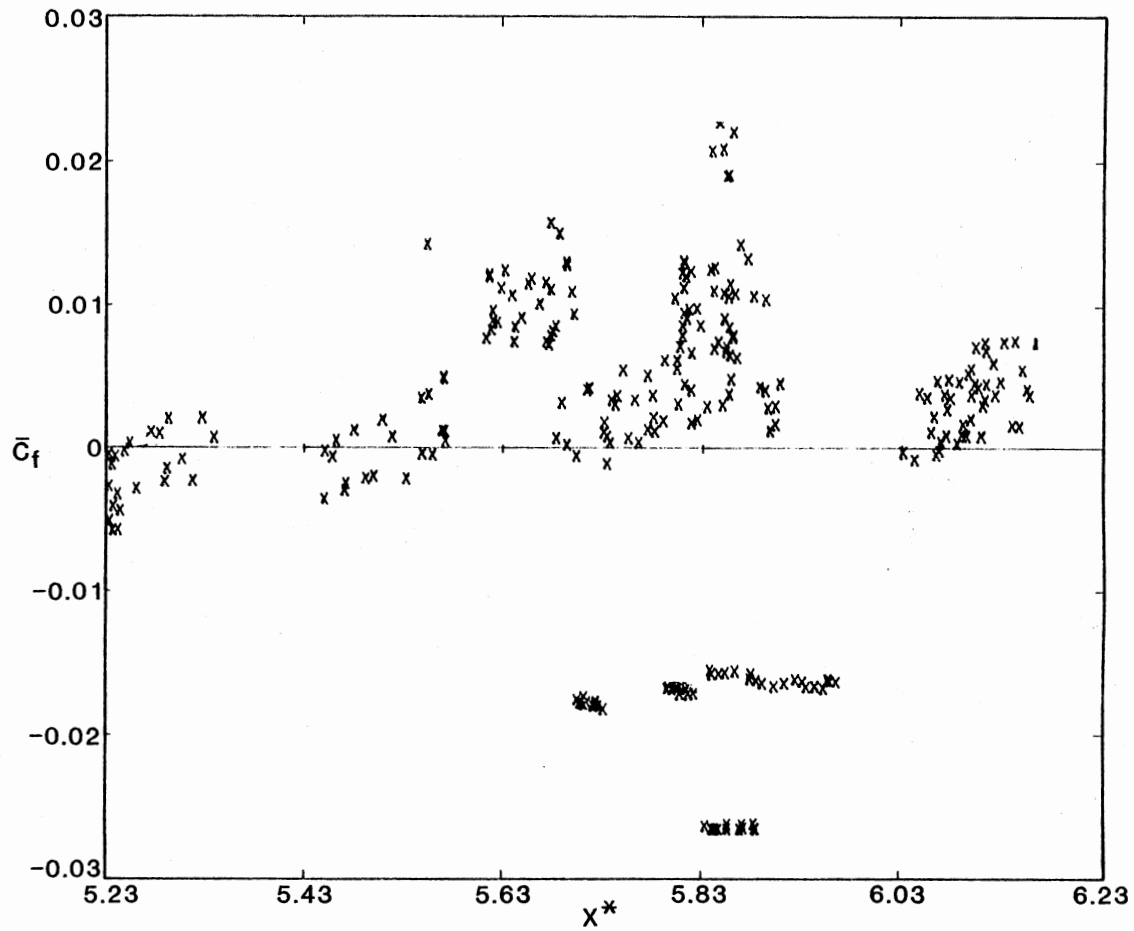


Figure 12. Deviation of Predicted Skin Friction Coefficient by Equation (5.5) from Theoretical Values

The corresponding rms value of \bar{c}_f is 1.175 percent. As expected, slightly higher scatter in the skin friction coefficient is observed when the effect of variations in temperature across the probe's face are ignored.

The boundary layer calculations have been repeated for two sample cases using the new correlation equation to estimate skin friction at the match point. One of these cases is Run Number 15.231 which was not included in the development of the correlation equation. The second typical case is Run Number 40.549 which was included. The skin friction coefficient at the match point is estimated by means of Equation (5.5). Then STAN-5 is set up to again solve the boundary-layer equations. Figure 13 and Figure 14 each show two sets of skin friction coefficients vs. surface distance. One distribution of skin friction coefficient corresponds to the estimation of c_f at the match point by means of the new correlation, and the other set of data corresponds to the estimation of c_f at the match point by means of Allen's correlation. Figure 14 further verifies that the method used to calculate skin friction coefficient is correct. Although in the example Allen's correlation under estimates the value of c_f at the match point, the values of c_f eventually converge as the boundary layer develops. The variation of effective center of the probe vs. surface distance along the cone for the two sample cases is presented in Figure 15 and Figure 16. Figures 17 and 18 show the corresponding k_{eff} values plotted vs. $U_{\tau}h/\nu_w$. Here again one distribution corresponds to the estimation of c_f at the match point by means of the new correlation equation, and the other distribution corresponds to the estimation of c_f at the match point by means of Allen's correlation. Based on these figures, it is concluded that the distribution of k_{eff}

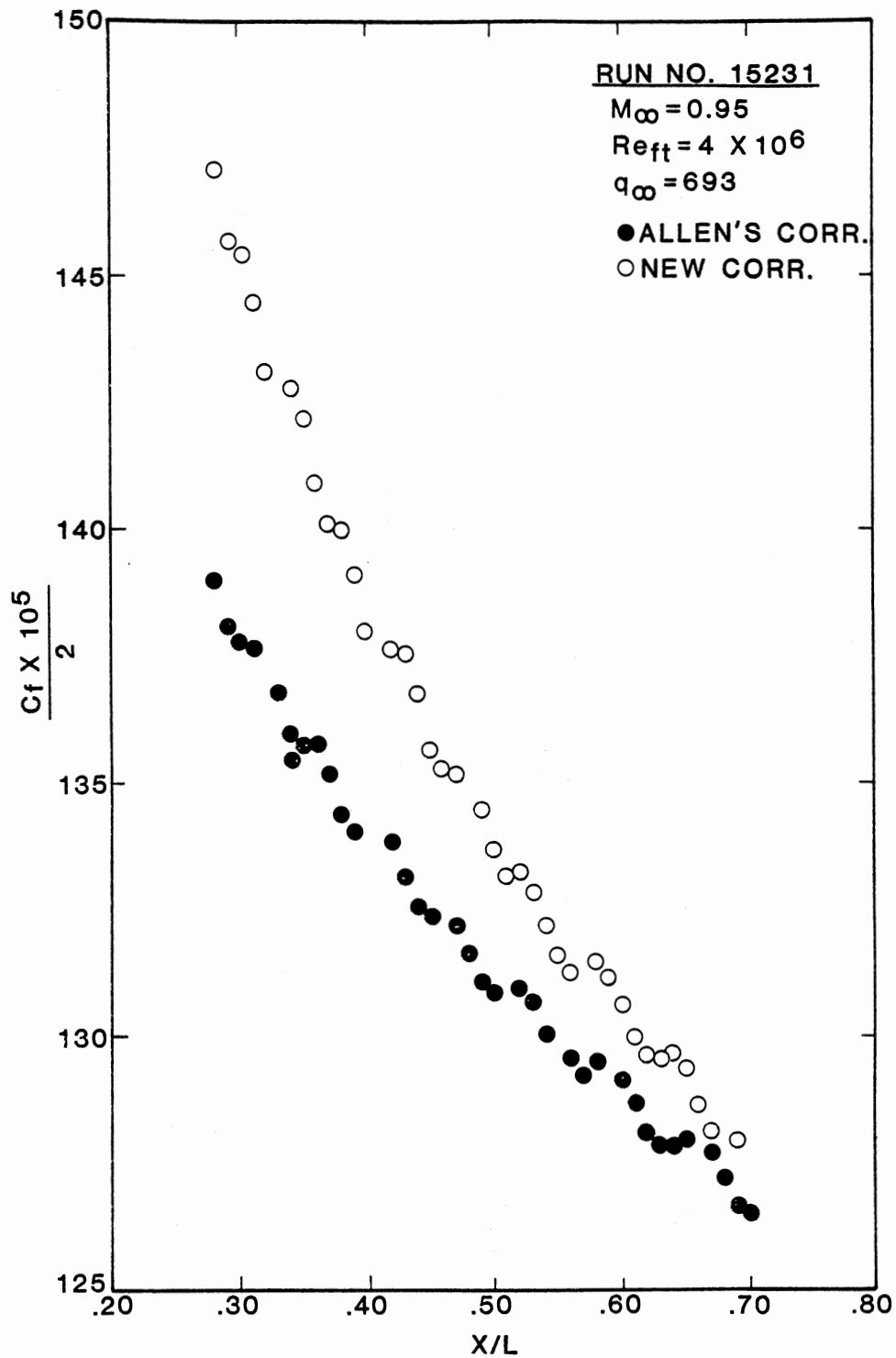


Figure 13. Skin Friction Distribution Along the Surface of the Cone for Run Number 15.231

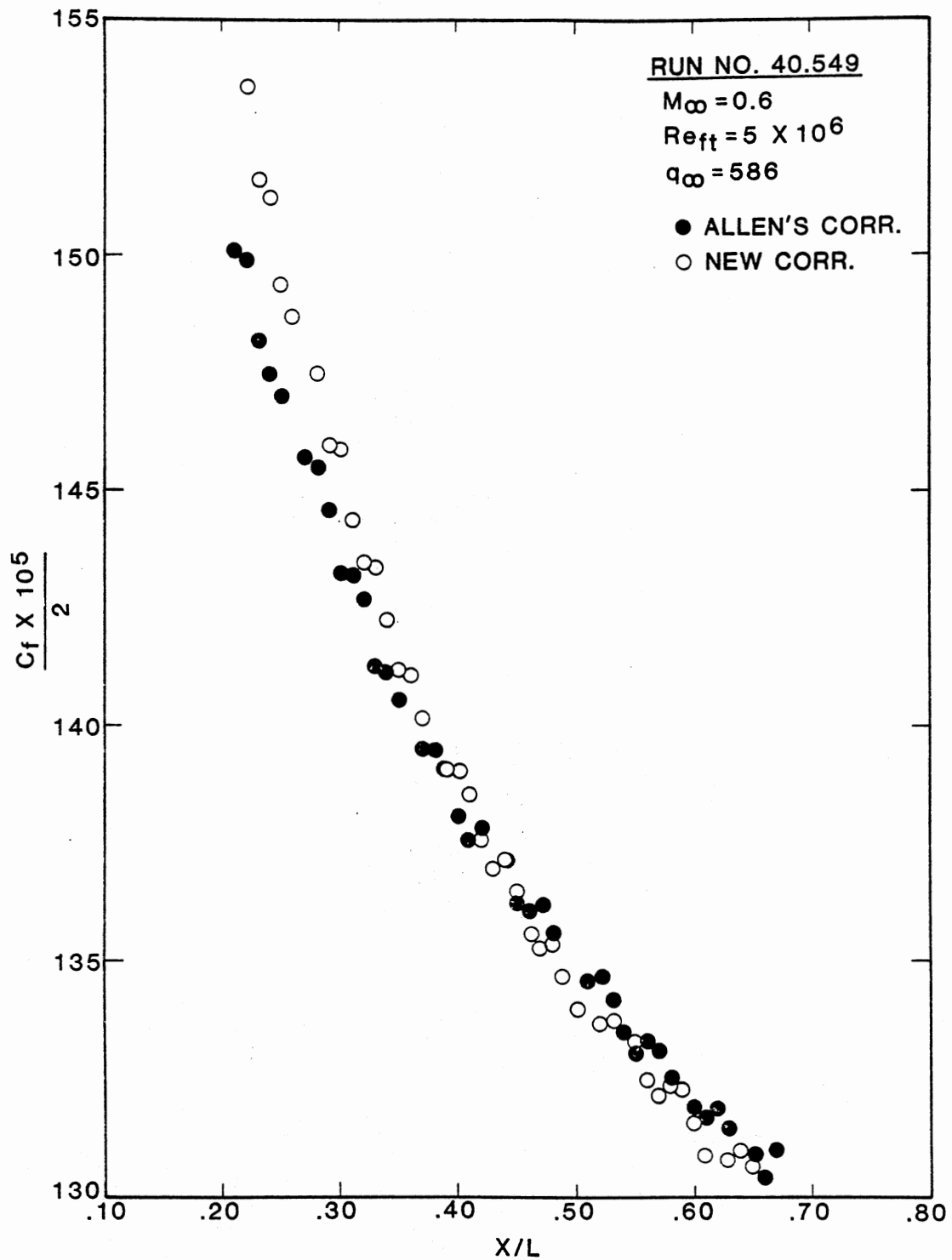


Figure 14. Skin Friction Distribution Along the Surface of the Cone for Run Number 40.549

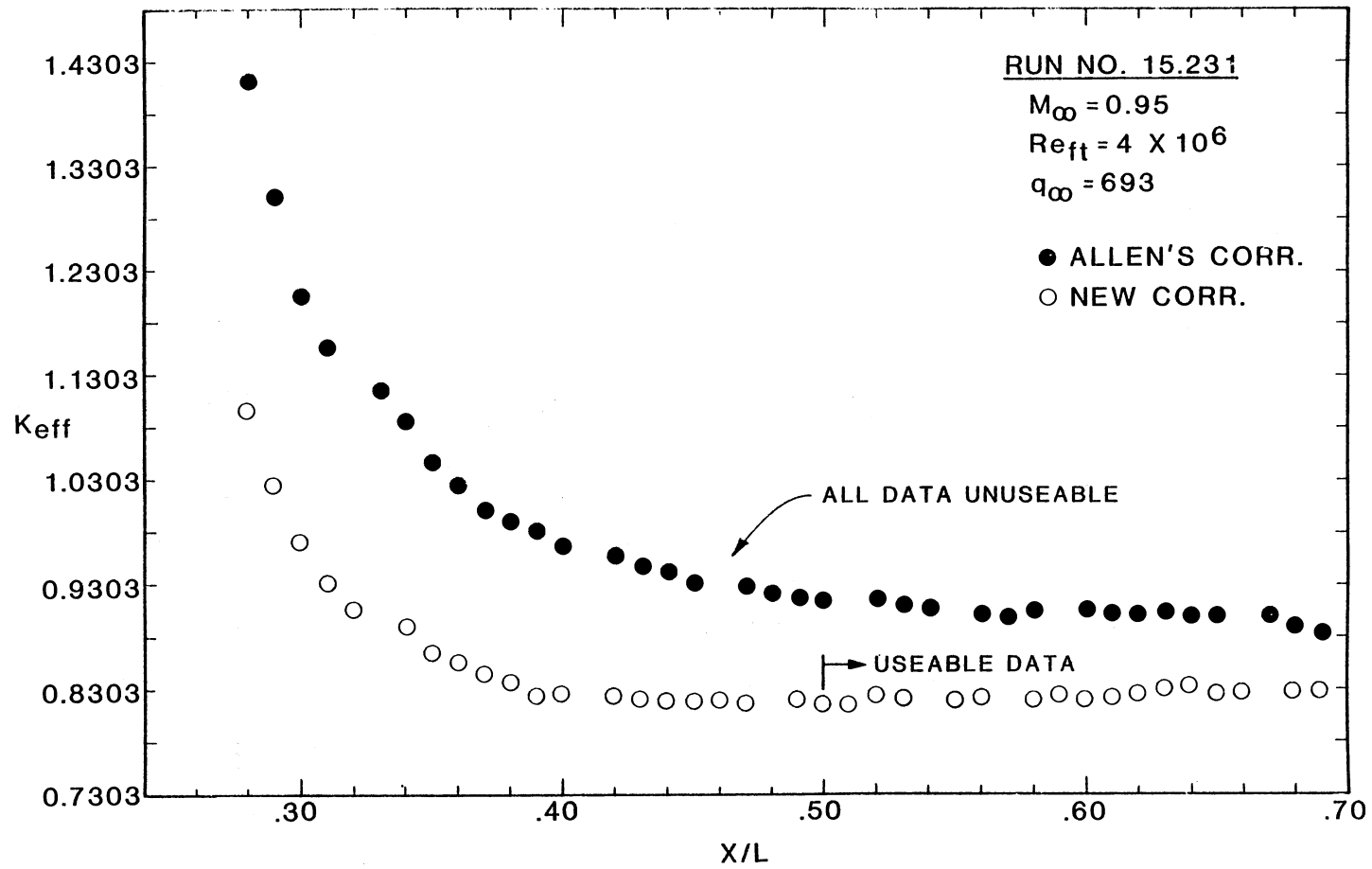


Figure 15. Comparison of k_{eff} Distribution Along the Surface of the Cone Using the New Correlation and Allen's Correlation for Run Number 15,231

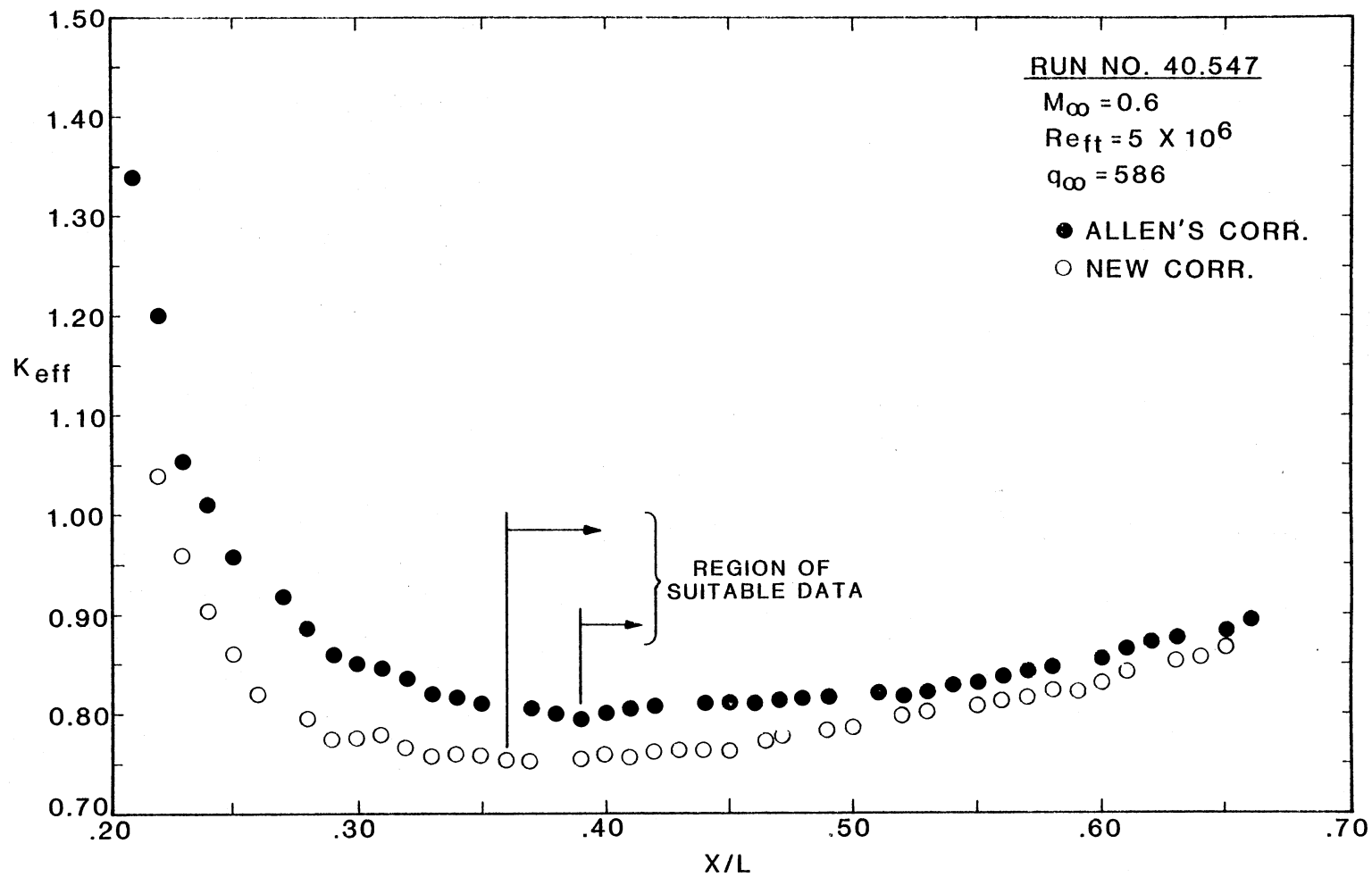


Figure 16. Comparison of k_{eff} Distribution Along the Surface of the Cone Using the New Correlation and Allen's Correlation for Run Number 40.549

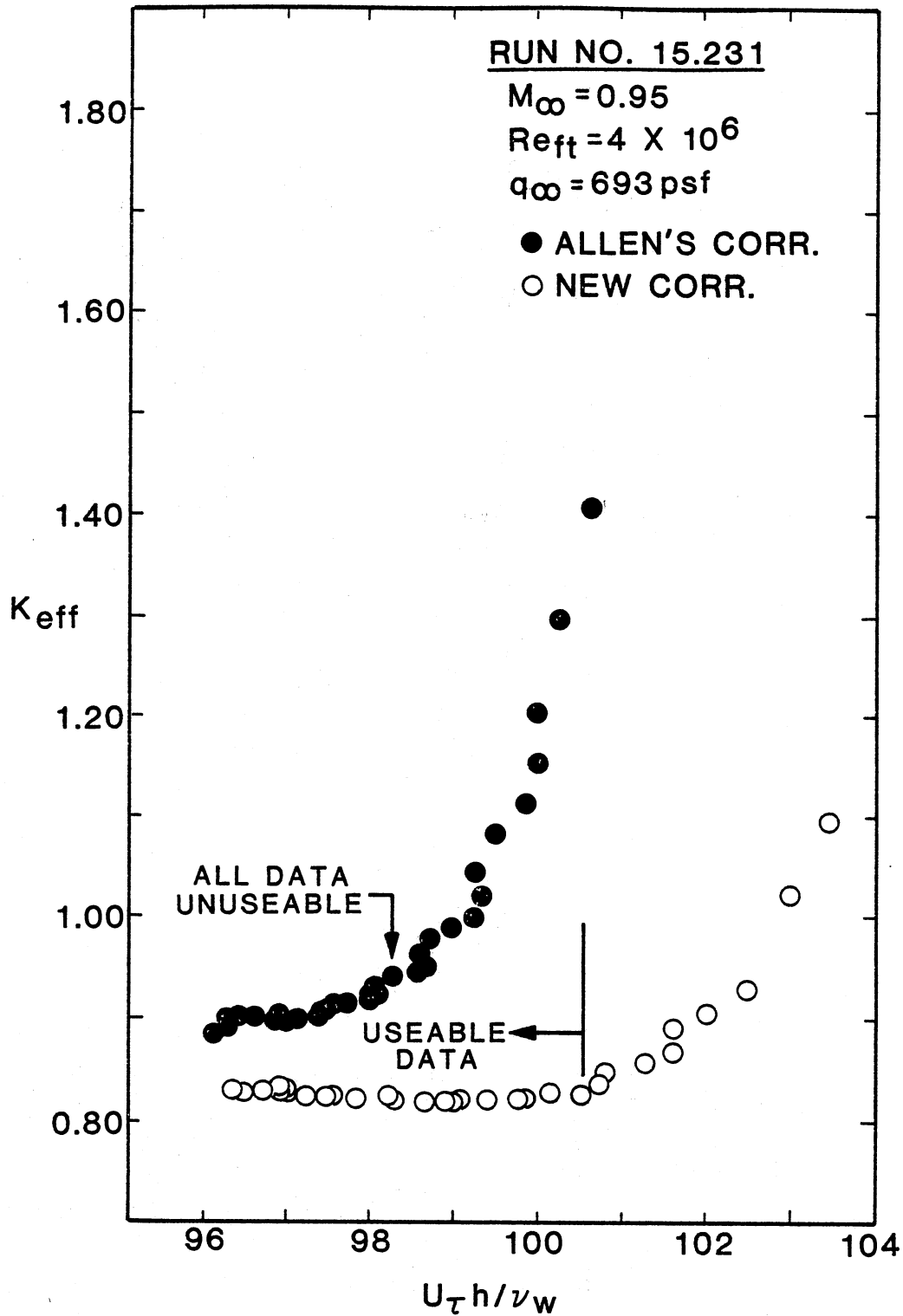


Figure 17. Comparison of k_{eff} Distribution as a Function of $U_\tau h / \nu_w$ Using Allen's Correlation and New Correlation for Run Number 15,231

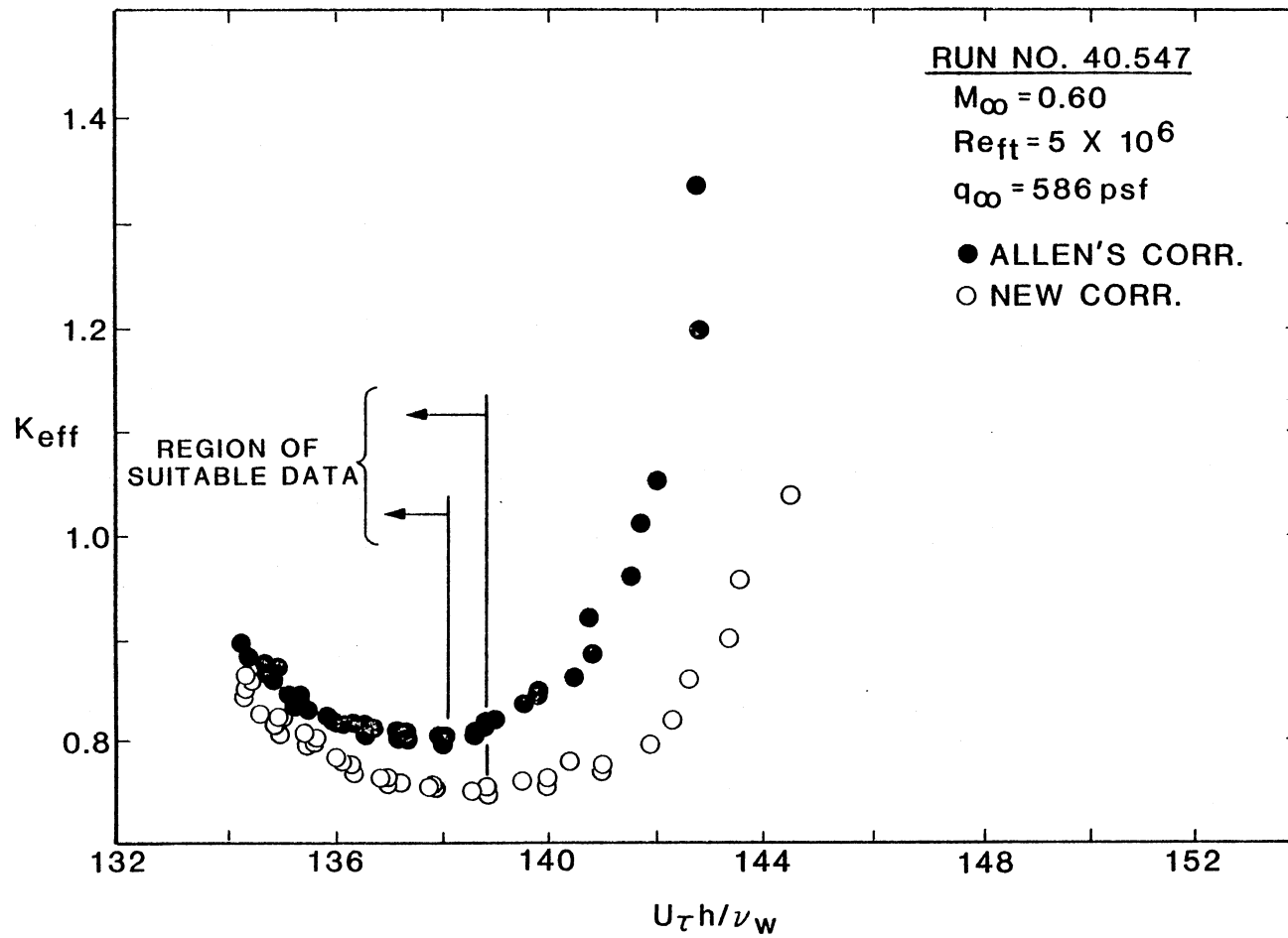


Figure 18. Comparison of k_{eff} Distribution as a Function of $U_{\tau}h/\nu_w$ Using Allen's Correlation and New Correlation for Run Number 40.549

resulting from the author's correlation (Eq. 5.5) exhibits the expected pattern of increasing k_{eff} better than the distribution obtained using Allen's correlation. The following observations are made concerning Figures 15, 16, 17, and 18

1. The minimum value of k_{eff} using correlation Equation (5.5) occurs upstream of that obtained by means of Allen's correlation.
2. The k_{eff} 's seem to approach a common asymptote as the boundary layer develop, independent of the initial values.

It should be noted that Allen's correlation was derived based on simultaneous measurement of skin friction and circular Preston-tube pressures within flat-plate, turbulent boundary layers in supersonic free-streams. The above discussion was primarily done to demonstrate that the new correlation equation is valid in spite of the fact that the initial values of skin friction and k_{eff} are erroneous. Comparison of correlation Equation (5.5) with Allen's correlation shows that one should use this equation to estimate the skin friction coefficient on a ten-degree cone at high subsonic Mach numbers.

In order to estimate skin friction on the AEDC Cone, one should use the following method.

1. Estimate the value of k_{eff} from the appropriate tables of Appendix B for a given location on the surface of the cone.
2. Use Equation (5.3) and solve for X^* .
3. Use either Equation (5.5) or Equation (5.7) and solve for Y^* .
4. Use Equation (5.2) and solve for U_τ . Then skin friction is calculated from the following relation.

$$c_f = U_\tau^2 \frac{\rho_w}{\rho_e} \cdot \frac{2}{U_e^2} \quad (5.8)$$

5. Obtain $U_\tau h/\nu_w$ and use Figure 10 to estimate a new value for k_{eff} .
6. Iterate the procedure until no improvement in the value of k_{eff} is observed.

It should be noted that one may have to interpolate or extrapolate the values of k_{eff} if the exact freestream Mach number and unit Reynolds number is not found in the tables of Appendix B. The user is warned not to use Tables XI, XV, and XX since the corresponding cases were not included in the development of the correlation equations, Equations (5.5) and (5.7).

CHAPTER VI

SUMMARY AND CONCLUSIONS

The distribution of Preston-tube pressures within turbulent boundary layers along the surface of a sharp-nosed, ten-degree cone have been correlated with theoretical value of turbulent skin friction for freestream Mach numbers less than one. The Mini-Basic computer code, the Wu and Lock computer code and the STAN-5 computer code were used to analyze the data and to solve the boundary layer conservation equations.

This is the first Preston-tube/turbulent-skin friction correlation for flow about a cone. The skin friction which results from using Preston-tube pressures in the correlation equation, has a rms error of 1.125 percent. This precision is very satisfactory and is comparable to previous Preston-tube correlations obtained by Patel (9) for pipe flows. A comparison of two sample cases using both Allen's correlation and correlation Equation (5.5) to estimate the skin friction at the match point suggests that this new correlation is sufficiently accurate for engineering uses.

In the course of this study, it was found that the effective center of the probe is not a constant. The distance above the wall of the effective center of the probe is a function of h , U_τ , ν_w and M_∞ . The variation of the effective center of the probe becomes less as $U_\tau h/\nu_w$ increases. The effective center of the probe increases as the surface

distance increases. For a specified unit Reynolds number, the effective center of the probe decreases as the Mach number increases. Furthermore, for a specified unit Reynolds number and Mach number the effective center of the probe increases as $U_{\tau} h / \nu_w$ decreases.

It is also found out that the variation of the fluid (air) properties across the probe's face may be neglected for subsonic flows.

Finally, the possible transverse errors caused by the use of the concept of a virtual origin for the turbulent boundary layer was investigated and found to be negligible.

The developed correlation equation, Equation (5.5), is restricted to turbulent boundary layers on a sharp and smooth ten-degree cone at subsonic freestream Mach numbers. Furthermore, this correlation equation is restricted to Preston-tube measurements carried out at NASA-Ames 11-ft TWT by means of an oval-shaped Pitot-probe whose height and aspect ratio are 0.0097 inches and 1.8, respectively.

The ten-degree cone under study, which is referred to as the AEDC Boundary Layer Transition Cone, was mounted on the nose of a McDonnell-Douglas F-15 aircraft and tested in flight during 1978. The procedure developed herein for analysis of the wind-tunnel tests is expected to be applicable to the flight data. This work is currently being performed by another graduate student. When this correlation becomes available, it will be possible to compare it with the wind-tunnel correlation and thereby define an "effective" unit Reynolds number for the 11-ft Transonic Wind Tunnel at NASA Ames. This new method is needed because the classical definition of a turbulence factor for wind tunnels (e.g., Pope and Harper [11]) is invalid when $M_{\infty} > 0.35$.

A SELECTED BIBLIOGRAPHY

1. Welty, James R., Charles E. Wicks and Robert E. Wilson. Fundamentals of Momentum, Heat, and Mass Transfer. 2nd ed. New York: John Wiley & Sons, Inc., 1976.
2. Dougherty, N. S. Jr. and D. F. Fisher. "Boundary Layer Transition on a 10-Degree Cone: Wind Tunnel/Flight Data Correlation." AIAA Paper No. 80-0154. Pasadena, California, January 14-16, 1980.
3. Crawford, M. E. and W. M. Kays. "STAN-5-A Program for Numerical Computation of Two-Dimensional Internal/External Boundary Layer Flows." Report No. HMT-23, Department of Mechanical Engineering, Stanford University, December, 1975.
4. Wu, T. and R. C. Lock. "A Theory for Subsonic and Transonic Flow Over a Cone - With and Without Small Yaw Angle." Technical Report RD-74-2, U.S. Army Missile Command, December, 1973.
5. Allen, T. M. "Reevaluation of Compressible-Flow Preston Tube Calibrations." NASA TM X-3488, February, 1977.
6. Musker, A. T. "Explicit Expression for the Smooth Wall Velocity Distribution in a Turbulent Boundary Layer." AIAA Journal, Vol. 17, No. 6 (June, 1979), pp. 655-657.
7. Patankar, S. V. and D. B. Spalding. Heat and Mass Transfer in Boundary Layers. 2nd Ed. London: Intertext Books, 1970.
8. Tetervin, N. "A Transformation Between Axisymmetric and Two-Dimensional Turbulent Boundary Layers." AIAA Journal, Vol. 8, No. 5 (May, 1970), pp. 985-987.
9. Patel, V. E. "Calibration of the Preston Tube and Limitations on its use in Pressure Gradients." Jour. Fluid Mechanics, Vol. 23 (1965), pp. 185-205.
10. Reed, T. D. and A. Abu-Mostafa. "Study of Boundary-Layer Transition Using Transonic-Cone Preston-Tube Data." (Unpublished paper presented to the NASA Ames Research Center, Moffett Field, California, 1981.) Stillwater, Oklahoma: Oklahoma State University, Dept. of Mechanical and Aerospace Engineering, 1981.
11. Pope, A. and T. T. Harper. Low-Speed Wind Tunnel Testing. New York: Wiley, 1966.

APPENDIXES

APPENDIX A

THE MINI-BASIC COMPUTER CODE

The Mini-Basic computer code was developed on an AppleTM II Plus Computer. The two primary reasons for developing this computer code were: (1) to become familiar with the basic features of micro-computers, in general, and (2) to reduce the calculation costs. This computer code requires 48 thousand bytes of memory. It is intended to store most of the variables and parameters as the program is calculating the necessary information. This gives the user the advantage of obtaining the values of different variables and parameters directly from the terminal rather than inserting a lot of commands to check the value of a specified variable in the course of calculation. The logic of the computer code is presented by the flow chart shown in Figure 19.

This Appendix is designed to guide the reader through the complete turbulent-boundary-layer calculations. In order to further clarify this matter, Run Number 59.634 is used as an example run. The following is a step by step procedure that should be followed to complete a turbulent-boundary-layer calculation for this sample run.

1. Use Table I and find Case Number 5 corresponds to Run Number 59.634.
2. Use the wind tunnel data sheets and estimate the following.
 - a. The location of the match point, $X_{MP} = 14.69$ in.
 - b. The Preston-tube pressure corresponding to the match point,
 $P_{pt} = 148.26$ lbf/ft.²
 - c. The location in the laminar boundary layer region that has

TMApple II Plus is a trade mark of Apple Computer, Inc.

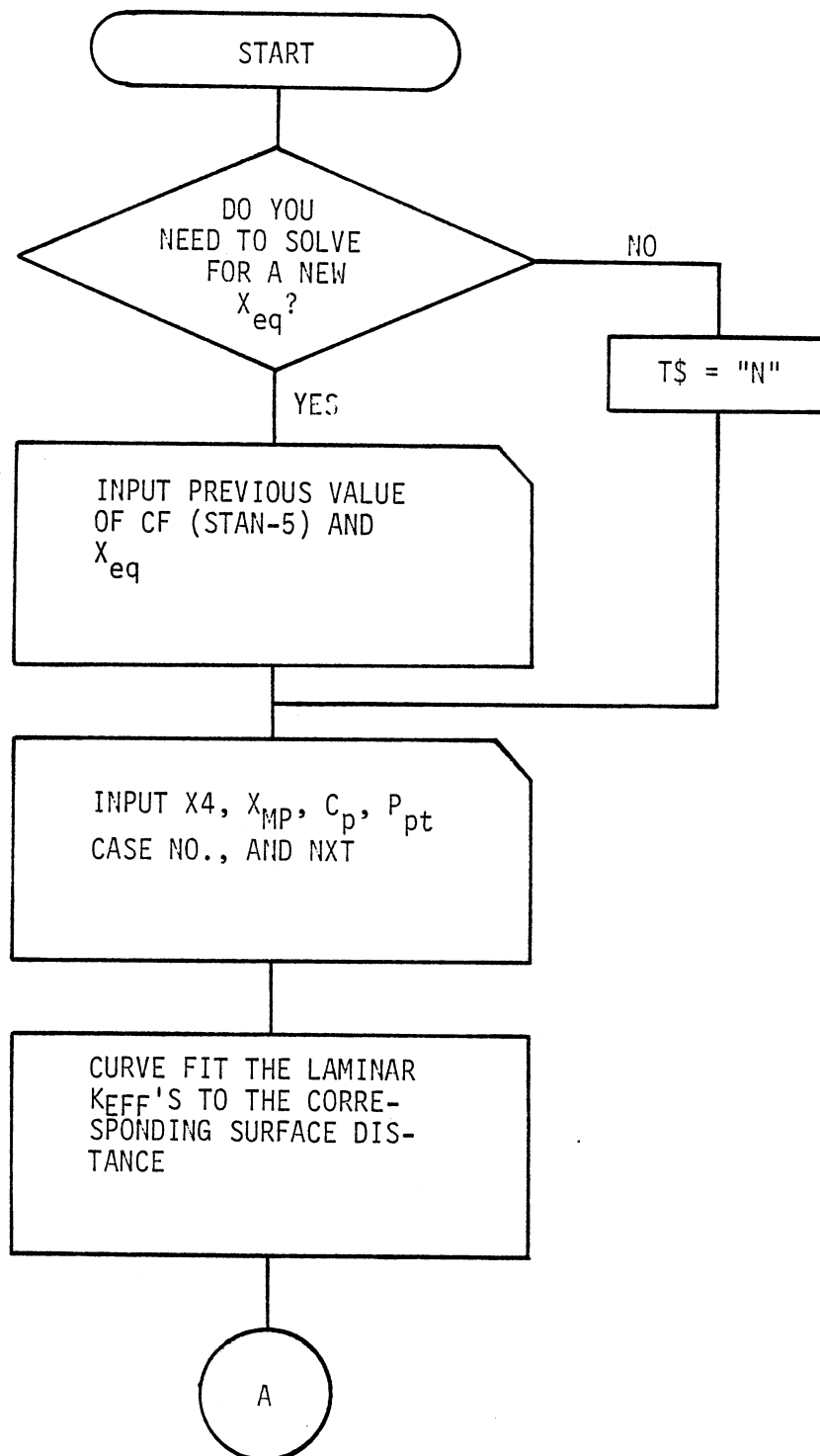


Figure 19. Simplified Flow Chart for the Mini-Basic Computer Code

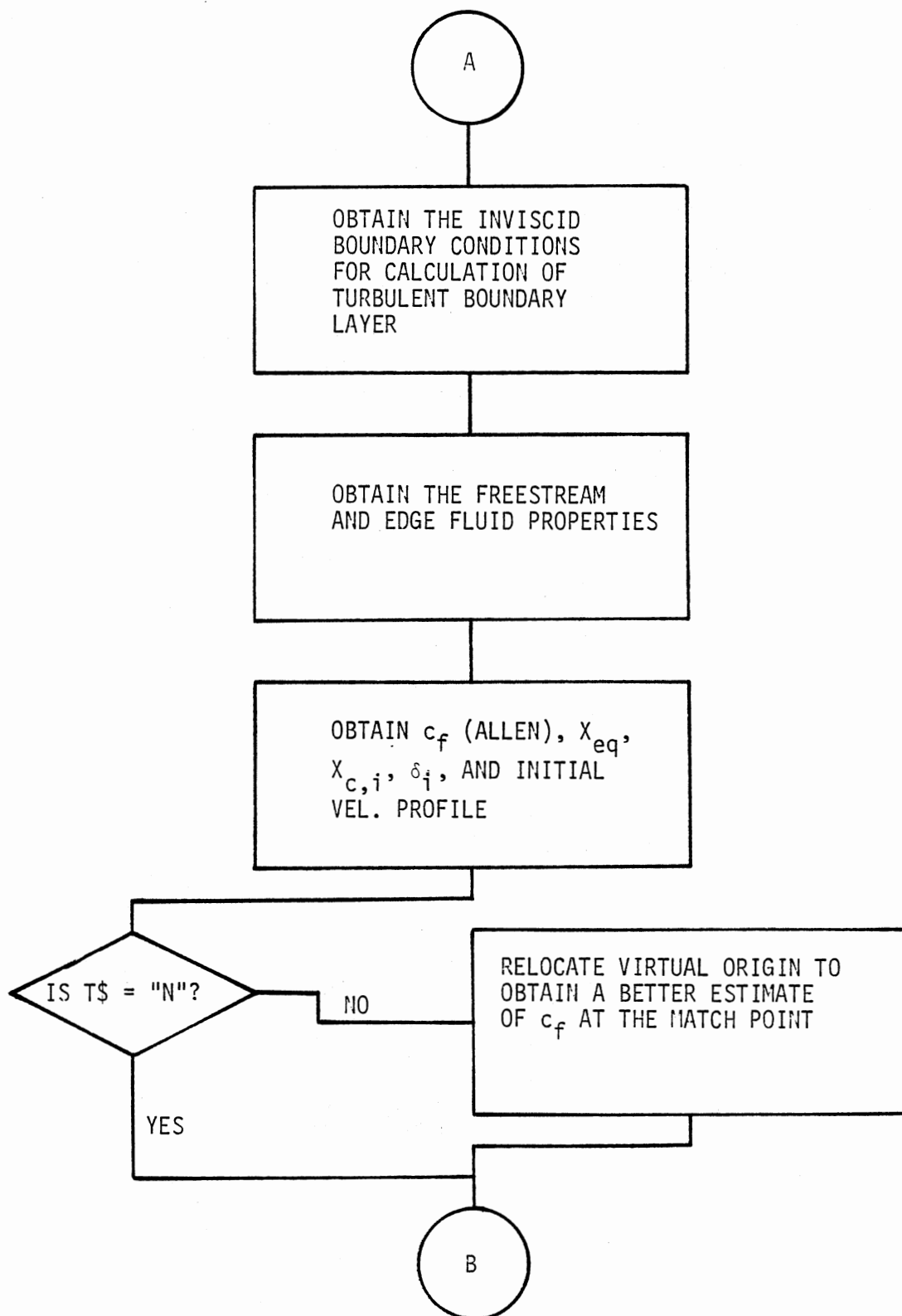


Figure 19. (Continued)

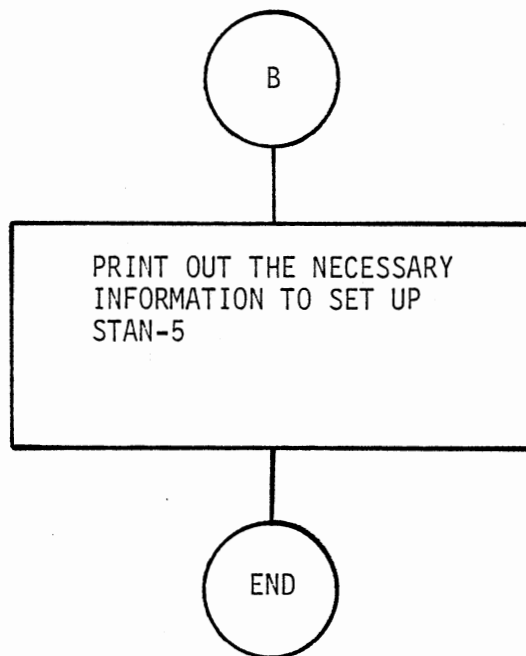


Figure 19. (Continued)

the same Preston-tube pressure as that of the match point,

$$X_4 = 5.25 \text{ in.}$$

- d. The value of X_L . $X_L = X_{MP}$ if $\left| \frac{c_f (\text{Allen}) - c_f (\text{STAN-5})}{c_f (\text{STAN-5})} \right| > 0.01$; otherwise, X_L is equal to the location at which the wind-tunnel data

3. Obtain the Wu and Lock printout and do the following.
 - a. Obtain the pressure coefficient, c_p , at the match point, $c_p = 0.03755$.
 - b. Input the first eighty-two X/L values into the Mini-Basic program as three data statements in line numbers 2570, 2580, and 2590. Then, input the corresponding values of edge velocity as three data statements in line numbers 2640, 2650, and 2660. Be sure not to include the point corresponding to $X/L = 0$.
 - c. Obtain the value of NXT . NXT is the index corresponding to the i th ($1 \leq i \leq 82$) element of X/L values that corresponds to the location of the match point. If the exact location of the match point is not found in the Wu and Lock table of X/L values, then choose the match point such that it coincides with the nearest value of X/L occurring downstream of that found in step 2-a. NXT is equal to 32 for this sample run.
4. Run the Mini-Basic computer code. This program will ask for some or all of the above information depending on the input option. Mini-Basic has four options. The first option is a first-order curve fit of laminar k_{eff} 's to the corresponding X/L values for the nineteen cases under study. The second option

calculates the initial velocity profile, and the third option calculates the inviscid boundary conditions. Finally, the fourth option should be used when the user is ready to make a STAN-5 run. In order to clarify the operation of the Mini-Basic computer code, two sample printouts are included in pp. 66-71. The first run uses option one, and the second printout uses option four.

5. Run STAN-5 computer code and obtain the skin friction at the match point: $c_f = 0.003127$.
6. Re-run the Mini-Basic program, and be sure to let the Mini-Basic code know that a new X_{eq} needs to be calculated. Mini-Basic asks for this information. Again, run STAN-5 and obtain c_f at the match point: $c_f = 0.003340$. If $\left| \frac{c_f(\text{Allen}) - c_f(\text{STAN-5})}{c_f(\text{STAN-5})} \right| < 0.01$, then proceed to step 7; otherwise, go to step 6. For this example, one has to go back to step 6 and obtain the third value of c_f calculated by STAN-5: $c_f = 0.003238$.
7. Re-run the Mini-Basic computer code, and this should be the final run. Set $XL = 32.0$ inches which is at the end of the traverse for this wind-tunnel test. A sample output of the final run of the Mini-Basic computer code for Run Number 59.639 is presented in pp. 72-75. Running STAN-5 for the fourth time should result in a c_f at the match point that is within 0.50 percent of that calculated by Allen's correlation. Running STAN-5 for the fifth time, one obtains: $c_f = 0.003288$, which is about 0.5 percent of that calculated by means of Allen's correlation.
9. Run the modified STAN-5 computer code to obtain the values of k_{eff} along the surface of the cone. The total Preston-tube

XX

HERE IS THE MENU

-
- 1- THE CURVE FIT RESULTS OF THE
LAMINAR KEFF VS. X/L
 - 2- THE INITIAL VELOCITY PROFILE
 - 3- THE INVISCID BOUNDARY CONDITIONS
 - 4- OPTION TWO AND OPTION THREE
-

INPUT YOUR CHOICE NUMBER

I.E. 1,2,3, OR 4 ;1

WOULD YOU LIKE A HARD COPY?

INPUT 'Y' OR 'N' ;Y

 STRAIGHT LINE CURVE FIT OF LAMINAR

KEFF VS. X/L

MINF = .3	REFT E-06 = 4	QINF = 230
	K1 = 0.33949*X/L + (1.0024)	
MINF = .4	REFT E-06 = 3	QINF = 246
	K2 = 2.05428*X/L + (0.94101)	
MINF = .5	REFT E-06 = 3	QINF = 302
	K3 = 1.86152*X/L + (0.96149)	
MINF = .5	REFT E-06 = 4	QINF = 404
	K4 = 1.84934*X/L + (0.90642)	
MINF = .6	REFT E-06 = 3	QINF = 357
	K5 = 1.73699*X/L + (0.97296)	
MINF = .6	REFT E-06 = 4	QINF = 477
	K6 = 1.64683*X/L + (0.92758)	
MINF = .6	REFT E-06 = 5	QINF = 586
	K7 = 1.23162*X/L + (0.84371)	
MINF = .7	REFT E-06 = 3	QINF = 408
	K8 = 1.8469*X/L + (0.91105)	
MINF = .7	REFT E-06 = 4	QINF = 538
	K9 = 1.68853*X/L + (0.8361)	
MINF = .7	REFT E-06 = 4	QINF = 548
	K10 = 1.47198*X/L + (0.9408)	
MINF = .7	REFT E-06 = 5	QINF = 680
	K11 = 1.30436*X/L + (0.8264)	
MINF = .8	REFT E-06 = 3	QINF = 453
	K12 = 1.238*X/L + (0.80214)	
MINF = .8	REFT E-06 = 4	QINF = 605
	K13 = 1.94761*X/L + (0.7616)	
MINF = .8	REFT E-06 = 4	QINF = 617
	K14 = 1.95792*X/L + (0.89866)	
MINF = .8	REFT E-06 = 5	QINF = 761
	K15 = 1.24183*X/L + (0.8531)	
MINF = .9	REFT E-06 = 3	QINF = 492
	K16 = 2.41218*X/L + (0.68914)	
MINF = .9	REFT E-06 = 5	QINF = 842
	K17 = 1.49198*X/L + (0.7427)	
MINF = .95	REFT E-06 = 4	QINF = 693
	K18 = 1.60379*X/L + (0.87261)	
MINF = .95	REFT E-06 = 5	QINF = 873
	K19 = 1.3133*X/L + (0.7202)	

HERE IS THE MENU

-
- 1- THE CURVE FIT RESULTS OF THE
LAMINAR KEFF VS. X/L
 - 2- THE INITIAL VELOCITY PROFILE
 - 3- THE INVISCID BOUNDARY CONDITIONS
 - 4- OPTION TWO AND OPTION THREE
- -----

INPUT YOUR CHOICE NUMBER
I.E. 1,2,3, OR 4 :4

WOULD YOU LIKE A HARD COPY?
INPUT 'Y' OR 'N' :Y

DO YOU NEED TO SOLVE FOR NEW XEQ(CONE)?
I.E. INPUT 'Y' OR 'N' :N

INPUT THE VALUE OF XL IN INCHES :14.69

INPUT THE VALUE OF X4 IN INCHES :5.25

INPUT THE VALUE OF X(MP) IN INCHES :14.69

INPUT THE VALUE OF 'CP' :0.03755

INPUT THE VALUE OF 'PPT' IN 'PSF' :148.26

WHAT IS THE CASE NUMBER :5

USE THE WU&LOCK PRINT OUT
TO INPUT THE VALUE OF 'NXT' :32

 THE INITIAL VELOCITY PROFILE OF THE
 TURBULENT BOUNDARY LAYER

	DIST. FROM WALL FT*10 ⁺⁶		VELOCITY FT/SEC
1	0.000	*	0.000
2	5.689	*	142.838
3	11.434	*	197.913
4	17.237	*	230.319
5	23.098	*	253.455
6	29.017	*	271.519
7	34.996	*	286.382
8	41.034	*	299.042
9	47.133	*	310.094
10	53.293	*	319.922
11	59.514	*	328.790
12	65.798	*	336.885
13	72.145	*	344.345
14	78.555	*	351.275
15	85.029	*	357.757
16	91.567	*	363.856
17	98.172	*	369.624
18	104.842	*	375.104
19	111.579	*	380.332
20	118.383	*	385.338
21	125.255	*	390.147
22	133.502	*	395.628
23	143.398	*	401.843
24	155.274	*	408.853
25	169.524	*	416.724
26	186.625	*	425.525
27	207.146	*	435.336
28	231.771	*	446.255
29	261.320	*	458.402
30	296.780	*	471.925
31	339.332	*	487.009
32	390.394	*	503.861
33	451.669	*	522.687
34	525.198	*	543.614
35	613.434	*	566.532
36	719.316	*	590.768
37	846.375	*	614.463
38	998.846	*	633.394
39	1137.703	*	639.477

 INVISCID BOUNDARY CONDITIONS

	SURFACE DIST. FT	RADIUS FT*100	EDGE VEL. FT/SEC
1	0.0833	0.72	639.476
2	0.1192	1.03	639.600
3	0.1571	1.36	639.730
4	0.1949	1.69	639.860
5	0.2328	2.02	639.990
6	0.2706	2.35	640.120
7	0.3085	2.68	640.250
8	0.3463	3.01	640.380
9	0.3842	3.34	640.510
10	0.4221	3.67	640.640
11	0.4599	4.00	640.770
12	0.4978	4.33	640.900
13	0.5356	4.66	641.030
14	0.5735	4.99	641.160
15	0.6113	5.32	641.290
16	0.6492	5.65	641.420
17	0.6871	5.98	641.550
18	0.7249	6.31	641.680
19	0.7628	6.64	641.810
20	0.8006	6.97	641.940
21	0.8385	7.30	642.070
22	0.8763	7.63	642.200
23	0.9142	7.96	642.330
24	0.9521	8.29	642.460
25	0.9899	8.62	642.590
26	1.0278	8.95	642.720
27	1.0656	9.28	642.850
28	1.1035	9.61	642.980
29	1.1414	9.94	643.110
30	1.1792	10.27	643.240
31	1.2171	10.60	643.370
32	1.2549	10.93	643.500
33	1.2928	11.26	643.630
34	1.3306	11.59	643.760
35	1.3685	11.92	643.890
36	1.4064	12.25	644.020
37	1.4442	12.58	644.150
38	1.4821	12.91	644.360

THE VALUE OF THE 'XEQ' IS = 1.4487 FT

THE VALUE OF X-INITIAL IS = 0.0833 FT

THE VALUE OF CF(ALLEN) = 3.270E-03

INITIAL STATIC PRESSURE INPUT
TO STAN-5 = 1435.22 PSF

HERE IS THE MENU

-
- 1- THE CURVE FIT RESULTS OF THE
LAMINAR KEFF VS. X/L
 - 2- THE INITIAL VELOCITY PROFILE
 - 3- THE INVISCID BOUNDARY CONDITIONS
 - 4- OPTION TWO AND OPTION THREE
-

INPUT YOUR CHOICE NUMBER
I.E. 1,2,3, OR 4 :4

WOULD YOU LIKE A HARD COPY?
INPUT 'Y' OR 'N' :Y

DO YOU NEED TO SOLVE FOR NEW XEQ(CONE)?
I.E. INPUT 'Y' OR 'N' :Y

INPUT THE VALUE OF 'CF' :0.003233

THE VALUE OF 'XEQ' IN 'FT' :1.2272

INPUT THE VALUE OF XL IN INCHES :32.00

INPUT THE VALUE OF X4 IN INCHES :5.25

INPUT THE VALUE OF X(MP) IN INCHES :14.69

INPUT THE VALUE OF 'CP' :0.03755

INPUT THE VALUE OF 'PPT' IN 'PSF' :148.26

WHAT IS THE CASE NUMBER :5

USE THE WU&LOCK PRINT OUT
TO INPUT THE VALUE OF 'NXT' :32

THE INITIAL VELOCITY PROFILE OF THE
TURBULENT BOUNDARY LAYER

	DIST. FROM WALL FT*10 ⁺⁶		VELOCITY FT/SEC
1	0.000	*	0.000
2	6.673	*	151.741
3	13.412	*	205.948
4	20.218	*	237.845
5	27.093	*	260.616
6	34.036	*	278.396
7	41.049	*	293.025
8	48.132	*	305.485
9	55.286	*	316.363
10	62.512	*	326.037
11	69.809	*	334.766
12	77.180	*	342.733
13	84.624	*	350.075
14	92.143	*	356.896
15	99.737	*	363.276
16	107.407	*	369.279
17	115.153	*	374.956
18	122.977	*	380.350
19	130.880	*	385.496
20	138.861	*	390.423
21	146.922	*	395.156
22	156.595	*	400.551
23	168.203	*	406.668
24	182.133	*	413.568
25	198.848	*	421.315
26	218.907	*	429.977
27	242.977	*	439.634
28	271.862	*	450.381
29	306.523	*	462.336
30	348.117	*	475.647
31	398.029	*	490.494
32	457.924	*	507.081
33	529.797	*	525.610
34	616.046	*	546.207
35	719.544	*	568.764
36	843.742	*	592.619
37	992.779	*	615.941
38	1171.624	*	634.574
39	1334.501	*	640.561

 INVISCID BOUNDARY CONDITIONS

	SURFACE DIST. FT	RADIUS FT*100	EDGE VEL. FT/SEC
1	0.0833	0.72	640.561
2	0.1063	0.92	640.640
3	0.1441	1.25	640.770
4	0.1820	1.58	640.900
5	0.2199	1.91	641.030
6	0.2577	2.24	641.160
7	0.2956	2.57	641.290
8	0.3334	2.90	641.420
9	0.3713	3.23	641.550
10	0.4091	3.56	641.680
11	0.4470	3.89	641.810
12	0.4849	4.22	641.940
13	0.5227	4.55	642.070
14	0.5606	4.88	642.200
15	0.5984	5.21	642.330
16	0.6363	5.54	642.460
17	0.6741	5.87	642.590
18	0.7120	6.20	642.720
19	0.7499	6.53	642.850
20	0.7877	6.86	642.980
21	0.8256	7.19	643.110
22	0.8634	7.52	643.240
23	0.9013	7.85	643.370
24	0.9392	8.18	643.500
25	0.9770	8.51	643.630
26	1.0149	8.84	643.760
27	1.0527	9.17	643.890
28	1.0906	9.50	644.020
29	1.1284	9.83	644.150
30	1.1663	10.16	644.360
31	1.2042	10.49	644.530
32	1.2420	10.82	644.700
33	1.2799	11.15	644.870
34	1.3177	11.48	645.040
35	1.3556	11.81	645.210
36	1.3934	12.14	645.380
37	1.4313	12.47	645.550
38	1.4692	12.80	645.730
39	1.5070	13.13	645.900
40	1.5449	13.46	646.080
41	1.5827	13.79	646.260
42	1.6206	14.12	646.440

43	1.6585	14.45	646.620
44	1.6963	14.78	646.810
45	1.7342	15.11	647.000
46	1.7720	15.44	647.190
47	1.8099	15.77	647.390
48	1.8477	16.10	647.590
49	1.8856	16.43	647.791
50	1.9235	16.76	648.000
51	1.9613	17.09	648.221
52	1.9992	17.42	648.440
53	2.0370	17.75	648.671
54	2.0749	18.08	648.901
55	2.1127	18.41	649.141
56	2.1506	18.74	649.381
57	2.1885	19.07	649.641
58	2.2263	19.40	649.901
59	2.2642	19.73	650.171
60	2.3020	20.06	650.452
61	2.3399	20.39	650.742
62	2.3777	20.72	651.052
63	2.4156	21.05	651.372
64	2.4535	21.38	651.702
65	2.4913	21.71	652.043
66	2.5292	22.04	652.413
67	2.5670	22.37	652.793
68	2.6049	22.70	653.194
69	2.6428	23.03	653.624

 THE VALUE OF THE 'XEQ' IS = 1.1329 FT

THE VALUE OF X-INITIAL IS = 0.0833 FT

THE VALUE OF CF(ALLEN) = 3.270E-03

INITIAL STATIC PRESSURE INPUT
 TO STAN-5 = 1434.06 PSF

pressures downstream of the match point at about one-half inch intervals of surface distance must be input to the modified STAN-5 computer code.

Obtaining the values of k_{eff} concludes the turbulent boundary layer calculations.

A complete listing of the Mini-Basic computer code is presented on the following pages.

```

*****
10    REM *****
20    REM  MINI-BASIC
30    REM    BY
40    REM  AMIR NASSIRHARAND
50    REM *****
60    REM  KEEP IN MIND THAT ALL
70    REM  CHR$(X) COMMANDS ADDRESS
80    REM  THE PRINTER IN
90    REM  DECIMAL NOTATIONS
100   REM  THESE ARE CENTRONICS
110   REM  MODEL 739-1 COMPATIBLE
120   REM  COMMAND HOME CLEARS
130   REM  THE SCREEN
-----
140   HOME
150   DIM MINF(21),REFT(21),QINF(21),Z(
      50),L0(50),C$(50),T(3),D$(50),A(3
      ),B(3),C(3),X(153),Y(153),A1(22),
      B1(22),MJ(21),MG(21),MH(21),X1(25
      0),X2(250),R(250),U1(250),UT(250)
      ,U(50),H$(50),P9(19),P8(21)

*****
160   REM  PUT THE CASES IN ORDER
170   REM  CASE NUMBERS 1-19
-----
180   FOR I = 1 TO 19:
      READ P9(I):
      NEXT I
190   DATA  11,10,5,4,3,2,1,8,13,6,7,1
      7,15,14,16,18,19,20,21
200   FOR I = 1 TO 21:
      READ P8(I):
      NEXT I
210   DATA  7,6,5,4,3,10,11,8,0,2,1,0,1
      5,16,13,14,12,16,17,18,19
220   HOME :
      Q1 = 0:
      THETA = (5 * 3.1415927) / 180:
      D$ = "*****
      *****":
      D9$ = "-----"
-----
230   S$ = D$

*****
240   REM  SET THE MAIN MENU
-----
250   PRINT D$

```

```

260   Z5 = 1:
      INVERSE :
      PRINT "          HERE IS THE MENU
          ";
      NORMAL :
      PRINT D9#:
270   Z5 = 1:
      PRINT :
      PRINT "1- THE CURVE FIT RESULTS O
          F THE":
      PRINT "    LAMINAR KEFF VS. X/L":
      PRINT :
      PRINT "2- THE INITIAL VELOCITY PR
          OFILE":
      PRINT :
      PRINT "3- THE INVISCID BOUNDRY CO
          NDITIONS":
      PRINT :
      PRINT "4- OPTION TWO AND OPTION T
          HREE"
280   PRINT :
      PRINT D9#:
      PRINT D9#:
290   PRINT :
      PRINT "INPUT YOUR CHOICE NUMBER":

      INVERSE :
      INPUT "    I.E. 1,2,3, OR 4 :";V
      1:
      NORMAL

*****
300   REM  OBTAIN THE INPUT VALUES
310   REM  AND CHECK THE INPUT
320   REM  CHOICE NUMBERS
-----
330   IF (V1 = 1 OR V1 = 2 OR V1 = 3 OR
          V1 = 4)
          THEN
          GOTO 380
340   HOME :
      FLASH :
      SPEED= 100
350   PRINT "YOU HAVE TO INPUT 1,2,3, O
          R 4":
      NORMAL :
      SPEED= 255
360   PRINT :
      Q1 = 1
370   GOTO 270

```

```

380 PRINT :
PRINT "WOULD YOU LIKE A HARD COPY
?";
INVERSE :
INPUT "          INPUT 'Y' OR 'N' :
";P$:
:
PRINT D9$:
NORMAL :
IF (P$ < > "Y" AND P$ < > "N")

    THEN
    HOME :
GOTO 380
390 HOME
400 IF (V1 = 1)
    THEN
    GOTO 550

*****
410 REM CHECK TO SEE IF
420 REM ITERATION IS REQUIRED
-----
430 T1$ = "DO YOU NEED TO SOLVE FOR N
EW XEQ(CONE)? ";
PRINT T1$:
INVERSE :
INPUT "          I.E. INPUT 'Y' OR 'N'
";T$:
NORMAL :
PRINT :
IF (T$ < > "Y" AND T$ < > "N")

    THEN
    HOME :
GOTO 430
440 PRINT D9$
450 IF (T$ = "Y")
    THEN
    INPUT "INPUT THE VALUE OF 'CF' :
";CSF:
PRINT :
INPUT "THE VALUE OF 'XEQ' IN 'FT'
";OX:
PRINT
460 IF (V1 < > 1)
    THEN
    INPUT "INPUT THE VALUE OF XL IN
INCHES ";E0:
E0 = E0 / 12

```

```
*****
470  REM  OBTAIN THE INPUT DATA
-----
```

```
480  PRINT :
      INPUT "INPUT THE VALUE OF X4 IN I
      NCHES :";X4;
      PRINT :
      INPUT "INPUT THE VALUE OF X(MP) I
      N INCHES :";XM;
      PRINT :
      INPUT "INPUT THE VALUE OF 'CP' :";
      ;CP;
      PRINT :
      INPUT "INPUT THE VALUE OF 'PPT' I
      N 'PSF' :";PPT
490  PRINT :
      INPUT "WHAT IS THE CASE NUMBER :";
      ;I1;
      Z3 = P9(I1)
500  PRINT :
      PRINT "USE THE WU&LOCK PRINT OUT
      ";
      INPUT " TO INPUT THE VALUE OF '
      NXT' :";NXT
```

```
*****
510  REM  ALL THE INPUT
520  REM  INFORMATION IS OBTAINED
-----
```

```
530  PRINT D9$;
      PRINT D$
540  HOME
```

```
*****
550  REM  READ THE FLUID CONSTSNTS
560  REM  P IS PIE IN
570  REM  MUSKER'S EGN.
580  REM  RF IS THE RECOVERY
590  REM  FACTOR
-----
```

```
600  READ R,GC,GAMA,E,K,P,RF
610  DATA 53.35,32.174,1.4,5.,.41,.5,
      .884
620  GDSUB 1390
```

```
*****
630  REM  DO NOT PRINT THE
640  REM  KEFF VS. X/L
650  REM  IF IT IS NOT ASKED FOR
-----
```

```
660  IF (V1 < > 1)
      THEN
      GOTO 740
```

```

670 C# = "STRAIGHT LINE CURVE FIT OF
      LAMINAR ":
      C1# = "          KEFF VS. X/L "
      :
      PRINT D#:
      PRINT C#:
      PRINT :
      PRINT C1#:
      PRINT D9#:
      PRINT
680 FOR J = 1 TO Z1
690   B1(J) = B1(J) * 44.5 / COS (
      HETA):
      B1(J) = INT (B1(J) * 100000 +
      .5) / 100000:
      A1(J) = INT (A1(J) * 100000 +
      .5) / 100000:
      NEXT J
700 FOR I = 1 TO 19
710   J = P9(I):
      IF (A1(J) > 1)
          THEN
              GOTO 730
720   INVERSE :
      PRINT "MINF = ";MINF(J);" REF
      T E-06 = ";REFT(J);" QINF = "
      ;QINF(J):
      NORMAL :
      PRINT "          K";I;" = ";B1(J);
      "*X/L + (0";A1(J);)"":
      GOTO 740
730   INVERSE :
      PRINT "MINF = ";MINF(J);" REF
      T E-06 = ";REFT(J);" QINF = "
      ;QINF(J):
      NORMAL :
      PRINT "          K";I;" = ";B1(J);
      "*X/L + (";A1(J);)"":
740 NEXT I:
      PR# 0:
      END
750 GOSUB 2530

```

```

*****
760 REM CALCULATION OF THE FREE
770 REM STREAM PROPERTIES, ME
780 REM UE, AND ETC.
-----
790 REFT(Z3) = REFT(Z3) * (10 ^ 6)
800 PINF = (2 * QINF(Z3)) / (GAMA * (
      MINF(Z3) ^ 2))

```

```

*****
810  REM  ** PTINF=PTOTAL-INFT **
-----
820  PTINF = ((2 * QINF(Z3)) * ((1 + (
      (GAMA - 1) / 2) * (MINF(Z3) ^ 2))
      ^ (GAMA / (GAMA - 1)))) * (1 / (
      GAMA * (MINF(Z3) ^ 2)))

*****
830  REM  ** MSE=ME^2 **
-----
840  MSE = (((1 + (QINF(Z3)) * (CP / P
      INF)) ^ (- 1 / 3.5)) * (5 + (MIN
      F(Z3) ^ 2))) - 5
850  ME = SQR (MSE)

*****
860  REM  KAX*(TINF^2)+KB*TINF+KC=0
-----
870  KA = (1 / (2 * QINF(Z3))) * ( SQR
      (GAMA * R * GC)) * (2.27E - 08)
      * (MINF(Z3) * REFT(Z3));
      KB = - 1;
      KC = - 198.6
880  DTA = KB ^ 2 - (4 * KA * KC);
      TINF = (1 / (2 * KA)) * (- KB +
      SQR (DTA))
890  IF (TINF < 0)
      THEN
      TINF = (1 / (2 * KA)) * (- KB -
      SQR (DTA))

*****
900  REM  CALCULATION OF OTHER
910  REM  AIR PROPERTIES
-----
920  TTL = (TINF) * (((MINF(Z3)) ^ 2)
      * (.5) * (GAMA - 1)) + 1)
930  TE = TTL * ((1 + (.2 * MSE)) ^ -
      1)
940  UE = (ME) * ( SQR (GAMA * GC * R
      * TE))

*****
950  REM  PPT IS THE PRESTON-
960  REM  TUBE PRESSURE
-----
970  PPT = PPT + PINF
980  PE = PINF + (CP * QINF(Z3))
990  TAW = (TE) * (1 + (RF / 2) * (GAM
      A - 1) * (ME ^ 2))
1000 TSTAR = (TE) * (.55 + (.035) * (M
      E ^ 2)) + .45 * TAW

```

```

*****
1010  REM  A=ROW,B=MUE,C=NUE:
-----

```

```

SUBSCRIPTS 1,2,AND 3 CORRESPOND T
O THE FLUID PROPERTIES EVALUATED
AT TEDGE, TSTAR, AND TWALL RESPEC
TVELY

```

```

1020  T(1) = TE:
      T(2) = TSTAR:
      T(3) = TAW
1030  FOR I = 1 TO 3:
      A(I) = (PE) / (R * T(I));
      B(I) = (2.27) * (T(I) ^ 1.5) *
            (10 ^ - 8) / (T(I) + 198.6);
      C(I) = B(I) * GC / A(I);
      NEXT

```

```

*****
1040  REM  CALCULATION OF CF(ALLEN)
-----

```

```

1050  MPT =  SQR ((2 / (GAMA - 1)) * ((
      (PPT / PE) ^ ((GAMA - 1) / GAMA))
      - 1))
1060  UPT =  SQR ((1 + ((GAMA - 1) * (M
      E ^ 2) / 2)) / (1 + ((GAMA - 1) *
      (MPT ^ 2) / 2))) * (MPT / ME) *
      (UE)
1070  KEFF = A1(Z3) + B1(Z3) * X4;
      DEQ = .0075 * KEFF / 12
1080  RD = (UE * DEQ) / (C(1))
1090  F1 = (A(2) / A(1)) * (B(1) / B(2)
      ) * RD * UPT / UE

```

```

*****
1100  REM  ** CALCULATION OF F2 **
-----

```

```

1110  F3 = LOG (F1) / LOG (10);
      F4 = (.01239) * (F3 ^ 2) + (.7814
      ) * (F3) - .4723;
      F2 = 10 ^ F4

```

```

*****
1120  REM  ** END OF F2 CAL. **
-----

```

```

1130  Z1 = (B(1) / B(2)) * RD * ( SQR (
      A(2) / A(1)))
1140  CF = (F2 / Z1) ^ 2

```

```

*****
1150  REM  END OF CF-ALLEN
1160  REM  CALCULATION
-----

```



```

*****
1170  REM  CALCULATION OF
1180  REM  XEQ(F.P.),XEQ(CONE),...
1190  REM  ** XEQ = XEQ(F.P.)
-----
1200  X1 = (.455 * A(2)) / (A(1) * CF);

      X2 = EXP (X1 ^ .5);
      X3 = (GC * B(2)) / (.06 * A(2) *
      UE);
      XEQ = X2 * X3

*****
1210  REM  ** XC=XEQ(CONE) **
-----
1220  XC = (2.268) * (XEQ)

*****
1230  REM  ** X0=XCONE-INITIAL **
-----
1240  X0 = XC - .5 / ( COS (THETA)) - X
      M / (12 * ( COS (THETA)))

*****
1250  REM  SET THE INITIAL
1260  REM  STATION OF STAN-5
-----
1270  IF (X0 < 0)
      THEN
      X0 = 1 / 12

*****
1280  REM  ** LG=XEQ(F.P.) - INITIAL **
-----
1290  LG = (1 / 2.268) * X0

*****
1300  REM  ** LF=CF(INITIAL) **
-----
1310  LF = (CF) * ((XEQ / LG) ^ (1 / 7)
      )

*****
1320  REM  ** L1=LAMDA(REF.) **
-----
1330  L1 = SQR ((2 * A(2)) / (LF * A(1)
      )))

```

```

*****
1340 REM L4=DELTA(REF.)*UG
1350 REM INITIAL
-----
1360 IF (T# = "Y")
      THEN
          GOTO 1810
1370 L3 = EXP ((L1 - B - (2 * P / K))
              * K):
          L4 = L3 * (C(2) * L1 / 1)
1380 GOTO 1810

*****
1390 REM FIRST ORDER LEAST SQUARE CUR
      VE FIT
-----
1400 Z4 = 0

*****
1410 REM X(I) IS THE SURFACE DISTANCE

1420 REM Y(I) IS THE CORRESPONDING
1430 REM LAMINAR KEFF
1440 REM DATA OBTAINED FROM
1450 REM WORK DONE
1460 REM BY
1470 REM REED AND ABU-MOSTAFA
-----
1480 FOR I = 1 TO 153:
      READ X(I),Y(I):
      NEXT I
      DATA 4.5,.965,5,.979,5.5,.999
          ,6,1.013,6.5,1.027,7,1.032,7.5,1.
          049,4,1.077,4.5,1.101,5,1.105,5.5
          ,1.118,6,1.163,6.5,1.159,7,1.185,
          7.5,1.208,8,1.223,6.5,1.209,7,1.2
          38,7.5,1.258
1490 DATA 8,1.280,8.5,1.36, 9,1.32
          4,9.5,1.342,10,1.358,10.5,1.381,1
          1,1.382,5,1.106,5.5,1.139,6,1.158
          ,6.5,1.177,7,1.197,7.5,1.217,8,1.
          236,8.5,1.257,9,1.279,0,0,0,0,0,0
          ,0,0,0,0,6.5,1.219,7,1.237,7.5,1.
          272,8,1.308,8.5,1.324,9,1.356,9.5

1500 DATA 1.371,10,1.385,10.5,1.3
          92,11,1.416,11.5,1.422,4.5,1.1,5,
          1.105,5.5,1.111,6,1.135,6.5,1.153
          ,7,1.171,7.5,1.191,8,1.208,4.5,.9
          55,5,.971,5.5,.993,6,1.005,6.5,1.
          011,5.5,1.126,6,1.152,6.5,1.183,7
          ,1.207,7.5,1.23,8,1.245,8.5,1.269
          ,9

```

```

1510 DATA 1.293,9.5,1.303,10,1.319,1
0.5,1.333,6.5,1.039,7,1.056,7.5,1
.073,8,1.097,8.5,1.110,6.5,1.226,
7,1.261,7.5,1.282,8,1.314,8.5,1.3
39,9,1.369,9.5,1.393,10,1.402,10.
5,1.422,11,1.426,6.5,1.054,7,1.05
3
1520 DATA 7.5,1.056,8,1.069,8.5,1.06
5,4,1.312,4.5,1.358,5,1.391,5.5,1
.411,6,1.441,6.5,1.464,7,1.474,6.
5,1.082,7,1.1,7.5,1.12,8,1.139,8.
5,1.157,5.5,1.138,6,1.162,6.5,1.1
84,7,1.208,7.5,1.228,8,1.247
1530 DATA 7,1.067,7.5,1.088,8,1.111
,8.5,1.132,4.5,.973,5,.996,5.5,1.
009,6,1.023,6.5,1.029,8,1.021,8.5
,1.035,9,1.057,9.5,1.069,10,1.081
,10.5,1.088,8.5,1.149,9,1.176
1540 DATA 9.5,1.203,10,1.229,10.5,1.
250,11,1.283,11.5,1.314,5,.911,5.
5,.923,6,.946,6.5,.959,4,1.015,4.
5,1.032,5,1.053,5.5,1.069,6,1.087
,6.5,1.108,7,1.129,7.5,1.147,8,1.
16,8.5,1.17,5,.868,5.5,.88,6,.898
,6.5,.911

```

```
*****
```

```

1550 REM ISOLATE THE DATA
1560 REM OF DIFFERENT CASES
-----
1570 FOR J = 1 TO 21:
      READ MG(J),MJ(J):
      NEXT
1580 DATA 1,7,8,16,17,26,27,35,41,51
,52,59,60,64,65,75,76,80,81,90,91
,95,96,102,103,107,108,113,114,11
7,118,122,123,128,129,135,136,139
,140,149,150,153
1590 FOR J = 1 TO 21:
      READ MINF(J),REFT(J),QINF(J):
      NEXT J:
      DATA .6,5,586,.6,4,477,.6,3,357,
.5,4,404,.5,3,302,.7,4,548,.7,5,6
80,.7,3,408,.4,4,403,.4,3,246,.3,
4,230,.4,2.5,396,.7,4,538,.8,4,61
7,.8,4,605,.8,5,761,.8,3,453,.9,3
,492,.9,5,842,.95,4
1600 DATA 693,.95,5,873

```

```

1610 IF (V1 = 1)
      THEN
        FOR J = 1 TO 21
1620   IF (V1 < > 1)
        THEN
          FOR J = Z3 TO Z3

*****
1630   REM USE THE ABOVE DATA
1640   REM AND OBTAIN THE S.L.
1650   REM CURVE FIT
-----
1660   S1 = 0:
        S2 = 0:
        S3 = 0:
        S4 = 0:
        FOR I = MG(J) TO MJ(J):
          S1 = S1 + X(I):
          S2 = S2 + X(I) ^ 2:
          S3 = S3 + X(I) * Y(I):
          S4 = S4 + Y(I):
        NEXT I:
        MH(J) = MJ(J) - MG(J) + 1:
        Z2 = MH(J) * S2 - (S1 ^ 2)
1670   B1(J) = ((MH(J) * S3) - (S1
        * S4)) / Z2:
        A1(J) = ((S2 * S4) - (S1 *
        S3)) / Z2:
        NEXT J
1680   IF (V1 < > 1)
        THEN
          RETURN

*****
1690   REM SET UP THE PRINTER
1700   REM IF IT IS ASKED FOR
1710   REM THE INTERFACE BOARD
1720   REM IS ASSUMED TO BE
1730   REM IN SLOT#1
-----
1740   IF (P# = "N")
        THEN
          RETURN
1750   PR# 1
1760   PRINT CHR# (9);"60N"
1770   PRINT :
        PRINT :
        PRINT
1780   PRINT CHR# (9);"20L"
1790   PRINT :
        PRINT
1800   RETURN

```

```

*****
1810 REM CALCULATION OF THE
1820 REM INITIAL TURBULENT
1830 REM VELOCITY PROFILE

```

```

-----
1840 IF (T# = "Y")
      THEN
        GOTO 2870

```

```

*****
1850 REM USE WU&LOCK RESULTS

```

```

-----
1860 IF (T# = "N")
      THEN
        YU = X0;
        WP = XC
1870 GOTO 1900

```

```

*****
1880 REM REF. THE B.C'S
1890 REM TO THE V.O.

```

```

-----
1900 HOME :
      UV = 0;
      XG = WP - (XM / (12 * ( COS (THET
      A)))));
      FOR I = 1 TO NREAR:
        X2(I) = X2(I) + XG;
        R(I) = X2(I) * ( SIN (THETA));

        IF (UV = 1)
          THEN
            NEXT I:
            GOTO 1930
1910 IF (X2(I) > YU)
          THEN
            SI = I;
            UV = 1
1920 NEXT I

```

```

*****
1930 REM Z=VERTICAL DISTANCE FROM THE
      SURFACE OF THE CONE:

```

```

-----
      U(I)=INITIAL VELOCITY PROFILE;
      U0=WALL FRICTION VELOCITY

```

```

*****
1940 REM SOLVE FOR THE EDGE
1950 REM VELOCITY AT THE
1960 REM INITIAL STATION

```

```

1970 IS = SI - 1;
      UG = (((U1(SI) - U1(IS)) / (X2(SI)
      ) - X2(IS))) * (YU - X2(IS)) + U
      1(IS)
1980 L4 = L4 / UG;
      U0 = UG / L1
1990 U(1) = 0
2000 Z(1) = 0;
      Z(2) = .005 * L4

```

```

*****

```

```

2010 REM AND SOLVE FOR INITIAL

```

```

2020 REM EDGE VELOCITY

```

```

-----
2030 Z5 = 0
2040 FOR I = 3 TO 50
2050     IF (I < = 21)
           THEN
               Z(I) = Z(I - 1) + 1.010 * (Z(I
               - 1) - Z(I - 2))
2060     IF (I > 21)
           THEN
               Z(I) = Z(I - 1) + 1.20 * (Z(I
               - 1) - Z(I - 2))
2070     IF (Z5 = 1)
           THEN
               GOTO 2090
2080     IF (Z(I) > L4)
           THEN
               X8 = I - 1;
               Z5 = 1
2090 NEXT
2100 FOR I = 1 TO X8;
           L0(I) = Z(I) / L4;
           NEXT
2110 X8 = X8 + 1;
           Z(X8) = L4;
           L0(X8) = 1;
           FOR I = 2 TO X8
2120             O1 = (Z(I) * U0) / C(2);
                   O2 = LOG (O1)
2130             O3 = 1 / K;
                   O4 = P * O3;
                   O5 = (6) * (L0(I) ^ 2)
2140             O6 = (4) * (L0(I) ^ 3);
                   O7 = (O4) * (O5 - O6);
                   O8 = O3 * O2;
                   O9 = (O3) * (L0(I) ^ 2) * (1 -
                   L0(I));
                   U(I) = (U0) * (O8 + O7 + O9 +
                   B)
2150 NEXT

```

```

2160 IF (V1 = 1 OR V1 = 3)
      THEN
      GOTO 2420

```

```

*****

```

```

2170 REM PRINT OUT THE
2180 REM VEL. PROFILE

```

```

-----
2190 IF (P# = "N")
      THEN
      GOTO 2260

```

```

*****

```

```

2200 REM CHECK AND SEE IF A
2210 REM HARD COPY IS ASKED FOR

```

```

-----
2220 PR# 1
2230 PRINT CHR# (9);"60N"
2240 PRINT
2250 PRINT CHR# (9);"20L"
2260 PRINT D#:
      PRINT " THE INITIAL VELOCITY PRO
      FILE OF THE":
      PRINT " TURBULENT BOUNDRY
      LAYER":
      PRINT D9#:
      PRINT :
      PRINT " DIST. FROM WALL
      VELOCITY":
      PRINT " FT*10^6
      FT/SEC":
      PRINT :
      PRINT D9#:
      PRINT :
      PRINT
2270 FOR I = 1 TO X8:
      U(I) = INT (U(I) * 1000 + .5)
      / 1000:
      D$(I) = STR# (U(I)):
      D$(I) = D$(I) + "000000"

```

```

*****

```

```

2280 REM USE STRINGS TO FORMAT
2290 REM THE TABLE OF VALUES

```

```

-----
2300 Z(I) = Z(I) * 1000000:
      Z(I) = INT (Z(I) * 1000 + .5)
      / 1000:
      X(I) = INT (Z(I)):
      C$(I) = STR# (Z(I)):
      H$(I) = STR# (X(I))

```

```

2160 IF (V1 = 1 OR V1 = 3)
      THEN
      GOTO 2420

```

```

*****

```

```

2170 REM PRINT OUT THE
2180 REM VEL. PROFILE

```

```

-----
2190 IF (P# = "N")
      THEN
      GOTO 2260

```

```

*****

```

```

2200 REM CHECK AND SEE IF A
2210 REM HARD COPY IS ASKED FOR

```

```

-----
2220 PR# 1
2230 PRINT CHR# (9);"60N"
2240 PRINT
2250 PRINT CHR# (9);"20L"
2260 PRINT D#:
      PRINT " THE INITIAL VELOCITY PRO
      FILE OF THE":
      PRINT " TURBULENT BOUNDRY
      LAYER":
      PRINT D9#:
      PRINT :
      PRINT " DIST. FROM WALL
      VELOCITY":
      PRINT " FT*10^+6
      FT/SEC":
      PRINT :
      PRINT D9#:
      PRINT :
      PRINT
2270 FOR I = 1 TO X8:
      U(I) = INT (U(I) * 1000 + .5)
      / 1000:
      D$(I) = STR# (U(I)):
      D$(I) = D$(I) + "000000"

```

```

*****

```

```

2280 REM USE STRINGS TO FORMAT
2290 REM THE TABLE OF VALUES

```

```

-----
2300 Z(I) = Z(I) * 1000000:
      Z(I) = INT (Z(I) * 1000 + .5)
      / 1000:
      X(I) = INT (Z(I)):
      C$(I) = STR# (Z(I)):
      H$(I) = STR# (X(I))

```



```

2310     IF ( LEN (H$(I)) = 1)
           THEN
           C$(I) = " " + C$(I) + "00000"
           "
2320     C$(1) = " 0.000";
           D$(1) = " 0.000";
           IF ( LEN (H$(I)) > 3)
           THEN
           C$(I) = C$(I) + "0000"
2330     IF ( LEN (H$(I)) = 2)
           THEN
           C$(I) = " " + C$(I) + "0000"
2340     IF ( LEN (H$(I)) = 3)
           THEN
           C$(I) = " " + C$(I) + "0000"
2350     I$ = STR$(I);
           IF ( LEN (I$) = 1)
           THEN
           I$ = " " + I$
2360     IF ( LEN (H$) = 4)
           THEN
           C$(I) = LEFT$(C$(I),6)
2370     IF (I = 1)
           THEN
           2400
2380     IF ( INT (Z(I)) = Z(I))
           THEN
           C$(I) = " " + STR$(Z(I)) + "
           ,0000000"
2390     IF ( VAL (D$(I)) = INT ( VAL
           (D$(I))))
           THEN
           D$(I) = STR$(U(I)) + ".000000"
           "
2400     PRINT " ";I$;" "; LEFT$(C$(I)
           ),8);" * "; LEFT$(
           D$(I),7);
           NEXT I:
           PRINT D9$
2410     IF (V1 = 2)
           THEN
           PR$ 0:
           END
2420     IF (T$ = "N")
           THEN
           GOTO 3140
2430     IF (O$ = "NEW")
           THEN
           RETURN

```

```

*****
2440 REM OBTAIN THE INVISCID
2450 REM BOUNDARY CONDITIONS
2460 REM NP1=NUMP1
2470 REM NS=NSHIFT
2480 REM BY CHANGING NSHIFT
2490 REM THE BC'S OVER A
2500 REM WIDER RANGE CAN
2510 REM BE DETERMINED
2520 REM THE VALUS OF NUM AND NSHIFT
      ARE BASED ON EXPERIENCE

```

```

-----
2530 NUM = 80:
      NS = 30:
      NP1 = NUM + 1

```

```

*****
2540 REM
      X1(I)=X/L (FT) FROM WU & LOC
      K** X1(I) IS MEASURED ALONG THE A
      XIS OF THE CONE ** X2(I)=X ALONG
      THE SURFACE OF THE CONE

```

```

-----
2550 FOR I = 1 TO NP1:
      READ X1(I):
      NEXT

```

```

*****
2560 REM X/L DATA FROM WU & LOCK

```

```

-----
2570 DATA .01281,.02307,.03332,.0
4355,.05379,.06401,.07423,.08445,
.09466,.10487,.11508,.12528,.1354
8,.14568,.15588,.16607,.17626,.18
645,.19664,.20682,.21701,.22719,.
23737,.24755,.25772,.26790,.27807
,.28824,.29841,.30858
2580 DATA .31874,.32891,.33907 ,0.34
9230,.35939,.36955,.37970,.38986,
.40001,.41016,.42031,.43046,.4406
0,.45074,.46089,.47103,.48116,.49
130,.50143,.51157,.52170,.53182,.
54195,.55207,.56220,.57232,.58243
,.59255,.60266,.61277,.62288,.632
98
2590 DATA .64308,.65318,.66328 .67337
,.68346,.69354,.70363,.71371,.723
76,.73385,.74392,.75398,.76403,.7
7408,.78413,.79417,.80420,.81422,
.82424

```

```

*****
2600 REM

```

```

2610  FOR I = 1 TO NP1:
      X2(I) = (X1(I) * 44.5) / (12 *
      COS (THETA)):
      R(I) = X2(I) * SIN (THETA):
      NEXT I
2620  FOR I = 1 TO NP1:
      READ U1(I):
      NEXT

```

```

*****
2630  REM  DATA FROM WU & LOCK
-----

```

```

2640  DATA  633.32,635.22,636.32,637.09
      ,637.71,638.21,638.65,639.03,639.
      39,639.70,640.640.28,640.54,640.7
      8,641.01,641.24,641.46,641.66,641
      .87,642.07,642.26,642.45,642.63,6
      42.81,642.99,643.17,643.34,643.51
      ,643.69,643.86,644.02,644.15,644.
      36
2650  DATA  644.53,644.70,644.87,645.04
      ,645.21,645.38,645.55,645.73,645.
      90,646.08,646.26,646.44,646.62,64
      6.81,647.00,647.19,647.39,647.59,
      647.79,648.00,648.22,648.44,648.6
      7,648.90,649.14,649.38,649.64,649
      .90,650.17,650.45,650.74,651.05
2660  DATA  651.37,651.70,652.04,652.41
      ,652.79,653.19,653.62,654.07,654.
      55,655.05,655.60,656.18,656.81,65
      7.49,658.22,659.03
2670  DX = X2(NXT) - X2(NXT - 1)
2680  DU = U1(NXT) - U1(NXT - 1)
2690  XXT = X2(NXT)
2700  UXT = U1(NXT)
2710  NFR = NXT + NSH
2720  NREAR = NUM + NSH + 1

```

```

*****
2730  REM  NT=NTOT
-----

```

```

2740  NT = NUM + NSH + NSH

```

```

*****
2750  REM  NXT1=N1XT
-----

```

```

2760  N1XT = NXT + 1:
      FOR I = N1XT TO NUM:
          VZ = (U1(I + 1) - U1(I)) / (X2
          (I + 1) - X2(I)):
          UT(I) = U1(I) + VZ * (DX - X2(
          I) + X2(I - 1)):
      NEXT

```

```

2770 V2 = DUDX
2780 FOR I = N1XT TO NUM
2790     X2(I + NSH) = XXT + DX * (I -
        NXT)
2800     R(I + NSH) = X2(I + NSH) * ( S
        IN (THETA))
2810     U1(I + NSH) = UT(I);
        NEXT
2820 FOR I = 1 TO NFR:
        J = NFR + 1 - I;
        X2(J) = XXT - (I - 1) * DX;
        R(J) = X2(J) * SIN (THETA);
        U1(J) = UXT - (I - 1) * DU;
        NEXT
2830 FOR I = NREAR TO NT:
        X2(I) = X2(I - 1) + DX;
        R(I) = X2(I) * SIN (THETA);
        U1(I) = 0;
        NEXT
2840 HOME ;
        RETURN
2850 PRINT ;
        PRINT
2860 PRINT ;
        PRINT ;
        HTAB 20 - INT ( LEN (D2#) / 2);
        PRINT D2#;
        PRINT ;
        PRINT ;
        INPUT "" ; C#

*****
2870 REM MOVE U.O.
2880 REM ** CF(STAN-5)=CSF **
2890 REM ** NEW XEQ(CONE)=XN **
-----
2900 XN = OX * ((CF / CSF) ^ - 7)

*****
2910 REM ** NEW XEQ(F.P.)=NF
-----
2920 NF = XN / 2.268

*****
2930 REM ** NEW X(CONE-INITIAL)=NC **
-----
2940 NC = XN - .5 / ( COS (THETA)) - X
        M / (12 * ( COS (THETA)))
2950 IF (NC < 0)
        THEN
        NC = 1 / 12

```

```

*****
2960 REM ** NEW X(F.P. INITIAL)=NI **

```

```

-----
2970 NI = NC / 2.268

```

```

*****
2980 REM ** NEW CF(ALLEN-INITIAL)=NA
**

```

```

-----
2990 NA = (CF) * ((NF / NI) ^ (1 / 7))

```

```

*****
3000 REM ** CAL. DELTA(INITIAL) **
3010 REM ** NEW LAMDA = N1 **

```

```

-----
3020 N1 = SQR ((2 * A(2)) / (NA * A(1
)))

```

```

*****
3030 REM ** NEW DELTA(REF.)=N4

```

```

-----
3040 N3 = EXP ((N1 - B - (2 * F / K))
* K):

```

```

N4 = N3 * (C(2) * N1 / 1)

```

```

3050 L1 = N1:

```

```

L4 = N4:

```

```

HOME

```

```

3060 O# = "NEW":

```

```

YU = NC:

```

```

WP = XN:

```

```

GOSUB 1900

```

```

3070 L1 = SQR ((2 * A(2)) / (LF * A(1
)))

```

```

3080 L3 = EXP ((L1 - B - (2 * F / K))
* K):

```

```

L4 = L3 * (C(2) * L1 / UG)

```

```

3090 PRINT :

```

```

PRINT :

```

```

PRINT :

```

```

HTAB 20 - INT ( LEN (D2#) / 2):

```

```

PRINT D2#:

```

```

PRINT :

```

```

PRINT :

```

```

IF (P# = "N")

```

```

THEN

```

```

INPUT "HIT THE <RETURN> KEY TO C
ONTINUE ";C#

```

```

*****
3100 REM OBTAIN THE 1ST TABLE
3110 REM OF STAN-5
3120 REM SET UP THE PRINTER
3130 REM IF IT IS ASKED FOR
-----
3140 IF (P# = "N")
      THEN
          GOTO 3190
3150 PR# 1
3160 PRINT CHR# (9);"132N":
      PRINT :
3170 PRINT
3180 PRINT CHR# (9);"20L"
3190 IF (V1 = 1)
      THEN
          GOTO 3380
3200 HOME :
      PRINT D#:
      PRINT "          INVISCID BOUNDRY CO
NDITIONS":
      PRINT D9#:
      PRINT
3210 PRINT " SURFACE DIST. RADIUS
      EDGE VEL.":
      PRINT " FT FT*100
      FT/SEC":
      PRINT :
      PRINT D9#:
      PRINT :
      PRINT
3220 E0 = E0 + XG + .9 / 12:
      J = 0:
      FOR I = SI - 1 TO NREAR - 1:
          IF (X2(I) > E0)
              THEN
                  NEXT I:
                  GOTO 3380
3230 J = J + 1:
      X2(SI - 1) = YU:
      R(SI - 1) = X2(SI - 1) * ( SIN
      (THETA)):
      U1(SI - 1) = UG
3240 X2(I) = INT (10000 * X2(I) +
      .5) / 10000:
      R(I) = R(I) * 100:
      R(I) = INT (R(I) * 1000 + .5)
      / 1000:
      U1(I) = INT (10000 * U1(I) +
      .5) / 10000

```

```

3250     J# = STR# (J);
        C# = STR# (X2(I));
        D# = STR# (R(I));
        E# = STR# (U1(I));
        E# = E# + "0000";
        ;
        C# = C# + "0000";
        IF ( LEN (J#) = 1)
            THEN
        J# = " " + J#

*****
3260     REM  STRINGS ARE USED
3270     REM  TO FORMAT THE NUMBERS
-----
3280     IF ( VAL (D#) < 10)
            THEN
        D# = " " + D# + "0000"
3290     IF ( VAL (C#) < 1)
            THEN
        C# = "0" + C#
3300     IF ( VAL (E#) = INT ( VAL (E#
        )))
            THEN
        E# = STR# (U1(I)) + ".00000"
3310     IF ( VAL (D#) < 1)
            THEN
        D# = STR# (R(I));
        D# = " 0" + D# + "0000"
3320     IF ( VAL (D#) > 10)
            THEN
        D# = D# + "00000"
3330     PRINT J#;
        PRINT "      "; LEFT# (C#,6);"
            "; LEFT# (D#,5);"      "
            ; LEFT# (E#,7);
        NEXT
3340     PRINT S#;
        PRINT D9#

*****
3350     REM  OBTAIN THE INITIAL
3360     REM  STATIC PRESSURE
3370     REM  INPUT TO STAN-5
-----
3380     EPI = (((1 + (.2) * (MINF(Z3) ^ 2
        )) / (1 + (.2) * ((UG ^ 2) / ((GA
        MA * GC * R * TTL) - (.2) * (UG ^
        2)))))) ^ (3.5)) * (PINF)
3390     EPI = INT (EPI * 100 + .5) / 100

```

```

*****
3400 REM PRINT OUT SOME USEFUL
3410 REM INFORMATION
-----
3420 PRINT S$:
      PRINT D9$
3430 IF (T$ = "N")
      THEN
      NC = X0:
      XN = XC
3440 XN = INT (XN * 10000 + .5) / 100
      00:
      NC = INT (NC * 10000 + .5) / 100
      00:
      XN$ = STR$ (XN):
      NC$ = STR$ (NC):
      IF (XN < 0)
      THEN
      XN$ = "0" + XN$ + "00000"
3450 IF (XN > 1)
      THEN
      XN$ = XN$ + "00000"
3460 IF (NC < 1)
      THEN
      NC$ = "0" + NC$ + "00000"
3470 IF (NC > 1)
      THEN
      NC$ = NC$ + "000000"
3480 PRINT :
      PRINT CHR$ (10):
      CF$ = STR$ (CF)
3490 PRINT D9$:
      PRINT "THE VALUE OF THE 'XEQ' IS
      = "; LEFT$ (XN$,6);" FT":
      PRINT D9$:
      PRINT "THE VALUE OF X-INITIAL IS
      = "; LEFT$ (NC$,6);" FT":
      PRINT D9$
3500 PRINT "THE VALUE OF CF(ALLEN) = "
      ; LEFT$ (CF$,5);"E-03":
      PRINT D9$:
      PRINT "      INITIAL STATIC PRESSU
      RE INPUT":
      PRINT "      TO STAN-5 = ";EPI
      ;" PSF":
      PRINT D9$
3510 PRINT D9$:
      PRINT S$:
      PR$ 0

```



```
*****  
3520 REM END THE MINI-BASIC  
3530 REM  
3540 REM COMPUTER CODE  
-----  
3550 END
```

APPENDIX B

TABULATED VALUES OF TOTAL PRESTON-TUBE PRESSURE,
EFFECTIVE CENTER OF THE PROBE, AND SKIN
FRICTION COEFFICIENT ALONG THE
SURFACE OF THE CONE FOR
19 CASES

TABLE III
 PRESTON-TUBE PRESSURE, EFFECTIVE CENTER
 OF THE PROBE AND SKIN FRICTION
 COEFFICIENT ALONG THE SURFACE
 OF THE CONE FOR RUN
 NUMBER 29.440

Case No. = 1					
$X_{MP} = 0.9767 \text{ ft}$					
$X_{eq} = 0.7008 \text{ ft}$					
No.	X_c ft	X_o ft	P_{pt} pst	k_{eff}	$c_f \times 10^6$
1	0.7015	0.97734	3758.2	1.3834	3470
2	0.7422	1.01804	3754.9	1.2957	3432
3	0.7849	1.06074	3752.5	1.2462	3410
4	0.8263	1.10217	3750.5	1.2136	3360
5	0.8697	1.14554	3748.8	1.1878	3346
6	0.9113	1.18714	3747.7	1.1854	3300
7	0.9548	1.23064	3746.4	1.1725	3288
8	0.9961	1.27194	3744.9	1.1536	3246
9	1.0391	1.31494	3743.9	1.1479	3238
10	1.0796	1.35544	3743.5	1.1650	3202
11	1.1216	1.39744	3742.4	1.1508	3190
12	1.1647	1.44054	3741.8	1.1605	3164
13	1.2050	1.48084	3741.1	1.1633	3136
14	1.2467	1.52254	3740.5	1.1667	3134
15	1.2892	1.56504	3739.8	1.1556	3100
16	1.3331	1.60894	3739.1	1.1672	3084
17	1.3786	1.64944	3738.7	1.1677	3078
18	1.4149	1.69074	3737.8	1.1667	3046
19	1.4574	1.73324	3737.5	1.1810	3042
20	1.5009	1.77674	3737.0	1.1818	3028
21	1.5502	1.82604	3736.7	1.2017	2996
22	1.5909	1.86674	3736.4	1.2108	2998
23	1.6323	1.90814	3736.0	1.2167	2984
24	1.6743	1.95014	3735.3	1.2093	2958
25	1.7174	1.99324	3735.0	1.2227	2950
26	1.7560	2.03184	3734.7	1.2301	2948
27	1.8006	2.07644	3734.3	1.2358	2924
28	1.8461	2.12194	3733.8	1.2435	2908
29	1.8870	2.16284	3733.5	1.2494	2910
30	1.9285	2.20434	3733.1	1.2499	2900
31	1.9704	2.24624	3732.7	1.2529	2880
32	2.0133	2.28914	3732.5	1.2662	2870
33	2.0571	2.33294	3732.4	1.2792	2874
34	2.1015	2.37734	3732.3	1.2948	2862
35	2.1464	2.42224	3732.1	1.3122	2844
36	2.1858	2.46164	3731.8	1.3162	2838
37	2.2259	2.50174	3731.7	1.3278	2842

TABLE IV
 PRESTON-TUBE PRESSURE, EFFECTIVE CENTER
 OF THE PROBE AND SKIN FRICTION
 COEFFICIENT ALONG THE SURFACE
 OF THE CONE FOR RUN
 NUMBER 61.636

Case No. = 2					
$X_{MP} = 1.3183 \text{ ft}$					
$X_{eq} = 1.4481 \text{ ft}$					
No.	X_c ft	X_o ft	P_{pt} psf	k_{eff}	$c_f \times 10^6$
1	1.4684	1.3386	2298.36	1.9050	3576
2	1.5096	1.3798	2295.79	1.8269	2990
3	1.5514	1.4216	2295.08	1.7484	3199
4	1.5943	1.4645	2293.65	1.6504	3088
5	1.6328	1.5030	2292.94	1.6212	3108
6	1.6774	1.5476	2292.23	1.6032	3080
7	1.7172	1.5879	2291.52	1.6032	3062
8	1.7580	1.6282	2290.09	1.5896	3064
9	1.7996	1.6698	2289.80	1.5348	3058
10	1.8416	1.7118	2288.95	1.5425	3036
11	1.8846	1.7548	2288.81	1.5234	3020
12	1.9286	1.7988	2288.52	1.5440	3024
13	1.9668	1.8370	2288.38	1.5533	3014
14	2.0054	1.8756	2288.09	1.5673	2996
15	2.0447	1.9149	2287.81	1.5760	2983
16	2.0849	1.9551	2287.38	1.5863	2982
17	2.1257	1.9959	2287.10	1.5843	2978
18	2.1668	2.0370	2286.95	1.5917	2962
19	2.2085	2.0787	2286.81	1.6098	2946
20	2.2511	2.1213	2286.67	1.6284	2941
21	2.2945	2.1647	2286.53	1.6447	2942
22	2.3383	2.2085	2285.67	1.6608	2933
23	2.3825	2.2527	2285.53	1.6368	2914
24	2.4276	2.2978	2285.39	1.6584	2902
25	2.4659	2.3361	2285.10	1.6788	2901
26	2.5125	2.3827	2284.96	1.7023	2902
27	2.5515	2.4217	2284.81	1.7152	2892
28	2.5989	2.4691	2284.67	1.7375	2876
29	2.6473	2.5175	2284.39	1.7526	2866
30	2.6883	2.5585	2284.10	1.7583	2872
31	2.7297	2.5999	2283.53	1.7455	2870
32	2.7714	2.6416	2282.96	1.7356	2860

TABLE V
 PRESTON-TUBE PRESSURE, EFFECTIVE CENTER
 OF THE PROBE AND SKIN FRICTION
 COEFFICIENT ALONG THE SURFACE
 OF THE CONE FOR RUN
 NUMBER 60.635

Case No. = 3					
$X_{MP} = 1.3250 \text{ ft}$					
$X_{eq} = 1.3586 \text{ ft}$					
No.	X_c ft	X_o ft	P_{pt} psf	k_{eff}	$c_f \times 10^6$
1	1.3691	1.3355	1848.3	1.4802	3196
2	1.4091	1.3755	1846.2	1.4282	3178
3	1.4500	1.4164	1844.0	1.3798	3160
4	1.4918	1.4582	1842.6	1.3579	3144
5	1.5346	1.5010	1841.2	1.3340	3126
6	1.5783	1.5447	1839.8	1.3114	3110
7	1.6231	1.5895	1838.3	1.2896	3094
8	1.6688	1.6352	1837.3	1.2799	3076
9	1.7156	1.6820	1836.5	1.2758	3060
10	1.7633	1.7297	1835.5	1.2687	3046
11	1.7998	1.7662	1835.1	1.2735	3032
12	1.8495	1.8159	1834.6	1.2854	3018
13	1.8874	1.8538	1834.3	1.2959	3008
14	1.9389	1.9053	1834.1	1.3108	2992
15	1.9915	1.9579	1833.9	1.3341	2978
16	2.0452	2.0116	1833.2	1.3356	2962
17	2.0862	2.0526	1832.9	1.3465	2952
18	2.1279	2.0943	1832.6	1.3567	2942
19	2.1702	2.1366	1832.5	1.3745	2930
20	2.2132	2.1796	1832.3	1.3905	2922
21	2.2569	2.2233	1832.2	1.4074	2912
22	2.3012	2.2676	1831.9	1.4193	2902
23	2.3462	2.3126	1831.5	1.4264	2892
24	2.3918	2.3582	1831.2	1.4404	2882
25	2.4382	2.4046	1830.6	1.4424	2872
26	2.4852	2.4516	1830.4	1.4568	2862
27	2.5329	2.4993	1829.9	1.4640	2856
28	2.5814	2.5478	1829.4	1.4674	2846
29	2.6305	2.5961	1828.8	1.4703	2836
30	2.6803	2.6467	1828.4	1.4807	2828

TABLE VI

PRESTON-TUBE PRESSURE, EFFECTIVE CENTER
OF THE PROBE AND SKIN FRICTION
COEFFICIENT ALONG THE SURFACE
OF THE CONE FOR RUN
NUMBER 25.376

Case No. = 4					
$X_{MP} = 0.9867 \text{ ft}$					
$X_{eq} = 1.3711 \text{ ft}$					
No.	X_c ft	X_o ft	P_{pt} psf	k_{eff}	$c_f \times 10^6$
1	1.3732	0.9888	2481.5	1.5635	3024
2	1.4110	1.0266	2477.2	1.4669	3008
3	1.4594	1.0750	2471.7	1.3431	2988
4	1.4990	1.1146	2468.7	1.2871	2974
5	1.5395	1.1551	2465.8	1.2386	2958
6	1.5809	1.1965	2463.1	1.1928	2946
7	1.6232	1.2388	2461.3	1.1705	2932
8	1.6663	1.2819	2458.8	1.1347	2916
9	1.7103	1.3259	2457.4	1.1212	2902
10	1.7553	1.3709	2456.1	1.1136	2888
11	1.8012	1.4168	2454.6	1.0982	2874
12	1.8480	1.4636	2453.1	1.0849	2862
13	1.8838	1.4636	2452.3	1.0803	2850
14	1.9323	1.5479	2450.3	1.0562	2838
15	1.9818	1.5974	2449.6	1.0604	2824
16	2.0196	1.6352	2448.7	1.0561	2814
17	2.0708	1.6864	2447.4	1.0438	2804
18	2.1099	1.7255	2446.0	1.0275	2794
19	2.1630	1.7786	2445.6	1.0388	2780
20	2.2035	1.8191	2445.0	1.0413	2770
21	2.2445	1.8601	2444.4	1.0438	2762
22	2.2862	1.9018	2443.3	1.0327	2752
23	2.3285	1.9441	2442.7	1.0322	2746
24	2.3714	1.9870	2441.4	1.0187	2736
25	2.4149	2.0305	2440.3	1.0074	2728
26	2.4591	2.0747	2439.9	1.0125	2720
27	2.5038	2.1194	2438.7	1.0007	2712
28	2.5493	2.1649	2438.4	1.0073	2706
29	2.5953	2.2109	2437.6	1.0017	2700
30	2.6421	2.2577	2437.3	1.0134	2692
31	2.6895	2.3051	2437.3	1.0257	2686
32	2.7376	2.3532	2437.3	1.0395	2678

TABLE VII

PRESTON-TUBE PRESSURE, EFFECTIVE CENTER
OF THE PROBE AND SKIN FRICTION
COEFFICIENT ALONG THE SURFACE
OF THE CONE FOR RUN
NUMBER 59.634

Case No. = 5					
$X_{MP} = 1.2243 \text{ ft}$					
$X_{eq} = 1.1452 \text{ ft}$					
No.	X_c ft	X_o ft	P_{pt} psf	k_{eff}	$c_f \times 10^6$
1	1.1483	1.2274	1565.7	1.4538	3286
2	1.1909	1.2700	1562.8	1.4067	3264
3	1.2304	1.3095	1559.7	1.3478	3256
4	1.2706	1.3497	1557.4	1.3159	3222
5	1.3121	1.3912	1554.6	1.2669	3208
6	1.3547	1.4338	1552.6	1.2399	3198
7	1.3982	1.4773	1550.6	1.2185	3164
8	1.4430	1.5221	1548.4	1.1884	3160
9	1.4838	1.5629	1547.2	1.1775	3146
10	1.5253	1.6044	1546.3	1.1818	3116
11	1.5679	1.6470	1545.0	1.1733	3104
12	1.6060	1.6851	1544.3	1.1699	3102
13	1.6502	1.7293	1543.5	1.1759	3078
14	1.6897	1.7688	1542.7	1.1784	3058
15	1.7302	1.8093	1542.3	1.1862	3060
16	1.7714	1.8505	1541.9	1.1945	3048
17	1.8131	1.8922	1541.6	1.2104	3024
18	1.8557	1.9348	1541.3	1.2253	3010
19	1.8994	1.9785	1541.0	1.2380	3012
20	1.9436	2.0227	1540.6	1.2463	2994
21	1.9885	2.0676	1539.9	1.2519	2972
22	2.0279	2.1070	1539.6	1.2650	2964
23	2.0882	2.1673	1539.3	1.2844	2962
24	2.1290	2.2081	1539.0	1.2960	2946
25	2.1703	2.2494	1538.9	1.3151	2928
26	2.2124	2.2915	1538.6	1.3293	2920
27	2.2554	2.3345	1538.3	1.3405	2924
28	2.2989	2.3780	1538.2	1.3573	2912
29	2.3428	2.4219	1537.6	1.3639	2894
30	2.3874	2.4665	1536.6	1.3569	2882
31	2.4330	2.5121	1536.3	1.3702	2880
32	2.4792	2.5583	1535.8	1.3741	2878
33	2.5258	2.6049	1535.2	1.3812	2866
34	2.5731	2.6522	1534.2	1.3736	2850

TABLE VIII

PRESTON-TUBE PRESSURE, EFFECTIVE CENTER
OF THE PROBE AND SKIN FRICTION
COEFFICIENT ALONG THE SURFACE
OF THE CONE FOR RUN
NUMBER 23.346

Case No. = 6					
$X_{MP} = 0.9975 \text{ ft}$					
$X_{eq} = 1.4616 \text{ ft}$					
No.	X_c ft	X_o ft	P_{pt} psf	k_{eff}	$c_f \times 10^6$
1	1.4674	1.0033	2092.6	1.5060	2968
2	1.5072	1.0431	2087.6	1.4118	2954
3	1.5479	1.0838	2082.7	1.3236	2938
4	1.5895	1.1254	2079.0	1.2688	2924
5	1.6320	1.1679	2075.6	1.2165	2910
6	1.6753	1.2112	2072.6	1.1781	2896
7	1.7196	1.2555	2069.8	1.1409	2882
8	1.7648	1.3007	2067.6	1.1202	2868
9	1.8109	1.3468	2065.6	1.1028	2852
10	1.8580	1.3939	2064.1	1.0919	2840
11	1.8939	1.4298	2062.6	1.0785	2832
12	1.9427	1.4786	2061.2	1.0728	2818
13	1.9924	1.5283	2059.8	1.0663	2804
14	2.0432	1.5791	2058.4	1.0540	2790
15	2.0949	1.6308	2057.1	1.0347	2778
16	2.1477	1.6836	2055.1	1.0258	2768
17	2.1880	1.7239	2053.8	1.0212	2758
18	2.2289	1.7648	2052.8	1.0256	2748
19	2.2704	1.8063	2052.2	1.0195	2738
20	2.3125	1.8484	2051.1	1.0133	2730
21	2.3552	1.8911	2050.0	1.0097	2720
22	2.3985	1.9344	2049.1	1.0057	2714
23	2.4425	1.9784	2048.1	1.0021	2706
24	2.4871	2.0230	2047.1	0.9886	2696
25	2.5323	2.0682	2045.7	0.9946	2690
26	2.5781	2.1140	2045.3	0.9996	2682
27	2.6247	2.1606	2044.8	1.0015	2674
28	2.6719	2.2078	2044.3	1.0015	2670
29	2.7198	2.2557	2044.0	1.0109	2662
30	2.7684	2.3043	2043.0	1.0055	2656
31	2.8176	2.3535	2042.7	1.0153	2650
32	2.8676	2.4035	2042.3	1.0213	2644

TABLE IX

PRESTON-TUBE PRESSURE, EFFECTIVE CENTER
OF THE PROBE AND SKIN FRICTION
COEFFICIENT ALONG THE SURFACE
OF THE CONE FOR RUN
NUMBER 40.547

Case No. = 7					
$X_{MP} = 0.7750$ ft					
$X_{eq} = 1.1229$ ft					
No.	X_c ft	X_o ft	P_{pt} psf	k_{eff}	$c_f \times 10^6$
1	1.1260	0.7781	2578.8	1.3423	3002
2	1.1679	0.8200	2568.8	1.2006	2998
3	1.2107	0.8628	2557.5	1.0055	2964
4	1.2510	0.9031	2552.7	1.0096	2950
5	1.2922	0.9443	2547.4	0.9575	2940
6	1.3344	0.9865	2542.5	0.9174	2912
7	1.3736	1.0257	2538.8	0.8873	2910
8	1.4135	1.0656	2535.3	0.8602	2892
9	1.4542	1.1063	2533.1	0.8531	2866
10	1.4915	1.1436	2531.6	0.8469	2864
11	1.5342	1.1863	2529.6	0.8383	2852
12	1.5777	1.2293	2526.7	0.8230	2826
13	1.6225	1.2746	2525.3	0.8208	2824
14	1.6683	1.3204	2523.3	0.8108	2812
15	1.7148	1.3669	2521.7	0.8074	2790
16	1.7575	1.4096	2520.4	0.8037	2790
17	1.8009	1.4530	2519.0	0.7979	2782
18	1.8450	1.4971	2518.3	0.8036	2762
19	1.8845	1.5366	2517.5	0.8071	2752
20	1.9249	1.5770	2516.7	0.8077	2756
21	1.9716	1.6237	2515.9	0.8104	2744
22	2.0132	1.6653	2514.9	0.8109	2726
23	2.0558	1.7079	2514.2	0.8126	2722
24	2.0993	1.7514	2513.5	0.8135	2724
25	2.1432	1.7953	2512.8	0.8165	2712
26	2.1879	1.8400	2511.9	0.8181	2996
27	2.2337	1.8858	2511.3	0.8210	2692
28	2.2736	1.9257	2510.8	0.8175	2694
29	2.3139	1.9660	2510.0	0.8241	2684
30	2.3547	2.0068	2509.6	0.8299	2670

TABLE IX (Continued)

Case No. = 7					
$X_{MP} = 0.7750 \text{ ft}$					
$X_{eq} = 1.1229 \text{ ft}$					
No.	X_c ft	X_o ft	P_{pt} psf	k_{eff}	$c_f \times 10^6$
31	2.3963	2.0484	2509.2	0.8336	2662
32	2.4388	2.0909	2509.0	0.8432	2666
33	2.4817	2.1338	2508.6	0.8468	2662
34	2.5251	2.1772	2507.9	0.8471	2650
35	2.5691	2.2212	2507.5	0.8569	2638
36	2.6140	2.2661	2507.2	0.8672	2634
37	2.6598	2.3119	2506.8	0.8726	2638
38	2.7059	2.3580	2506.5	0.8792	2630
39	2.7525	2.4046	2505.9	0.8850	2618
40	2.8000	2.4521	2505.6	0.8970	2608

TABLE X

PRESTON-TUBE PRESSURE, EFFECTIVE CENTER
OF THE PROBE AND SKIN FRICTION
COEFFICIENT ALONG THE SURFACE
OF THE CONE FOR RUN
NUMBER 58.633

Case No. = 8					
$X_{MP} = 1.2063 \text{ ft}$					
$X_{eq} = 1.2241 \text{ ft}$					
No.	X_c ft	X_o ft	P_{pt} psf	k_{eff}	$c_f \times 10^6$
1	1.2282	1.2104	1356.0	1.4172	3236
2	1.2686	1.2508	1352.5	1.3443	3206
3	1.3100	1.2922	1349.4	1.3010	3182
4	1.3527	1.3349	1346.5	1.2603	3178
5	1.3962	1.3784	1344.0	1.2311	3148
6	1.4359	1.4181	1342.5	1.2262	3128
7	1.4767	1.4589	1340.0	1.1883	3128
8	1.5182	1.5004	1338.4	1.1781	3104
9	1.5605	1.5427	1336.6	1.1637	3080
10	1.6097	1.5919	1335.4	1.1618	3078
11	1.6485	1.6307	1334.1	1.1537	3062
12	1.6937	1.6759	1333.6	1.1578	3034
13	1.7343	1.7165	1332.3	1.1661	3026
14	1.7758	1.7580	1331.8	1.1746	3024
15	1.8177	1.7999	1331.3	1.1884	3002
16	1.8604	1.8426	1330.8	1.2033	2984
17	1.9170	1.8992	1330.4	1.2075	2982
18	1.9489	1.9311	1330.0	1.2274	2974
19	1.9940	1.9762	1329.9	1.2376	2952
20	2.0334	2.0156	1329.4	1.2456	2938
21	2.0737	2.0559	1329.0	1.2565	2934
22	2.1146	2.0968	1328.7	1.2730	2932
23	2.1559	2.1381	1328.6	1.2921	2918
24	2.1977	2.1799	1328.4	1.3012	2898
25	2.2404	2.2226	1328.0	1.3168	2890
26	2.2840	2.2662	1327.9	1.3346	2894
27	2.3280	2.3102	1327.7	1.3388	2884
28	2.3725	2.3547	1327.6	1.3588	2866
29	2.4177	2.3999	1326.9	1.3598	2852
30	2.4639	2.4461	1326.1	1.3622	2850
31	2.5786	2.5008	1325.3	1.3251	2848

TABLE XI
 PRESTON-TUBE PRESSURE, EFFECTIVE CENTER
 OF THE PROBE AND SKIN FRICTION
 COEFFICIENT ALONG THE SURFACE
 OF THE CONE FOR RUN
 NUMBER 70.726

Case No. = 9					
$X_{MP} = 0.9767 \text{ ft}$					
$X_{eq} = 2.5189 \text{ ft}$					
No.	X_c ft	X_o ft	P_{pt} psf	k_{eff}	$c_f \times 10^6$
1	2.5224	0.98019	1754.3	1.2495	2636
2	2.5631	1.02089	1751.5	1.2043	2630
3	2.6042	1.06199	1745.9	1.1035	2626
4	2.6457	1.10349	1741.8	1.0391	2622
5	2.6876	1.14539	1738.4	0.9868	2616
6	2.7301	1.18789	1733.2	0.9504	2612
7	2.7730	1.23079	1731.5	0.9218	2608
8	2.8163	1.27409	1729.4	0.9034	2602
9	2.8601	1.31789	1727.1	0.8776	2600
10	2.8981	1.35589	1726.0	0.8515	2594
11	2.9428	1.40059	1724.5	0.8447	2590
12	2.9880	1.44579	1723.2	0.8325	2584
13	3.0271	1.48489	1721.5	0.8214	2580
14	3.0666	1.52439	1721.5	0.8047	2576
15	3.1065	1.56429	1720.8	0.8019	2572
16	3.1535	1.61129	1719.8	0.7955	2568
17	3.1941	1.65189	1718.8	0.7875	2564
18	3.2352	1.69299	1718.3	0.7873	2560
19	3.2767	1.73449	1717.0	0.7752	2556
20	3.3115	1.76929	1716.7	0.7766	2554
21	3.3607	1.81849	1716.0	0.7743	2548
22	3.4105	1.86829	1715.3	0.7729	2544

TABLE XII

PRESTON-TUBE PRESSURE, EFFECTIVE CENTER
OF THE PROBE AND SKIN FRICTION
COEFFICIENT ALONG THE SURFACE
OF THE CONE FOR RUN
NUMBER 21.318

Case No. = 10					
$X_{MP} = 0.9383 \text{ ft}$					
$X_{eq} = 1.2813 \text{ ft}$					
No.	X_c ft	X_o ft	P_{pt} pst	k_{eff}	$c_f \times 10^6$
1	1.2869	0.94398	1827.5	1.3578	3022
2	1.3228	0.97988	1819.7	1.2391	3006
3	1.3596	1.01668	1815.4	1.1871	2990
4	1.4066	1.06368	1809.0	1.1098	2970
5	1.4550	1.11208	1805.4	1.0795	2952
6	1.5046	1.16168	1801.6	1.0455	2932
7	1.5453	1.20238	1798.7	1.0209	2918
8	1.5869	1.24398	1796.2	1.0028	2902
9	1.6293	1.28638	1794.0	0.9896	2888
10	1.6836	1.34068	1791.7	0.9778	2872
11	1.7281	1.38518	1789.7	0.9674	2858
12	1.7735	1.43058	1787.6	0.9535	2844
13	1.8198	1.47688	1786.2	0.9506	2830
14	1.8552	1.51228	1785.8	0.9583	2820
15	1.9032	1.56028	1784.6	0.9604	2806
16	1.9522	1.60928	1783.3	0.9580	2796
17	2.0022	1.65928	1781.9	0.9548	2782
18	2.0532	1.71028	1780.5	0.9517	2768
19	2.0921	1.74918	1779.1	0.9448	2758
20	2.1449	1.80198	1777.2	0.9360	2746
21	2.1852	1.84228	1776.4	0.9340	2736
22	2.2260	1.88308	1775.6	0.9242	2730
23	2.2675	1.92458	1774.1	0.9277	2720
24	2.3096	1.96668	1773.2	0.9293	2712
25	2.3523	2.00938	1772.1	0.9266	2702
26	2.3956	2.05268	1771.6	0.9343	2692
27	2.4395	2.09658	1770.6	0.9330	2684
28	2.4841	2.14118	1770.4	0.9391	2678
29	2.5293	2.18638	1769.1	0.9337	2670
30	2.5751	2.23218	1768.4	0.9372	2662
31	2.6216	2.27868	1767.8	0.9399	2656
32	2.6688	2.32588	1767.4	0.9497	2648
33	2.7006	2.35768	1766.9	0.9524	2644

TABLE XII (Continued)

Case No. = 10					
$X_{MP} = 0.9383 \text{ ft}$					
$X_{eq} = 1.2813 \text{ ft}$					
No.	X_c ft	X_o ft	P_{pt} pst	k_{eff}	$c_f \times 10^6$
34	2.7489	2.40598	1766.2	0.9516	2640
35	2.7979	2.45498	1765.5	0.9553	2634
36	2.8476	2.50468	1764.9	0.9609	2626
37	2.8811	2.53818	1764.2	0.9600	2624

TABLE XIII
 PRESTON-TUBE PRESSURE, EFFECTIVE CENTER
 OF THE PROBE AND SKIN FRICTION
 COEFFICIENT ALONG THE SURFACE
 OF THE CONE FOR RUN
 NUMBER 41.548

Case No. = 11					
$X_{MP} = 0.7850 \text{ ft}$					
$X_{eq} = 1.5914 \text{ ft}$					
No.	X_c ft	X_o ft	P_{pt} psf	k_{eff}	$c_f \times 10^6$
1	1.5946	0.78824	2256.9	1.2912	2808
2	1.6346	0.82824	2248.9	1.2256	2790
3	1.6758	0.86944	2241.9	1.1398	2792
4	1.7176	0.91124	2236.3	1.0804	2778
5	1.7547	0.94834	2231.3	1.0284	2760
6	1.7927	0.98634	2228.5	1.0090	2752
7	1.8427	1.03634	2225.2	0.4830	2752
8	1.8821	1.07574	2222.6	0.9646	2736
9	1.9281	1.12174	2219.8	0.9457	2720
10	1.9694	1.16304	2218.1	0.9386	2724
11	2.0112	1.20484	2215.8	0.9229	2716
12	2.0537	1.24734	2214.1	0.9168	2698
13	2.0970	1.29064	2212.4	0.9089	2688
14	2.1413	1.33494	2211.2	0.2052	2692
15	2.1863	1.37994	2209.5	0.8979	2682
16	2.2252	1.41884	2208.2	0.8933	2666
17	2.2649	1.45854	2207.0	0.8904	2658
18	2.3055	1.49914	2205.5	0.8832	2662
19	2.3466	1.54024	2204.7	0.8824	2662
20	2.3881	1.58174	2203.7	0.8842	2646
21	2.4231	1.61674	2203.0	0.8854	2634
22	2.4659	1.65954	2201.4	0.8768	2630
23	2.5095	1.70314	2201.0	0.8820	2634
24	2.5537	1.74734	2200.7	0.8889	2628
25	2.5983	1.79194	2199.4	0.8850	2616
26	2.6436	1.83724	2198.6	0.8874	2602
27	2.6898	1.88344	2198.3	0.8944	2600
28	2.7289	1.92254	2197.1	0.8880	2602
29	2.7763	1.96994	2196.3	0.8900	2596
30	2.8242	2.01784	2195.6	0.8942	2584

TABLE XIII (Continued)

Case No. = 11					
$X_{MP} = 0.7850 \text{ ft}$					
$X_{eq} = 1.5914 \text{ ft}$					
No.	X_c ft	X_o ft	P_{pt} psf	k_{eff}	$c_f \times 10^6$
31	2.8648	2.05844	2195.3	0.8998	2574
32	2.9060	2.09964	2194.6	0.8990	2572
33	2.9479	2.14154	2194.1	0.9025	2576
34	2.9901	2.18374	2194.0	0.9130	2572
35	3.0241	2.21774	2192.7	0.9046	2564
36	3.0670	2.26064	2192.1	0.9083	2554
37	3.1106	2.30424	2191.6	0.9117	2546
38	3.1549	2.34854	2191.3	0.9226	2544
39	3.1998	2.39344	2191.0	0.9279	2548
40	3.2450	2.43864	2190.6	0.9332	2544
41	3.2906	2.48424	2190.0	0.9389	2534

TABLE XIV

PRESTON-TUBE PRESSURE, EFFECTIVE CENTER
OF THE PROBE AND SKIN FRICTION
COEFFICIENT ALONG THE SURFACE
OF THE CONE FOR RUN
NUMBER 57.632

Case No. = 12		$X_{MP} = 1.23917$ ft	$X_{eq} = 0.91783$ ft		
No.	X_c ft	X_o ft	P_{pt} psf	k_{eff}	$c_f \times 10^6$
1	0.9181	1.2394	1192.1	1.0805	3386
2	0.9611	1.2824	1187.1	1.0353	3342
3	1.0021	1.3234	1182.8	0.9950	3332
4	1.0442	1.3655	1176.4	0.9283	3290
5	1.0880	1.4093	1176.2	0.9506	3282
6	1.1289	1.4502	1173.9	0.9402	3248
7	1.1710	1.4923	1172.0	0.9343	3222
8	1.2146	1.5359	1170.4	0.9315	3214
9	1.2546	1.5759	1169.1	0.9342	3180
10	1.2959	1.6138	1167.8	0.9366	3164
11	1.3383	1.6596	1166.4	0.9328	3156
12	1.3815	1.7028	1165.1	0.9353	3122
13	1.4261	1.7474	1164.5	0.9460	3116
14	1.4718	1.7931	1163.7	0.9518	3100
15	1.5132	1.8345	1163.1	0.9626	3070
16	1.5558	1.8771	1162.3	0.9653	3060
17	1.5993	1.9206	1161.8	0.9759	3054
18	1.6436	1.9649	1161.4	0.9899	3028
19	1.6889	2.0102	1160.8	0.9995	3012
20	1.7297	2.0510	1160.5	1.0103	3012
21	1.7709	2.0922	1160.3	1.0216	2996
22	1.8128	2.1341	1160.1	1.0380	2972
23	1.8557	2.1770	1160.0	1.0565	2964
24	1.9060	2.2273	1159.0	1.0573	2962
25	1.9440	2.2653	1158.0	1.0649	2946
26	1.9827	2.3040	1157.8	1.0731	2926
27	2.0221	2.3434	1156.8	1.0889	2918
28	2.0691	1.3904	1155.1	1.0879	2920
29	2.1167	2.4380	1155.0	1.0751	2904
30	2.1580	2.4793	1154.3	1.0912	2886
31	2.2001	2.5214	1153.4	1.0958	2876
32	2.2431	2.5644	1152.1	1.0960	2878
33	2.2866	2.6079	1150.7	1.0884	2870

TABLE XV
 PRESTON-TUBE PRESSURE, EFFECTIVE CENTER
 OF THE PROBE AND SKIN FRICTION
 COEFFICIENT ALONG THE SURFACE
 OF THE CONE FOR RUN
 NUMBER 72.748

Case No. = 13		$X_{MP} = 0.9667$ ft	$X_{eq} = 1.0689$ ft		
No.	X_c ft	X_o ft	P_{pt} psf	k_{eff}	$c_f \times 10^6$
1	1.0714	0.9692	1602.3	1.1976	3122
2	1.1133	1.0111	1595.2	1.1304	3084
3	1.1568	1.0546	1588.1	1.0621	3076
4	1.1974	1.0952	1580.9	0.9960	3050
5	1.2349	1.1327	1578.1	0.9858	3024
6	1.2779	1.1757	1574.5	0.9619	3022
7	1.3217	1.2195	1571.0	0.9425	2990
8	1.3624	1.2602	1568.1	0.9286	2974
9	1.4042	1.3020	1566.0	0.9209	2970
10	1.4467	1.3445	1564.0	0.9182	2942
11	1.4904	1.3882	1561.7	0.9103	2926
12	1.5353	1.4331	1560.3	0.9109	2922
13	1.5758	1.4736	1558.1	0.9030	2898
14	1.6173	1.5151	1556.7	0.0940	2880
15	1.6707	1.5685	1555.3	0.9072	2878
16	1.7140	1.6118	1554.0	0.9089	2854
17	1.7584	1.6562	1552.7	0.9125	2836
18	1.7982	1.6960	1551.9	0.9158	2838
19	1.8444	1.7422	1551.0	0.9220	2824
20	1.8854	1.7832	1549.9	0.9242	2802
21	1.9273	1.8251	1548.9	0.9297	2792
22	1.9702	1.8680	1548.2	0.9291	2796
23	2.0136	1.9114	1547.9	0.9410	2782
24	2.0576	1.9554	1547.0	0.9456	2762
25	2.1027	2.0005	1546.7	0.9541	2756
26	2.1487	2.0465	1546.3	0.9621	2758
27	2.1886	2.0464	1545.7	0.9621	2748
28	2.2357	2.1335	1544.6	0.9678	2728
29	2.2770	2.1748	1544.3	0.9796	2722
30	2.3191	2.2169	1544.0	1.9887	2726
31	2.3617	2.2595	1543.6	1.9943	2720
32	2.4047	2.3025	1543.5	1.0051	2706
33	2.4484	2.3462	1543.3	1.0203	2694
34	2.4930	2.3908	1543.0	1.0323	2692
35	2.5384	2.4362	1542.2	1.0333	2694
36	2.5843	2.4821	1541.7	1.0408	2686

TABLE XVI

PRESTON-TUBE PRESSURE, EFFECTIVE CENTER
OF THE PROBE AND SKIN FRICTION
COEFFICIENT ALONG THE SURFACE
OF THE CONE FOR RUN
NUMBER 19.289

Case No. = 14					
$X_{MP} = 0.9667 \text{ ft}$					
$X_{eq} = 1.5678 \text{ ft}$					
No.	X_c ft	X_o ft	P_{pt} psf	k_{eff}	$c_f \times 10^6$
1	1.5708	0.9697	1632.3	1.5223	2904
2	1.6124	1.0113	1623.3	1.3852	2898
3	1.6546	1.0535	1616.5	1.2939	2872
4	1.6923	1.0912	1611.1	1.2248	2860
5	1.7421	1.1410	1606.5	1.1785	2858
6	1.7814	1.1803	1602.4	1.1345	2824
7	1.8271	1.2260	1600.8	1.1352	2818
8	1.8681	1.2670	1598.0	1.1089	2814
9	1.9099	1.3088	1595.1	1.0852	2812
10	1.9521	1.3510	1593.7	1.0824	2792
11	1.9951	1.3940	1592.4	1.0814	2776
12	2.0392	1.4381	1590.1	1.0637	2776
13	2.0840	1.4829	1588.7	1.0600	2772
14	2.1294	1.5283	1587.3	1.0575	2752
15	2.1756	1.5745	1585.1	1.0399	2740
16	2.2161	1.6150	1583.7	1.0309	2738
17	2.2572	1.6561	1582.3	1.0242	2738
18	2.2988	1.6977	1580.9	1.0166	2726
19	2.3409	1.7398	1579.9	1.0130	2710
20	2.3838	1.7827	1578.0	1.0099	2704
21	2.4276	1.8265	1576.6	0.9968	2708
22	2.4719	1.8708	1575.2	0.9912	2702
23	2.5091	1.9080	1573.7	0.9827	2690
24	2.5545	1.9534	1572.3	0.9743	2676
25	2.5930	1.9919	1570.9	0.9607	2674
26	2.6400	2.0389	1570.2	0.9656	2680
27	2.6875	2.0864	1568.0	0.9486	2672
28	2.7680	2.1669	1566.6	0.9526	2658
29	2.8092	2.2081	1565.9	0.9532	2650
30	2.8511	2.2500	1564.9	0.9493	2646

TABLE XVI (Continued)

Case No. = 14					
$X_{MP} = 0.9667 \text{ ft}$			$X_{eq} = 1.5678 \text{ ft}$		
No.	X_c ft	X_o ft	P_{pt} psf	k_{eff}	$c_f \times 10^6$
31	2.9019	2.3008	1564.3	0.9549	2648
32	2.9361	2.3350	1563.8	0.9579	2646
33	2.9792	2.3781	1563.0	0.9618	2638
34	3.0229	2.4218	1562.5	0.9663	2618
35	3.0674	2.4663	1562.2	0.9734	2618
36	3.1035	2.5027	1561.6	0.9743	2622
37	3.1489	2.5388	1561.0	0.9797	2614
38	3.1947	2.3844	1560.0	0.9827	2604

TABLE XVII

PRESTON-TUBE PRESSURE, EFFECTIVE CENTER
OF THE PROBE AND SKIN FRICTION
COEFFICIENT ALONG THE SURFACE
OF THE CONE FOR RUN
NUMBER 42.549

Case No. = 15					
$X_{MP} = 0.8105 \text{ ft}$					
$X_{eq} = 1.5597 \text{ ft}$					
No.	X_c ft	X_o ft	P_{pt} psf	k_{eff}	$c_f \times 10^6$
1	1.5678	0.8186	2008.35	1.3354	2800
2	1.6074	0.8582	1998.38	1.2209	2776
3	1.6479	0.8987	1991.25	1.1492	2766
4	1.6999	0.9507	1984.12	1.0850	2764
5	1.7422	0.9930	1979.84	1.0539	2744
6	1.7854	1.0362	1975.57	1.0214	2730
7	1.8298	1.0806	1971.29	0.9889	2734
8	1.8692	1.1200	1968.44	0.9713	2722
9	1.9150	1.1658	1965.30	0.9525	2702
10	1.9560	1.2068	1962.74	0.9385	2696
11	2.0160	1.2668	1959.88	0.9259	2694
12	2.0586	1.3094	1958.46	0.9252	2676
13	2.1022	1.3530	1956.32	0.9171	2664
14	2.1467	1.3975	1954.32	0.9067	2668
15	2.1854	1.4362	1953.04	0.9038	2662
16	2.2245	1.4753	1952.04	0.9050	2648
17	2.2710	1.5218	1950.05	0.8954	2636
18	2.3117	1.5625	1949.19	0.8968	2634
19	2.3669	1.6177	1947.77	0.8947	2632
20	2.4088	1.6596	1947.05	0.8986	2620
21	2.4513	1.7021	1945.63	0.8981	2606
22	2.4947	1.7455	1944.20	0.8958	2604
23	2.5389	1.7897	1943.49	0.8955	2610
24	2.5836	1.8344	1942.78	0.9018	2600
25	2.6287	1.8795	1941.64	0.9026	2584
26	2.6747	1.9255	1941.07	0.9059	2580
27	2.7216	1.9724	1940.07	0.9061	2578
28	2.7931	2.0439	1939.21	0.9140	2576
29	2.8333	2.0841	1938.64	0.9184	2566
30	2.8740	2.1248	1938.22	0.9249	2554
31	2.9154	2.1662	1937.22	0.9237	2550
32	2.9575	2.2083	1936.93	0.9302	2554

TABLE XVIII
 PRESTON-TUBE PRESSURE, EFFECTIVE CENTER
 OF THE PROBE AND SKIN FRICTION
 COEFFICIENT ALONG THE SURFACE
 OF THE CONE FOR RUN
 NUMBER 56.631

Case No. = 16					
$X_{MP} = 1.3183 \text{ ft}$					
$X_{eq} = 0.6993 \text{ ft}$					
No.	X_c ft	X_o ft	P_{pt} psf	k_{eff}	$c_f \times 10^6$
1	0.7009	1.3199	1055.9	0.8198	3528
2	0.7418	1.3608	1050.9	0.7954	3492
3	0.7814	1.4004	1046.6	0.7750	3454
4	0.8227	1.4417	1043.3	0.7678	3420
5	0.8623	1.4813	1040.3	0.7601	3386
6	0.9034	1.5224	1038.6	0.7629	3362
7	0.9424	1.5614	1036.6	0.7631	3324
8	0.9830	1.6020	1035.2	0.7649	3314
9	1.0245	1.6435	1033.4	0.7672	3270
10	1.0679	1.6869	1031.8	0.7677	3262
11	1.1083	1.7273	1030.4	0.7704	3230
12	1.1542	1.7732	1029.4	0.7786	3200
13	1.1930	1.8120	1028.5	0.7824	3194
14	1.2370	1.8560	1027.4	0.7895	3156
15	1.2781	1.8971	1026.4	0.7955	3150
16	1.3201	1.9391	1026.1	0.8012	3132
17	1.3630	1.9820	1024.8	0.8098	3100
18	1.4073	2.0263	1024.7	0.8235	3096
19	1.4476	2.0666	1024.2	0.8323	3080
20	1.4886	2.1076	1023.4	0.8391	3050
21	1.5307	2.1497	1022.5	0.8429	3040
22	1.5739	2.1929	1021.7	0.8460	3036
23	1.6177	2.2367	1021.4	0.8596	3010
24	1.6569	2.2759	1022.4	0.8701	2992
25	1.7146	2.3336	1020.5	0.8804	2990
26	1.7556	2.3746	1020.2	0.8925	2970

TABLE XIX
 PRESTON-TUBE PRESSURE, EFFECTIVE CENTER
 OF THE PROBE AND SKIN FRICTION
 COEFFICIENT ALONG THE SURFACE
 OF THE CONE FOR RUN
 NUMBER 43.550

Case No. = 17					
$X_{MP} = 0.9525 \text{ ft}$					
$X_{eq} = 2.8075 \text{ ft}$					
No.	X_c ft	X_o ft	P_{pt} psf	k_{eff}	$c_f \times 10^6$
1	2.8133	0.9583	1786.80	1.2222	2514
2	2.8568	1.0018	1767.98	1.0066	2506
3	2.9008	1.0458	1778.67	1.1473	2494
4	2.9457	1.0907	1775.11	1.1182	2488
5	2.9851	1.1301	1765.70	1.0164	2488
6	3.0250	1.1700	1770.83	1.0868	2488
7	3.0650	1.2100	1768.69	1.0707	2484
8	3.1052	1.2502	1766.70	1.0578	2478
9	3.1457	1.2907	1765.27	1.0522	2468
10	3.1869	1.3319	1763.70	1.0463	2462
11	3.2289	1.3739	1762.28	1.0420	2458
12	3.2716	1.4166	1760.85	1.0350	2460
13	3.3291	1.4741	1760.14	1.0388	2456
14	3.3724	1.5174	1758.00	1.0245	2450
15	3.4159	1.5609	1757.29	1.0282	2440
16	3.4601	1.6051	1755.86	1.0234	2434
17	3.5128	1.6578	1754.72	1.0207	2432
18	3.5588	1.7038	1753.73	1.0181	2432
19	3.6129	1.7579	1751.87	1.0072	2432
20	3.6517	1.7969	1751.59	1.0135	2426
21	3.6906	1.8356	1751.02	1.0168	2420
22	3.7378	1.8828	1750.30	1.0200	2412
23	3.7778	1.9228	1749.88	1.0266	2406
24	3.8184	1.9634	1749.02	1.0274	2406
25	3.8679	2.0129	1748.59	1.0330	2406
26	3.9261	2.0711	1747.60	1.0329	2404

TABLE XX

PRESTON-TUBE PRESSURE, EFFECTIVE CENTER
OF THE PROBE AND SKIN FRICTION
COEFFICIENT ALONG THE SURFACE
OF THE CONE FOR RUN
NUMBER 15.231

Case No. = 18		$X_{MP} = 1.0333$ ft		$X_{eq} = 1.8595$ ft	
No.	X_c ft	X_o ft	P_{pt} psf	k_{eff}	$c_f \times 10^6$
1	1.8633	1.0371	1370.72	1.4120	2780
2	1.9049	1.0787	1362.16	1.3002	2762
3	1.9475	1.1213	1354.32	1.2073	2756
4	1.9910	1.1648	1349.47	1.1587	2754
5	2.0349	1.2087	1345.05	1.1162	2736
6	2.0716	1.2534	1341.49	1.0875	2720
7	2.1254	1.2992	1337.21	1.0490	2716
8	2.1654	1.3392	1334.36	1.0267	2716
9	2.2057	1.3795	1331.51	1.0037	2704
10	2.2466	1.4204	1329.66	0.9945	2688
11	2.2883	1.4621	1327.66	0.9827	2682
12	2.3308	1.5046	1325.24	0.9658	2686
13	2.3738	1.5476	1323.67	0.9558	2678
14	2.4173	1.5911	1322.24	0.9500	2664
15	2.4615	1.6355	1320.53	0.9444	2652
16	2.5143	1.6881	1318.25	0.9344	2648
17	2.5835	1.7573	1316.54	0.9300	2644
18	2.6224	1.7962	1315.12	0.9228	2634
19	2.6618	1.8356	1313.98	0.9198	2622
20	2.7019	1.8757	1312.98	0.9182	2618
21	2.7591	1.9329	1311.84	0.9160	2620
22	2.8087	1.9825	1310.84	0.9147	2614
23	2.8505	2.0293	1309.41	0.9079	2602
24	2.8928	2.0666	1308.13	0.9025	2592
25	2.9359	2.1097	1307.28	0.9005	2586
26	2.9885	2.1623	1306.71	0.9078	2590
27	3.0417	2.2155	1305.85	0.9085	2584
28	3.0864	2.2602	1304.42	0.9015	2574
29	3.1317	2.3055	1303.71	0.9043	2562
30	3.1778	2.3516	1302.71	0.9058	2558
31	3.2152	2.3890	1301.57	0.9032	2558
32	3.2625	2.4363	1300.15	0.9024	2560
33	3.3006	2.4744	1289.29	0.9045	2556
34	3.3486	2.5224	1296.58	0.8938	2546
35	3.3972	2.5710	1296.16	0.8860	2534

TABLE XXI

PRESTON-TUBE PRESSURE, EFFECTIVE CENTER
OF THE PROBE AND SKIN FRICTION
COEFFICIENT ALONG THE SURFACE
OF THE CONE FOR RUN
NUMBER 44.551

Case No. = 19					
$X_{MP} = 0.85917 \text{ ft}$					
$X_{eq} = 1.8964 \text{ ft}$					
No.	X_c ft	X_o ft	P_{pt} psf	k_{eff}	$c_f \times 10^6$
1	1.9007	0.8635	1713.45	1.1369	2678
2	1.9413	0.9041	1706.32	1.0801	2660
3	1.9827	0.9455	1699.08	1.0203	2652
4	2.0251	0.9879	1691.35	0.9595	2656
5	2.0680	1.0308	1685.94	0.9226	2644
6	2.1052	1.0680	1682.09	0.8985	2628
7	2.1496	1.1124	1677.81	0.8738	2620
8	2.1951	1.1579	1673.53	0.8493	2622
9	2.2345	1.1973	1670.68	0.8351	2616
10	2.2743	1.2371	1668.55	0.8282	2602
11	2.3149	1.2777	1665.69	0.8141	2590
12	2.3563	1.3191	1663.56	0.8034	2588
13	2.4196	1.3824	1660.42	0.7905	2586
14	2.4623	1.4251	1658.57	0.7851	2572
15	2.5058	1.4686	1656.43	0.7792	2560
16	2.5429	1.5057	1655.29	0.7769	2562
17	2.5877	1.5505	1653.86	0.7743	2564
18	2.6331	1.5959	1652.15	0.7690	2556
19	2.6714	1.6342	1561.15	0.7696	2546
20	2.7181	1.6809	1649.58	0.7686	2534
21	2.7577	1.7205	1649.30	0.7748	2530
22	2.8060	1.7688	1648.02	0.7727	2534
23	2.8466	1.8094	1647.16	0.7730	2528
24	2.8959	1.8587	1646.45	0.7772	2516
25	2.9376	1.9004	1645.31	0.7770	2506
26	2.9799	1.9427	1645.02	0.7826	2502
27	3.0229	1.9857	1644.60	0.7863	2504
28	3.0752	2.0380	1643.88	0.7899	2500
29	3.1191	2.0819	1643.60	0.7963	2492
30	3.1635	2.1263	1642.88	0.7994	2480
31	3.2086	2.1714	1641.89	0.7995	2474
32	3.2544	2.2172	1641.74	0.8061	2474
33	3.3005	2.2633	1641.46	0.8119	2476
34	3.3478	2.3106	1640.75	0.8151	2470
35	3.3950	2.3578	1640.46	0.8226	2460
36	3.4429	2.4057	1640.03	0.8288	2450

VITA²

Amir Nassirharand

Candidate for the Degree of

Master of Science

Thesis: CORRELATION OF THEORETICAL TURBULENT SKIN FRICTION WITH PRESTON-TUBE MEASUREMENTS ON A SUBSONIC CONE

Major Field: Mechanical Engineering

Biographical:

Personal Data: Born in Tehran, Iran, January 12, 1961, the son of Mr. and Mrs. Hassan Nassirharand.

Education: Graduated from Hadaf High School, Tehran, Iran, in May 1977; received Bachelor of Science in Mechanical Engineering degree from Oklahoma State University in December 1980; enrolled in Master of Science program at Oklahoma State University, January 1981; completed requirements for the Master of Science degree at Oklahoma State University in December, 1981.

Professional Experience: Graduate research assistant, January 1981-December 1981.